CHAPTER ONE

INTRODUCTION

1.1Background of the study

Adhesion is the ability of a material to stick to another, while adhesives are substances that possess this quality. Benedek, (2004) describes adhesives as non-metallic substances used to bind surfaces together. Adhesives flow during bonding and solidify after bonding. They are required to wet surfaces which they intend to bond. They undergo fortification upon application and remain firm. During the fortification process there is a change in the structure of the adhesives, and they remain taut in the bond. The American Adhesive Sealant Council describes adhesives as materials which flow at application and capable of bonding. Adhesives can be classified according to their operating capacity and respective chemistry (Ana, et al, 2020). They are classified as chemically susceptible adhesives, Evaporative adhesives and Thermoplastic adhesives. Evaporated adhesives are either solvent base or water base. Natural rubber is an example of solvent base evaporative adhesive. Animal hide is an example of water base evaporative adhesive.

Chemically susceptible adhesives are those that react to heat and moisture such as Epoxy, Silicon, and Acrylic. Thermoplastic adhesives flow when heated and set thereafter, example is Hot melts (Ana et al, 2020). Raw materials for making adhesives include inorganic materials, natural materials, semi-synthetic materials and synthetic materials. The inorganic materials are derived from soluble silicates, phosphates, cements, hydraulic cements, miscellaneous cements. Natural materials are derived from starch, dextrin, gelatin, asphalt, bitumen, natural rubber resins and shellac. Semi-synthetic materials are those derived from vinyls, acrylics, reactive acrylic bases,

synthetic rubber, aldehyde condensation resins, amine resins, epoxy resins, polyester resins, polyolefin polymers, (Ana et al, 2020). Adhesives can be classified according to application. This classification includes pressure sensitive adhesives, structural adhesives and thermosetting structural adhesives. Jaber (2019), describes structural adhesives as adhesives used below their glass transition point. They are capable of withstanding great physical force; examples are urethanes, and cyanoacrylate. Pressure sensitive adhesives are adhesives characterized by low elastic modulus. The low elastic modulus makes the adhesive alter its shape, on the application of minimum pressure.

Glue gums which are used in wide applications are examples of pressure sensitive adhesives. Thermosetting structural adhesives have limited shelf life and may come in two components forms resins and adhesive. They give extremely high output upon application. Pressure sensitive adhesives are materials which possesses the ability to form a bond with adherent surfaces on the application of minimum pressure and little contact time. According to (Benedek, 2004) pressure sensitive adhesive retain the ability to flow even after bonding. This makes it easier to delaminate from bonding surfaces with ease, and leaving no traces. Remarkably, pressure sensitive adhesives do not require activation, heating prior to application. Debonding and bonding involving these types of adhesives are energy driven (Benedek and Feldestein, 2019). Adhesives possess three principal properties namely: Tack, Peel and Shear. Tack measures the capacity of adhesive to adhere quickly. Peel measures the ability of adhesives to resist removal. Shear measures the ability of the adhesive to resist shear forces (Zbigniew et al, 2013).

An oil and gas multinational firm in the country, which places a high degree of attention on the safety of lives and properties within the firm, installed

emergency fire safety equipment at strategic places around the firm. Each installation must be indicated by special designated sign (made from Aluminum of 2mm thickness) and installed on vertical surfaces over head the safety installation, at particular heights of 2meters for offices, and 3meters for the firm workshops. These signs must never be bored with nails or pins, thus leaving the only alternative to install the safety sign with the use of adhesives.During the application of various adhesives (Pressure Sensitive Adhesives) most of the signs for the safety equipment failed to get pasted on the walls. The walls include those made from high density fibre wood, mild steel, ceramic wall tiles, and rubber wall tiles. This led to the suspicion that the cause of the failure might be from the surfaces or adhesives and could be linked to phenomenon of interfacial properties.

Interfacial properties such as the substrate surface free energy and surface free energy of the pressure sensitive adhesive affect tack movement. Tack was also found to be dependent on energy dissipated at the interface of bond formation (Zbigniew et al, 2013). The chemical composition of the adhesive and surface parameters like surface roughness, surface energies of the various substances affect the ability of the pressure sensitive adhesive to form bonds (Rudenauer, 2013). The adhesive force between substance and pressure sensitive adhesive was found to be dependent on the critical values of the surface free energy. The ability of a bond to exist between the two surfaces is affected by the thermodynamic work of adhesion (Toyama et al, 2013). The capacity for an adhesive to wet the surface of its adherent also affects the surface energy and aids its penetration capacity across the surface. Wetting in conjunction with surface roughness, and exchange of material across the surface/ adhesive interface impact on the bond strength (Li, et al, 2001).

The work of adhesion is an interfacial property, which as earlier explained affects the ability of bond to be formed between two materials. This phenomenon explains the inability of the aluminum plate to bond to the surfaces with the pressure sensitive adhesive.

Therefore this research will examine the role of work of adhesion in the process of attaching the aluminum plate likewise factors that affect the role of work of adhesion.Interfacial tensions (both of surfaces and liquids), contact angle, dissipation energy, fracture energy, chemical composition of the adhesive shall be investigated.More so high work of adhesion has been associated with lower contact angle (Bernardes, et al, 2012). It has been found that there is a relation between adhesive rheology and adherence particularly in case of strong adhesion with a solid substrate and soft adhesive (Marin and Derail, 2006).This work made use of the concept of thermodynamic work of adhesion and fracture energy to explore sources of improvement in adhesive/substrate bond formation between two dissimilar surfaces. Furthermore it shall add to the knowledge pool of the role played by the above two mentioned parameters in other areas beyond the research topic. These areas include pipe coating, corrosion treatment, fluid flows across surfaces.Summarily, interfacial factors affect adhesive performance in bond formation at adhesive/substrate interface, and this in turn affects the work of adhesion. The extent which these factors played in the bond performance, bond failure at the interface,likewise the effect of fracture energy on bond formation shall be investigated.

1.2 Statement of problem

The basic demand is that emergency signs (made from aluminum plate) be pasted on the vertical wall surface as a means to alert staff of the presence of first aid safety equipment for use in case of emergency situation such as inferno. The challenge to executing this task is that use of fasteners such as nails, pins and boring the surfaces will lead to destruction of surface aesthetic, increases stress concentration at the point where fasteners are used and adds to the weight the surfaces bear. However, adhesive offers alternative usageto fasteners and the above enumerated challenges are eased off, but upon the application of the adhesives to stick the sign on the vertical wall surfaces most failed to paste the signs. The major suspicion is that the failure of the signs to stick to the surface is as a result of failure of interfacial parameter to allow adherence between the surfaces. Remarkably the research employs the use of work of adhesion and fracture energy to find out the reason for the failure. The work of adhesion measures the relation between interfacial energy between adhesives and substrates (Rudenauer, 2013) and the fracture energy is fundamental to the process of delamination, (Mokhtari, et al, 2017). The delamination is as a result of debond across two materials which stop adhering to each other.

1.3 Aim and Objectives of the Study

The aim of the research is to evaluate the influence of interfacial parameters on the adhesion of pressure sensitive adhesives. Thus to achieve this, these objectives will be pursued:

1. To measure contact angles and hence calculate surface energies.
2. To measure the thermodynamic work of adhesion from interfacial energy, surface energy and surface energy component polarity.
3. To ascertain the role of adhesive rheology in adhesion across the interfaces.

4. To determine if a correlation exists between combinations of work of adhesion, work of cohesion, work of spread and tack calculate from tensile strength.
5. To identify the modifications that will enhance good bond formation.

1.4 Significance of the study.

The significance of this study centres on providing solutions to the inability of sign posts to bond to vertical surfaces using different pressure sensitive adhesives. The study will supply the correlation between physical adhesion (thermodynamic work of adhesion) and fracture energy in predicting the reason for these bond strength failures. Additionally, the study will describe the influence of various adhesive rheology interface parameters and adherence to the surface, thermodynamically. Finally, the study will provide corrective modifications that can be made on these surfaces to ensure sustenance of bond strength of the pressure sensitive adhesives on the bonding surfaces.

1.5 Scope of the study

The scope of this study covers the use of physical adhesion (thermodynamic work of adhesion) and fracture energy to predict failure and bond performance. Presently the available technology measures bond quality and predicts failure by bond destruction. Therefore, the study is confined to the application of the interfacial parameters (fracture energy and thermodynamic work of adhesion) to predict bond failure and quality. External factors like temperature, pressure, humidity and state of matter were not considered in the study.

CHAPTER TWO

LITERATURE REVIEW

2.1 Pressure Sensitive Adhesives, Properties and Applications.

Pressure sensitive adhesives are substances which on application to surfaces forms a strong bond, under light pressure, and extremely short contact time. They havecharacteristics stickiness that enable them grab on any surface upon application. They achieve immediate stickiness without the application of heat treatment or solvent treatment. Pressure sensitive adhesive are viscous materials, exhibits flow and dissipate energy. It is elastic which limits its flow ability while conserving its store energy. The store energy promotes adequate tack and peel properties. Bendek, (2004) describes adhesives as non-metallic materials used to bond other materials mainly on their surface through adhesion and cohesion. The adhesion forces acting between the adhesive and the substrate aid the instant stickiness upon application. The cohesive forces within the adhesive enable the adhesive to remain in shape under the action of shearing forces. The effectiveness of a pressure sensitive adhesive depends to an extent on its ability to wet its adherent surface. Zbigniew et al, (2013), identifies the capacity of an adhesive film to wet its adherent surface to be dependent on the softness of the adhesive. Furthermore, it prescribes that the adhesive must maintain the popular Dalhquist criterion. The criterion demands that the pressure sensitive adhesive must have a dynamic shear modulus of less than $3x10^{6}$dynes/cm and exhibit tack at 1second deformation. Pressure

sensitive adhesive when subjected to tensile stress, exhibits predictable debonding ability (Deplace et al, 2009). Pressure sensitive adhesive possess low modulus, which favors viscous flow, and produces a layer of linear elastic material across a substrate surface. This layer enhances the penetration of the adhesive into the surface crevices and cracks. The adhesive exhibits softcontinuous stream of stickiness across a boundary with adherence.Therefore they combine rheological, viscous, elastic properties to enhance shear (Geiss and Vogt,2007). They are durable on application and resist creep and cyclic loading. Pressure sensitive adhesive exhibit three principal properties. They are Tack, Shear, and Peel strength. Sun et al, (2012) held that these properties though basically viscoelastic properties, depend on the adhesive bulk properties. They also affect the rheology of the adhesive, its performance during bonding, debonding and performance with regard to contact pressure and bond formation. The three principal properties and their effect on the pressure sensitive adhesives are discussed below

2.1.1 Tack

Tack refers to the ability of an adhesive to stick to a surface at very little time space and little applied pressure. Adhesive tack enables it to oppose removal when it is applied on a surface. ASTM (2019), describes tack as an adhesive capacity to bond with another surface with measurable strength. This is done while allowing a specified force to debond the adhesive from the substrate. The bond between the adhesive and surface is formed at slight pressure and limited contact time. Tack depicts a reverse of the separation energy, where the separation energy is the ability to debond the substrate from an adhesive. The tack represents the capacity to enforce the bond formation. The composition of a pressure sensitive adhesive and its component synthesis affect the tack of an adhesive. Zbigniew et al, (2012), describe the ratio of

combination of free mono and solvent- base acrylic as influencing the tack of a pressure sensitive. The ratio was found to affect residual mechanical properties of the coated self-adhesive at higher synthesis, while reducing same at lower synthesis. The viscoelastic properties of a pressure sensitive adhesive affect its deformability enabling it to stretch and achieve required contact with different surfaces. (Teisseire, et al, 2006). Factors beyond tack, such as surface energy, contact time, adhesive properties influence bond quality. Mohammed, et al, (2016), describes the quality of bond between a pressure sensitive adhesive and a substrate as grossly affected by surface energies for both substrate and adhesive. Other factors include contact pressure, mechanical properties of the adhesives, temperature and humidity. Tack is also essential where adhesive debond is required by enabling a clean separation at existing bonded surface, and this assures greater tack ability. Polymers exhibit tack beyond their glass transition temperature.The glass transition temperature is the temperature point where a polymer changes state from the tough glassy form to a flowing liquid state. According to (Yang, 2006), low glass transition temperature indicates low viscosity, which favors wettability across a surface and better tack.However, when the glass transition temperature is high the adhesive is stiff, with an inability to wet surface and subsequent drop in tack. The presence of tackifiers resins, dissimilar polymers, adjusting molecular weight and distribution, cross-link co-polymerization affect the tack of a pressure sensitive adhesive (Ozawa, et al, 2001). Good radial flow, low elastic modulus improves tack. (Rudenauer, 2013). Tack is measured by the Loop Tack test, Probe Tack testand coefficient of friction method. The unit of measuring tack is in J/m^2.Creton, (2003) identifies fibril formation in debond as a show of tackiness. The fibril is formed at the interface between the adhesive and substrate, and enhances stickiness.

Once a bridging of the fibrils is formed, resistance to fracture of the bond is diminished, crack propagation is blunted and tack enhanced.

2.1.2 Shear

Shear measures the ability to resist and remain stable under the influence of shearing forces. When pressure sensitive adhesives have adequate chemical and physical cross links across their polymer chains, it ensures resistance to continuous shear. Bendek, (2004) describes shear resistance as a measure of force needed to pull an adhesive held parallel to the substrate surface under condition of definite pressure. Ozawa et al, (2001) states that balance between resistance to creep in shear for solid and peeling process for highly viscous liquids aids pressure sensitive adhesive to optimize its properties for its application. The implication is that for a pressure sensitive adhesive to remain stable on application across a substrate surface.The solid property of the adhesive material makes it not to be too fluid. More so the adhesive must not be highly viscous because it will not flow to wet the surface as such resist adhesion.It is expected that the adhesive must be capable of withstanding a moderate level of stress for a long period. Like other properties mentioned, the shear of an adhesive is controlled by tackifier blends, polymerization, and molecular weight adjustment and curing. The viscosity of a fluid characterizes its holding power and for adhesives undergoing elasticity it depicts its tensile bearing capacity.Shear measures the cohesive force strength within the molecules of a pressure sensitive adhesive. The shear power of an adhesive is improved when it comes from a homogenous source, because of similarity in based formulation cohesion and modifications. This impacts on adhesion, (Alyssa, et al, 2014) expresses the gecko feet ability to exhibit anti-wetting behavior on contact with water as a function of shear holding power. The shear holding power induces low contact angle hysteresis that makes water

drop bead up on the gecko toe and fall off. This water does not penetrate its adhesive pad. This exhibition of super hydrophobicity enhances its holding capacity. It explains the gecko feet self-cleaning dirt power and recovery after wetting.

2.1.3 Peel

Peel refers to the force needed to pull out the adhesive film from a substrate surface. Bendek, (2004) defines peel as the amount of force needed to remove a flexible coat from a pressure sensitive adhesive from a particular surface, at a particular angle and speed.During peeling of a pressure sensitive adhesive from a substrate, a certain amount of energy is expended. This is called the bond energy of dissipation.Peel force is dependent on the rate removal of the adhesive from substrate, peel angle and adhesive thickness. Rudenauer, (2013) describes peel as the resistance of an average load per width during the delamination of a flexible thin strip, bonded to a rigid substrate. The process of delamination occurs at an angle between 90^0-180^0. During peeling process two forms of energy are expended, namely the fracture energy, and the earlier mentioned dissipation energy. At peeling, there is a break down in the bond between adhesive and substrate surface; this is a break down in the bond between adhesive substrate surfaces. This leads to fracture of the joint. The point of fracture at the interface during peel presents irreversible entropy, which is accompanied with an evolution of energy. The dissipated energy during peel is a consequent of stress transfer and interaction of viscoelastic properties characteristic of deformation (Yang, 2006). The introduction of peel at the adhesive and substrate generates deformation. Deplace et al, (2009) held that this deformation supplies

information on maximal nominal stress, maximal strain, and adhesion energy at the point of debond.In addition, the peel adhesive is influence by factors which includes thickness of adhesive layer, cohesive failure, culminating in debond. During the process of debond adhesive rheology, viscoelastic properties and even mechanical properties of the substrate surface are involved (Ozawa et al, 2001). Peel Adhesion is influenced by the composition of the pressure sensitive adhesive, as viscosity of the adhesive determines its bonding capacity. It was earlier stated that excess viscosity will retard wetting, as such limit pressure sensitive adhesive spread across substrate surface. Bendek, (2004), revealed that peel resistance is influenced by the chemical nature and macromolecular characteristics of the base polymers. On the other hand, (Zbigniew, et al, 2012) resolved that residual monomers in a solvent based pressure sensitive acrylic adhesive affects its mechanical properties particularly peel adhesion. The composition of an adhesive is determined by the chemical interaction between the viscoelastic materials such as presence of tackifiers, cross-links, and synthesizers.

2.2 The Role of Interfacial Parameters on Bond Formation.

Adhesion occurs when two surfaces are joined together. The surfaces have peculiar characteristics which facilitate the joining processes. The mechanism of adhesion occurs via microscopic and macroscopic mechanism. The different parameter (cavitation, surface roughness, interfacial energy, adhesion, surface free energy, fracture energy and wetting) and mechanism are discussed below.

2.2.1 Cavitation

Cavitation is an interfacial phenomenon which takes place within an adhesive bulk. It occurs due to a failure in the adhesive cohesive strength or attraction

among similar molecules in the adhesive bulk. This leads to failure in the adhesive bulk, as it spreads across cavities and boundaries of cavities.Cavitation process is generated by attraction which surpass a threshold. Teisseir, et al, (2006), states that the on-set of cavitation is reflective of the materials elastic resistance. It also found that the materials elasticity inhibits inner pre-existing bubble growth within the bulk. Other properties like bubble surface tension, bubble dilation were found to facilitate the cavitation process. Cavitation is a good description of an interfacial mode controlled stress within a bulk, which triggers unstable stress condition. The stress within the bulk rises, till it reaches a threshold were it exceeds the modulus of elasticity. Cavitation is thus triggered with a generation of strain within the bulk, resulting in a low energy release from each cavity. Rudeneaur, (2013), identifies that cavitation occurs at a contact angle which exceeds 90^0, when there is an elastic extension which accompanies detachment. Environment, with low elastic modulus, high degree film confinement and strong interface bonds favors cavitation. Patil, et al, (2012), shows that cavitation followsdebond in both elastic and viscoelastic adhesive.It generates energy loss and facilitates to fracture toughness of an adhesive. The different in pressure between the atmospheric pressure and the internal bubble pressure generated during adhesive debond triggers adhesive cavitation.

2.2.2 Surface Roughness

Surface roughness is the distortion experienced in the surface texture of a material. Nori, (2015), describes surface roughness as an interfacial property, which results from mechanical bonding, surface deformation or dislocation. It affects the physical appearance of the surface by introducing distortions, and (Rudneauer, 2013) refers to it as the pressure of asperities or wave forms. The presence of asperities on a surface leads to the occurrence of an actual profile

across a length of measured surface profile. A profile, in this case, is the intercept between a perpendicular surface plane and a tactical part. Surface roughness leads to a non-uniform distribution of flatness across a surface. It can be a result of distortion arising from surface treatment, defects, asperities, or machining. Mitutoyo, (2009), categorized surface roughness as follows:

R_a Is the arithmetic mean surface roughness

R_{sm} Is the average groove width

R_t Is the total height of the roughness profile

R_z Is the maximum height of the roughness profile

R_{zTmAX} Is the maximum surface surfaces roughness

R_{zd} Is the surface roughness depth.

Boxin, (2004), divided surface roughness into three major parts namely:

Optical roughness; is at a scale of less than 1mm. It refers to the roughness available in individual fibers or pigment article.

Micro roughness; is scale at 1mm-100nm, akin to fiber network roughness.

Macro roughness; is at scale of 0.1mm-1mm

2.2.3 Interfacial Energy

Interfacial energy or adhesion energy is the energy existing between two bodies in diverse phases. It allows intermolecular attraction between molecules of different surfaces. Gommes, (2014) describe it as the energy at the interface between water (in liquid phase) and glass (in solid phase). Nori, (2015), stated that it affects peel velocity at interface and is intrinsic between two interfaces in contact.

2.2.4 Crack Propagation

Crack propagation is a process of initiating a separation between an adherent and adhesive. This is done through the application of tensile force acting normal to plane of crack propagation. A shear force acting parallel to the plane of crack propagation and at right parallel to plane in direction of crack initiates it. Crack propagation distorts the bulk in an adhesive, initiates a deform action used in deboned during a probe tack test, (Piltonen, 2013). This process occurs at the interface and results to an interfacial failure through cavitation, bulk fingering, and fibrillation. Crack is the region in a space where there is a detachment between a block and substrate. The region is traced from the edge of the crack, otherwise referred to as crack process zone. Persson and Tosatti, (2001) states that microscopic cavitation initiates crack propagation and nucleation occurs at interface. It causes a spatial distribution and concentration of cavity and evolves into fibrillar structures. Crack releases stress at interface between adhesive and substrate, and is caused by a profound velocity stretch resulting from traction. High elastic modulus in a material favors crack propagation, while in a low temperature environment or under condition of dense cross link. Teisseire et al, (2016), enumerates applied stress, elastic modulus, local separation, atmospheric pressure as factors influencing crack propagation at interface between adhesive and substrate. During crack propagation the contact area between an adhesive and adherent is separated as crack size increase. When the size increases the area of contact between the interfaces diminishes. Rudenaeur, (2013) showed that crack propagation, is accompanied by a drop in load, required to initiate a fixed displacement and limitation in spread of strain energy at interface.

2.2.5 Adhesive Film Degree of Confinement

The adhesive film degree of confinement is a measure of the relation between contact probe radius and the adhesive film thickness. Ghatak and Chaudhary,

(2007) describes it as a confine parameter.It is the ratio of two different length scales, thickness of a film and stress decay length along the film plate interface.

2.2.6 Adhesion

Adhesion refers to molecular attraction between dissimilar particles or surfaces. It is the act of joining two surfaces using a pressure sensitive adhesive. Adhesion is adhesive ability to stick to a surface, otherwise a measure of tack. It is characterized by low viscosity, good wettability and capacity to withstand shear within molecules of the adhesive bulk. Zibgniew et al, (2013) described adhesion as a measure of tack and adhesive ability to resist removal, while Nori, (2015),refered to it as a molecular interaction at material interface. Adhesion is aided by the process of adsorption of the adhesive into the substrate surface, electrostatic attraction and diffusion processes. Adhesion measures the work required to separate the adhered surface (Fuentes et al, 2015), and aided by increased roughness, surface porosity, and size compatibility (Kovacevic, 2008). Good adhesion is achieved through mechanical interlocking, chemical bonding and physical adhesion. Mechanical interlocking and chemical bonding is derived indirectly from destructive micromechanical test. This micromechanical testis like micro indentation measure practical adhesion. The practical adhesion measure the interfacial and chemical interaction. The mechanical property determines the local stress, matrix residual stress, external stress fracture site which is a result of interfacial stress and loading. The roughness of a substrate surfaces increases the propensity of mechanical interlocking between adhesive and substrate surfaces. This follows that an increase in the surface roughness site for higher bonding between the adhesive and substrates. Adhesion is facilitated by adsorption, as it provides adequate interfacial bond between

adherent components. Kovacevic, 2008 stipulated that adsorption helps spontaneous wetting, increase surface contact and reduce stress concentration. Adhesion involving chemical bonding is a process of ionic transfer among electrovalent bonds, covalent bonds to improve bond formation. This is achieved through diffusion bonding, and this supports inter diffusion between two interacting surfaces.

2.2.7 Contact Angle

Contact angle is the angle a liquid makes with a solid in conjunction with vapor. The contact angle a liquid makes with a solid varies for different liquid on the same substrate. Each liquid use for contact angle measurement has peculiar intrinsic characteristics. This explains the different values derived during interaction at each interface, during measurement. Fuentes, et al, (2014), stated that contact angles are used to determine physical adhesion of various surfaces by the application of different investigation liquids. Contact angles occurs in different forms such as advanced contact angle, receding contact angle, static contact angle. When a sessile liquid drop is placed on a substrate surface, Njobuenwu, et al, 2005 held that it spreads for some time then it halts. The contact angle measured at the halt of liquid spread is called the advanced contact angle. The receding contact angle is the angle that emerges when a liquid drop is withdrawn with the aid of a needle or pipette. The advanced contact angle is applicable during wetting of substrate surface, while the receding is present at dewetting. Static contact angle is the contact with which the contact area between liquid and solid remains unchanged from outside during measurement.Contact angle is influenced by the viscoelastic properties of an adhesive material during debond. The receding contact angle is as well deterred during bonding condition at substrate/adhesive interface. Julia, et al, (2010), state that viscoelastic

materials create good model process for predicting debond. Contact angle affects interfacial properties like wettability, spread ability and surface energy. Bhutani et al, (2012), experimented on the effect on contact angle during inclination (reduced contact angle). It was discovered that the contact angle reduced while the advanced contact remains constant, particularly when hydrophilic pendant is considered. This development is affected by the surface roughness.Static contact angle which remains constant during measurement aids in the analysis of dropwise condensation, biomimetic drug delivery lap-chip and adhesive technology. Contact angle undergoes a process of hysteresis, which is a difference between the advancing contact angle and receding contact angle. Piltonen (2013) described contact angle hysteresis as the phenomenon which makes a liquid ball up due to cohesive force within the contact liquid. The liquid spreads out when the adhesive forces between the surface and liquid increase, more than cohesive forces causing the liquid ball up. Boyd et al, (2007), observed contact angle hysteresis in crude oil extraction from water logged rocks containing petroleum. Here there are two layers (crude/water), where crude oil does not attach to the rock. This makes it incapable of altering the wettability of the system towards oil. This interaction result in the formation of advanced water contact angle which favors water displacement of oil from rock surface pores. The reverse process is receding water, which displace water from oil. When a drop of measuring liquid is dropped on a substrate surface, it takes some time for the liquid to halt its spread. The time it takes for the liquid to halt its spread and form a given contact angle is called contact time.Contact angle decreases with increase time due to surface reconstruction along line of hydrophobic component, (starting contact angle). Flinn and Ashley, (2010), stated that at equilibrium contact angle is influenced by the hydrophilic component of the

substrate surfaces. When test liquids are dropped on substrate surfaces, it spreads with time due to vapor absorption. Ducan, et al, (2005), identified that the volume of drop varies due to effects of moisture absorption and evaporation.Viscous liquids change in shape occurs when dropped on substrate surface. This pattern is a regular feature until an equilibrium shape is achieved.

2.2.8 Surface Free Energy

Surface energy is the work required to separate two surfaces with a force higher than the forces binding them together.It is measured as energy per unit area and referred to as surface tension.It is expressed as 1mN/Mequivalent to a surface free energy of $1mJ/m^2$ or 1dyn/cm. It is influenced by intermolecular forces acting along interfaces, and can be split into polar component and non-polar components.Ducan, et al, (2015), stipulated that the polar component of the surface free energy consists of electron acceptor or electron donor, while the non-polar component comprises Vander waals force. Furthermore the polar components can be divided into Lewis acid/base components, with one component dominating the other.Surface energy exists as stress at surface of solids.It reduces the area, and as the size diminishes as a lower energy level is attained. The mechanicalwork needed to raise the surface area is also a measure of surface energy. The unit is put at $1mJ/cm^2$. Rudenauer, (2013) explained that the interfacial molecules between two surface in contact have high potential energy that the molecules in the rest of the bulk. Bond is the result of forces holding molecules inside and on the surface of the medium; surface energy is the energy needed to break the bond. The bonds strength reflects the dispersion, by hydrogen and metallic components. Surface tension is interchangeably used with surface energy and relates substance to vacuum

with the respect to air and vapour. Kovacevic, (2008), held that surface tension refers intermolecular forces which try to separate the number of molecules at the surface. It went further to describe surface energy as intermolecular distance that keeps the molecules at surface together. Zbigniew,et al, (2013), explained that surface free energy measures an adhesive capacity to wet the yet to be bonded surface. Better wetting promotes penetration into surface asperities. This in turn promotes interlock of the adhesive on the substrate as well as mechanical bond. Mohammed, et al, (2016) pointed out that surface free energy of a substrate depends on contact angle measurement across the surface. The surface energy constitutes of dispersive and polar components. Peykova, et al, (2012), stated that tack of an adhesive and its adherence performance is a function of its surface energy. This is because adhesive with lower surface energy have better wettability over substrate surfaces with higher surface energy. Surface energy is the capacity of a body to induce attractive force into other materials with unfilled bonds such as chemical bond, hydrogen bond and Vander-waals. Qi, (2000) described it as energy needed to create unit area of a surface of material in a thermodynamically reversible manner.Flinn and Ashley, (2010) stated that surface energy can be used to characterize a surface. According to Simoncic (2004), it is a reflection of solid-liquid intermolecular interaction.

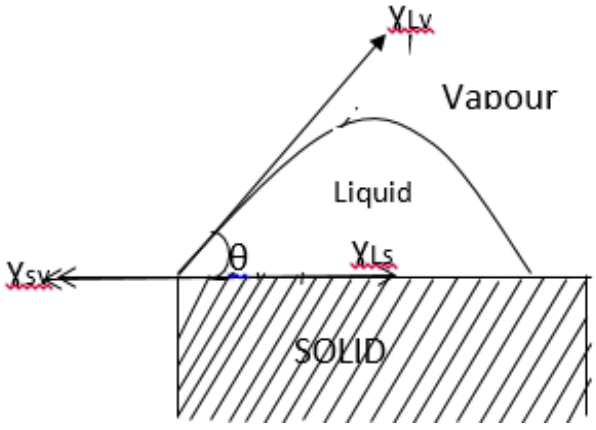

Figure 2.1 Liquid drop on a solid surface (Chaudhury, 1996)

Figure 2.1 shows a chemical equilibrium of a liquid drop on a solid surface. It shows a balance of three surface tension forces acting at the liquid-solid vapour contact line.

γ_{lv} represents the surface free energy at the liquid-vapour interface.

γ_{sv} represents the surface free energy at the solid-vapour interface.

γ_{sl} represents the surface free energy at the solid-liquid interface.

θ represents the contact angle.

A surface can be characterized as a low surface energy material when it tends to contract, shrivel and form droplet. Wolf and Sparavigna, (2010) states that surfaces which possess poor wettability, very scarce coating adhesion, need surface treatment to improve on its surface energy. Shaw and Williams (2013), gave examples of such surfaces polypropylene, polyethylene, nylon. Low surface do not wet well as such maximize contact area. Accordingly, a high surface energy material is easily wetted and allow droplet of liquid put on it to spread across its surface. It has good adhesion capacity and good bond ability. Examples are ABS, and Polycarbonate.

2.2.9 Fracture Energy

Fracture energy is an intrinsic property peculiar to a material. It is unaffected by load applied or shape of the body. It represents the energy that must be surmounted before crack initiation is felt on an adhesive bond or material. The amount of energy dissipated at point of bond failure is equivalent to the amount of energy expended during cracking initiation. Nori (2015), described it as energy required to overcome adhesion and a characteristics property of bonded interface. It is independent of viscoelastic or rheological properties of an adhesive. Fracture energy is needed to overcome practical adhesion. Practical adhesion is concerned with adhesion at point of pure interfacial

failure. The process of practical adhesion requires an external force use to break an adhesion through a distance.According to, (Boxin, 2004), practical adhesion relates to intermolecular interaction involving interfacial chemistry, rheology, and fracture mechanism. Toygar, et al, (2009), described fracture energy as interfacial property needed to determined resistance of a material to crack propagation. Rudeneaur, (2013) called the fracture energy, the energy which peel resistance exhibit, alongside the dissipated energy. Dissipated energy exist during fibrillation (Yang, 2006) explained it as interplay at the interface resulting in stress transfer.

During the transfer, the plastic and viscoelastic deformation properties are involved.There is an energy generated as a result of breaking down the forces which are bonding the adhesive filmto the accompanying flat surface. Feldstein et al, (2014) described it as energy expended in breaking the adhesive and cohesive intermolecular strength in a bond. When maximum force is applied to separate two surfaces bonded together by a pressure sensitive adhesive, it induces a complex debonding mechanism. The applied force is time dependent, and the result of the debond is heterogeneous cavitation, viscous fingering starting at cavity boundaries. In addition, there is a bubble growth between the walls, which leads the fibrils to thin out, elongate and fracture. Mohammed, et al, (2012) defined dissipation energy as work done expend to overcome tackiness between two surfaces bonded together. Connor andWillenbacher, (2004), described dissipation energy as energy expended on deformation of the pressure sensitive adhesive (polymer chain)alongside viscoelastic rheology. According to, Moslemi and Khoshrawan, (2015), dissipation energy predicts delamination onset and crack propagation in a bond. Surface roughness which influence, tack affects dissipation, because dissipation rises alongside tack (Zbigniew, et al, 2013). Qi, (2000)

described fracture energy as practical fracture roughness of an adhesive bond. The critical strain release energy is energy dissipated at the point of fracture formation across a unit of surface. It is same as fracture energy and larger than the thermodynamic work of adhesion. It is directly linked to work of adhesion. Fuentes, et al, (2008), refered to fracture energy as work dissipation required to spread a crack of unit area. Belnoue and Hallet, (2016) defined the critical release energy as sum of the stored elastic energy (released when the crack grows)and a dissipation term embracing the plastic dissipation. Fracture Energy or Critical strain release energy is energy need to create new surfaces, as the constituents G_c remain inseparable and intertwined with each other. During fracture energy, crack propagation is initiated and the elastic material is exerted by the normal tensile stress. The cracks in this region do not transmit stress, but spread it to nearby regions. This increases the interfacial energy as the crack width increases, and reduces the elastic energy (Teissere, et al, 2006). The fracture energy is as well called Griffith crack propagation.

2.2.10 Wetting

Wetting is the ability of a fluid to spread over a surface. It describes the preference of a solid to be in contact with a particular solid over another. According to Boyd, et al, (2007), wetting explains the displacement of a fluidby a wetting fluid across a surface, thus initiating spreading. It measures the interaction between the surface and liquid contact angle, while interfacial force promotes spreading and absorptivity (Bhutani, et al, 2012). The wettability between a solid and adhesive is influenced by contact time (Flinn and Tracey, 2010), while physical attraction emanates from intermolecular forces (Ducan, et al, 2005). Intermolecular forces are the forces present at the bonding interface. It consists of dispersive forces and polar forces. When water is dropped on a surface and it fails to spread. It shows that there is poor

intermolecular attraction between the surface and the water. However, when the water drop makes a contact angle which is greater than 90^0 with the surfaces, it is termed hydrophobicity. Surface which produce these effects are called hydrophobic surface. Moreover, when the surfaces trap air, and the contact angle of the water with the surface extends to 150^0. It is called super hydrophobicity. Banerjee, (2008) described super water repellant surfaces as substrate with hydrophobic contact angles exceeding 140^0. Hydrophobicity disallow wetting, encourages liquid bead up on surfaces. Hydrophilic surfaces encourages wettability and form contact angle below 90^0. Gommes, (2014), stated that liquids which allow wettability encourages the formation of thin layer on the surface. This process indicates spread on the surface.

2.2.11Dewetting

The inability of a liquid to spread when applied to a surface is dewetting.

Njobuewu et al, (2005), expresseddewetting as a surface phenomenon which occurs when the contact angle between a liquid and a solid is greater than 90^o. This phenomenon explains the bead up of mercury drops on grass surface. Hydrophobicity is example of dewetting, likewise super hydrophobicity. Spinodaldewetting occurs when film of an adhesive break up in a spinodal process as a result of long rangeVan der Waal forces. These forces evolve into an increase in film thickness variation, resulting in film break up. The process of spinodaldewet is a result of weak attraction existing between substrate and surrounding medium. The attractive force between the two plain surfaces is related by an interaction constant called Hamaker.

Autophobicity is a dewetting process which occurs as a result of variation of the equilibrium contact angle. This occurs when a fluid drop on a surface creates a layer which inhibit wetting. Geoghgan and Karusch, (2002) identifiedautophobicity as a dewetting process between homopolymer film

on polymer brushes. The reason for the dewet on the brush is the differential in entropy along the interface, variation in molecular weight and grafting density. According to Kovacevic(2008), dewetting signifies lack of mutual attraction between substrate and adhesive. This results in a high interfacial energy between both materials.

2.2.12 Nucleation

Nucleation is the emergence and growth of a phase within a polymer film. This is caused by the presence of impurities or molecules cluster within the adhesive film. When there is a drop in pressure within an adhesive bulk it results in nucleation. This pressure drop is influenced by strain, rate of strain within the adhesive bulk. It decreases when the substrate plate is removed from the adhesive surface. The drop in pressure within the adhesive bulk causes the growth of micro bubbles. The spread of nucleation is halted at contact between grain boundaries as a result of interfacial damage. Geoghegan and Karusch, (2002), described nucleation as a process of film rupture or discontinuation in the spread of a thin film across a flat substrate. The rupture or discontinuation is due to thermal agitation, presence of impurities such ass dust or scum in the adhesive film or substrate. According to Benedek, (2004), there is a discontinuation in the polymeric film material, when a flat probe is punched on it. The punching induces hydrostatic stress within the bulk adhesive and the development of regions of voids.

2.2.13 Surface Effects

Surface effects refer to the role of substrate surface in the adhesion between solid and adhesive. The nature of surface topology of a substrate and adhesive's viscoelastic properties affect the adhering capacity of a rough surface. The substrate surface topology affects rate of cavity growth. Smooth

surfaces express lateral growth while rough surface shows omini-directional growth of cavities. The viscoelastic properties of pressure sensitive adhesive determine the growth rate and amount of cavities at substrate/adhesive interface. Surface effect looks at interaction between the surface chemical properties and it structural composition. The process of assessing viscoelastic material performance according to Sun, et al, (2012), utilizes the stress relaxation inside contact zone of viscoelastic materials. In addition, the creep properties in the cohesive zone of the viscoelastic material aids in the assessment. Zhang, (2007), held that the substrate atomic structure and structural composition resulting from machine work and deformation influences adhesion. Such is manifest, in surface roughness waviness which affect contact angles, light absorption, adhesion and friction. Surface effect influences tribology of polymer interaction. This is done through the role it plays by wear, friction, adhesion between two surfaces, and asperities across the surface (Myshkin, et al, 2005).

2.2.14 Thermodynamic Work/Impacts in Adhesion.

Thermodynamic work of adhesion is a measure of the amount of energy spent to delaminate two surfaces bonded by an adhesive. During the interaction between a substrate and an adhesive, the thermodynamic work of adhesion derives the change in the surface free energy. The thermodynamic work of adhesion is equivalent to the work expended under equilibrium condition. It relate to the surface energy through the Drupe equation. Benedek, (2004), defines the thermodynamic work of adhesion as an interfacial property which reflects the separation or debonding energy of the adhesive joint. It is rate dependent on viscoelatic properties and temperature. According to Rudenaeur(2013), it measures the relation between the interfacial energy, between liquid (adhesive) and solid (substrate). It also measures the

respective surface free energy of both adhesives and substrates. It relates the liquid surface tension, contact angle the liquid form with the surface and interfacial tension between solid and liquid (Bernades, et al, 2012). Mohammed, et al, (2016) described it as the area under the load-displacement curve in a probe tack experiment.

The process of interfacial bonding between dissimilar materials with the aid of adhesive can be analyzed from thermodynamic approach. This is because there is an exchange of material across the interface to achieve the bonding. The boundary at the interface and the exchange of the material between the adherent and adhesive determines the strength and quality of the bond. The present research seek to study, the thermodynamic relation between the various pressure sensitive adhesive types and the various substrate adherents. Thus to study the relation the following laws applicable to the interfacial boundary with regards to material exchange are reviewed. The effect or roles they play in the adhesion are also examined.

2.2.14.1 Young Equation.

Young Equation (1805) relates the solid surface free energy in equilibrium, with the liquid vapor, liquid surface tension, interfacial solid/ liquid free energy and the contact angle.

The young equation is as follows

$$\gamma_{sv} = \gamma_{sl} + \gamma_{lv}\cos\theta \qquad (2.1)$$

where γ_{sv} represents the solid surface energy

γ_{sl} represents the solid/liquid interfacial free energy

γ_{lv} represents the liquid surface free energy

θ represents the contact angle

2.2.14.2 Thermodynamic Work of Adhesion (Wa)

The Drupe equation aids in the calculation of energy at the interface between two materials. The Drupe equation is as follows:

$$Wa = \gamma s + \gamma l - \gamma sl = \gamma l\,(1 + \cos\theta) \qquad (2.2)$$

Where γs represents the solid surface energy

γl represents the liquid surface tension

γsl represents the solid liquid/liquid interface free energy

θ represents the contact angle

When $W_a$is positive then there is an attraction between the solid and liquid leading to wetting. Thus when W_a is negative there is a repulsion between the solid and the liquid leading to a dewet of the liquid on the solid substrate.

2.2.14.3 Wenzel Equation

Bhutani, et al, (2012) stated that when a liquid droplet sits on a solid surface in two distinct configureuration, it is said to be conformal to Wenzel state. Wenzel equation shows the surface roughness factor **r**. This connects a solid wettability with its micro and macro structure. This factor relates with the contact angle of the rough surface. The Wenzel equation for contact is as follows

$$\cos\theta' = \mathbf{r}\cos\theta \qquad (2.3)$$

Where θ' represent the contact angle on rough surface

θ represent the contact angle on surface without roughness

r represent the surface roughness factor.

2.2.14.4 Cohesive Zone Model

Cohesive damage zone model relate traction to separation at an interface where a crack may initiate. The initiation of a crack is related to the cohesive

strength. The cohesive strength is the maximum traction-separation law. The traction force drops to zero when the traction-separation law reaches the fracture roughness. It is accompanied by the formation of a new crack regime (Moslemi and Khoshrawan, 2015). The cohesive zone model tracks the magnitude of crack damage across a crack plane. Belnoue and Hallett, (2016) described a position of damage across a crack plane as d, with an initial value$d^o = 0$. This condition persist till damage initiation continues to a failure value of 1. Here the crack faces completely separate and the value of d is given by the Traction-Separation law.

2.2.14.5 Spreading Coefficient

Spreading coefficient is the energy gain when a unit area of dry solid is covered with a liquid film of a particular thickness across a flat surface.

The spreading coefficient s is given as

$$S = \gamma s - (\gamma l + \gamma sl) \quad (2.4)$$

Where γ_s represents the solid surface energy

$\gamma_l$represent the liquid surface tension

γ_{sl}represents the solid/liquid interfacial free energy

The equilibrium spreading coefficient of a system can be described as the difference between the work of adhesion and cohesion. The equilibrium spreading coefficient is represented as S_o. Thus;

$$S_o = W_a - W_c \quad (2.5)$$

Where W_a represent the work of adhesion

W_c represents the work of cohesion

The equilibrium spreading pressure (equilibrium spreading coefficient) is defined as the reduction of surface energy of the solid covered by a layer of vapour (Kovacevic, 2008). Thus the relation is as follows:

$$\pi_s = \gamma_s - \gamma_{sv} = RT\int_o^{po} \Gamma d(Inp) \quad (2.6)$$

Where; P represents the vapour pressure

P_o represents the equilibrium vapour pressure

Γ represents the surface centration of adsorbed vapour

T represents the absolute temperature.

2.2.14.6 Owens-Wendt Model.

Owens-Wendt characterizes the interfacial surface energy, as a representation of the geometric mean of surface energy of solids (Kovacevic, 2008)

$$\gamma sl = \gamma sv + \gamma lv - 2\left(\gamma_{sv}^{d}\gamma_{lv}^{d}\right) - 2\left(\gamma_{sv}^{p}\gamma_{lv}^{p}\right)^{1/2} \quad (2.7)$$

where γsl represents interfacial surface energy and the geometric mean of surface energy of solids

γ_{lv}^{d} represents the disperse component of surface free energy of the test liquids

γ_{sv}^{p} represents the polar component of the surface free energy of the test liquids.

2.2.14.7 Zisman Law

Zisman law characterizes wetting as a condition in a liquid where the surface tension (γ) is equal to or less than the critical surface tension. This is represented as $\gamma \leq \gamma_c$. The result is a perfect spread of the liquid on solid. Contact angles are derived from dropping several test liquid on a particular surface. When the contact angles are graphically plotted against liquid surface area, it results in a linear relationship.

$$\frac{1}{\cos(\theta)} = \frac{\gamma}{\gamma_c} \quad (2.8)$$

When $\gamma = \gamma_c$,the contact angle is zero (Gommes, 2014)

The critical surface tension is the surface tension at which a liquid wets a solid completely.

2.2.14.8 Gibbs Free Energy

Gibbs free energy relates the enthalpy and entropy content of the system. In adhesion it gives an insight into the nature of reaction between an adhesive and adherent (substrate). It is the measure of compatibility at the interface between the adhesive and substrate. Kovacevic, (2008) describes the compatibility at the interface as follows:

$$\Delta G_M = \Delta H_M - T\Delta S_M \quad (2.9)$$

Where ΔH_M represents the enthalpy of mixing

ΔS_M represents the entropy of mixing

T represents the absolute temperature.

2.2.14.9 Young- Drupe Equation

Young-Drupe equation shows the thermodynamic relation between the contact angle, the work of adhesion and interfacial free energy. It follows that when the contact angle is low, the work of adhesion increases and separation energy between substrate and adhesive rises.

$$W_{sl} = \gamma_{lv}^{(1+\cos\theta)} \quad (2.10)$$

where $\gamma_{lv}^{(1+\cos\theta)} = \gamma_{lv} + \gamma_{sv} + \gamma_{sl}$ (2.10b)

When the contact angle between the test liquid and the surface is zero, there is perfect wetting thus:

At θ = 0, then $W_A = 2\gamma_{lv}$ (2.11)

At θ = 90^0, then $W_A = \gamma$ (2.12)

When the work of adhesion between the liquid and the surface is zero,

$\theta = 180^{o}$, then $W_A = 0$ (2.13)

2.2.14.10 Wetting Condition

Wetting occurs due to the difference between the surface free energy of adhesive and substrate. Zbigniew, et al, (2013) identifies the following interfacial condition as necessary for wetting, they are:

For spontaneous wetting,

$$\gamma_{sv} \geq \gamma_{sl} - \gamma_{lv} \quad (2.14)$$

where γ_{sv} represents the interfacial energy between the solid and vapor

γ_{lv} represents the interfacial energy between the solid and liquid

γ_{lv} represents the interfacial energy between the liquid and vapor.

For condition where the adhesive will spread on the substrate, the conditions:

$$\gamma_{sv} \geq \gamma_{sl} - \gamma_{lv} \text{ or } \gamma_{substrate} \geq \gamma_{adhesive} \quad (2.14b)$$

2.2.14.11Molecular Approach to Surface Free Energy and its Components.

Chauhury, (1996) describes surface free energy as the change in the total surfacefree energy (G) in relation to a unit change in surface area (A). This is done at constant temperature (T) pressure (P) and moles(n). Especially stated as follows:

$$\gamma_{sv} = (\delta G/\delta A)_{T,P,n} \quad (2.15)$$

Solids have defined surface area, thus a change in the surface area affects the molecular package structure and elastic forces in the solids. The liquid because of its behavior with reference to equation (2.15) has changeable surface area. The solid surface mechanics and bulk affect the behavior of a solid. When contact angles of non-swelling liquids are measured on ideal rigid surface, surface energetics can be derived. According to (Gibbs, 1926), the

surface free energy of a solid cannot be derived from contact angle, due to inability to derive interaction energy at solid-liquid interface.

Young-Drupe over-came this difficulty by utilizing a combination of the where $\cos\theta$is equal unity, the $\emptyset^2\gamma_{sv}$ is equivalent to γ_{lv} and this describes the Zisman critical surface free energy γ_c.

2.2.14.12Microscopic View to Interfacial Interaction.

Chaudhry, (1996), state that the pair wise additivity rule, for interaction energy involving two series-infinite flat slab. It is expressed as follows:

$G_{12} = \int_{V1} dv1 \int_{v2} n1n2\ g12\ dv2$ (2.20)

where d_{v1} and d_{v2}represents the volume element of bodies 1 and 2

$n_1$and$n_2$represents the number densities of oscillators in bodies 1 and 2

g_{12}represents the interaction energy between oscillating bodies 1 and 2

Good and Girifalco introduced Debye, Keeson and London forces to measure the interaction energy between two slabs. This led to the expression of g_{12} as follows:

g_{12} = - $(6kT/R^6)\sum_{n=0}^{\infty} \propto_1 (iw_n) \propto_2 (iw_n)$ (2.21)

$\propto (iw_n)$represents the polarization of the oscillator expressed along complex frequency axis iw_n. The interaction energy is simplified to the following:

G_{12} = - $A_{12}/(12\pi l^2)$ (2.22)

Where A_{12} represent the Hamaker constant

L represents the separate distance

The Hamaker constant A_{12} is given as follows:

$A_{12} = 6\pi^2 n_1 n_2\ KT\ \sum_{n=0}^{\infty 1} \propto_1 (iw_n) \propto_2 (iw_n)$ (2.23)

The polarization expressed in equation (2.23) is split into a d.c. photon. The d.c. photon arises from the zero frequency interaction. The other part of the split is from the higher frequency interaction. This split is represented as follows:

$$\propto_1 (iw_n) = (\mu^2/3KT)\left(1 + \frac{w_n}{w_{rot}}\right) + \propto_e (0)/\,(1 + (w_n/w_e)^2) \qquad (2.24)$$

where μ represent the dipole moment

w_{rot} represent the rotational frequency

$\propto_e (0)$represent the electronic polarizability

$w_e$represent the electronic excitation frequency

Work of adhesion at the solid-liquid, solid-vapor, and liquid-vapor interfaces

$$w_{sc} = \gamma_{sv} + \gamma_{lv} - \gamma_{sl} \qquad (2.25)$$

Further simplification of equation 2.25, (which estimate the total energy in a reversible adhesion process) result in the following equation:

$$\gamma_{lv}(1 + \cos\theta) = w_{sl} \qquad (2.26)$$

Good and Girifalco, (1957) simplified equation 2.26 (Young Drupe equation), by the introduction of Berthelot's (1898) intermolecular interaction rule. This expressed the work of adhesion as a geometric mean of the surface free energy of the solid and the surface tension of the liquid. Both quantities are represented as γ_{sv} and γ_{lv} respectively. The introduction of the Berthelot's rule reduces equation (2.26) as follows:

$$w_{sl} = 2\,\emptyset\,(\gamma_{sv}\,\gamma_{lv})^{1/2} \qquad (2.27)$$

where∅ is a correction factor for intermolecular attraction

∅is equivalent to unity.

∅equivalent to unity on the condition that interfacial forces are same.

∅is less than unity when the interfacial and intermolecular forces are not the same.

This led Good and Girifalco, to express $\emptyset$ as surface molecular level parameters like ionization, polarization, and dipole moment. Bradley, (1932), De Boer (1936), and Hamaker (1937), introduced the concept of pairwise additivity rule of intermolecular interactions. This led to the combination of Good-Girifalco and Young-Drupe equation to arrive at the following equation:

$$\gamma_{lv}(1+\cos\theta) = 2\,\emptyset\,(\gamma_{sv}\gamma_{lv})^{1/2} \qquad (2.28)$$

The value of the primary forces that make up the cohesive and adhesive interaction forces are at $\emptyset = 1$, when they are dispersive. This reduces equation (2.28) as follows:

$$\gamma_{sv} = \frac{\gamma_{lv}(1+\cos\,\theta)^2}{4} \qquad (2.28b)$$

2.2.14.13 Macroscopic Theory of Lifshitz.

According to (Lifshitz, 1961) the interaction energy between two surfaces is calculated from the Fourier transform. This is particularly applicable for a macroscopic model. The Fourier transform is for the normal component of the electromagnetic stress tensor. The simplified Hamaker constant of interaction at short distances can be expressed through the Lifshitz's theory. This is expressed as follows:

$$A_{12} = 1.5KT\ \sum_{n=o}^{\infty}\sum_{j=i}^{\infty}(\{([E_1\,(iw_n) - 1)\,/(E_1\,(iw_n)+1][(E_2(iw_n)-$$

$$1)/(E_2(iw_n+1)]\}\mathrm{i}/j^3 \qquad (2.29)$$

Where $E_{m\,(iw_n\,)}$ is the dielecteric susceptibility of the material $m\left(m_{E\,\{1,\ 2\}}\right)$ expressed along the complex frequency axis iw_n.

Lifshitz theory of interaction helps to calculate energy of interaction between condensed phases in terms of the dielectric susceptibilities of the materials. These are continum property that is valid for large separation distance. The Liftshitzcontinum method does not rigidly apply to wetting and adhesion with regard to separation distance.This is applicable when the separation distance

is comparable with molecular sizes. Fowkes, (1964), Isrealachvili (1974, Hough and White (1987), Van Oss et al, (1988). Chaudury, (1996) calculated the Hamaker constant of a non-polar liquid and solid. They discovered that dispersion component of the surface tension and Hamaker constant ratio. This ratio is approximately constant for several materials. It provides an empirical correlation which provides an estimated means of calculating surface tension of liquid from Hamaker constant, and contrariwise

2.2.14.14 Van der Waals repulsion between particles

According to Chaudhury, (1996) Lifshitz theory, states that the interaction between differentmaterials in a liquid can become repulsive. This is because of Van der Waals repulsion between the particles in a liquid medium.

Van der Waals phenomenon is comparable to a liquid medium where two particles P_1 and P_2 interact with the liquid. Particles P_1 have a smaller polarizability than the liquid, thus a negative polarizability state. Particles P2 have a higher polarizability than the liquid, thus a positive polarizability. When the values are implemented into equation 2.2.3, it reduces to

$$A_{12}|_{n=o}=\bar{\wedge}\, n_1 n_2[N^2 N_2^2/3KT)] + [m^2 \propto_{e1} (0)] + 3KT_{e1}(0) \propto_{e2} (0)] \quad (2.30)$$

The higher frequency component on the application of the Hamaker constant is reduced to the following:

$$A_{12}|_{n>o}= \left(\frac{3}{2}\right) \bar{\wedge}^2\, n_1 n_2 h w_{e2} \alpha_{e2}(0)\alpha_{e2}(0)/(w_{e1} + w_{e2}) \quad (2.31)$$

Equation 2.31 corresponds to London dispersion interaction. The ratio of work of adhesion to the geometric mean of work of cohesion acting along parallel plates is represented by the Good-Girifalco parameter Ø

$$\emptyset = w_{12}/(w_{11}w_{22})^{1/2} \quad (2.32)$$

Applying the value of Ø into equations 2.22 and 2.32

$$\emptyset = (j l_1 l_2/l_{12})(A_{12}/J A_{11} A_{22} \quad (2.33)$$

Where $l_1\ l_2\ l_{12}$ represent the equilibrium Van der Waals separation distances Fowke's law is introduced and it considers intermolecular interactions at solid surfaces. This is specified as follows:

$$\gamma = \gamma^d + \gamma^p + \gamma^i + \cdots \quad (2.34)$$

Where d represents the dispersion force

P represents the polar force

$i$represents the interaction force

The work adhesion is expressed alongside with equation 2.34 as follows:

$$w_{12} = 2\sqrt{(\gamma_1^d \gamma_2^d)} + 2\sqrt{(\gamma_1^p \gamma_2^p} + 2\sqrt{(\gamma_1^i \gamma_2^i)} \quad (2.35)$$

Thus the solid surface angle can be calculated when the surface free energy components of a solid surface, contact angles of various measuring liquids and surface free energy components of measuring liquid. The surface free energy components of the solid are determined as follows:

$$\gamma_{lv}(1 + cos\theta) = 2\sqrt{(\gamma_s^d \gamma_l^d)} + 2\sqrt{(\gamma_5^p \gamma_l^d)} + 2\sqrt{\gamma_s^{\iota}}\gamma_l^{\iota} \quad (2.31)$$

The Van der Waals repulsion mechanism deals with adhesion free energy. The adhesion free energy is equivalent to a hydrodynamic drag force. Neuman et al, (1983) described the free energy of adhesion as constituent of several surface free energy of several polymer particles. This is represented as follows:

$$\Delta G = \gamma_{ps} - \gamma_{pl} - \gamma_{sl} \quad (2.37)$$

where γ_{ps} represents the interfacial tension of the particles-solid

γ_{pl} represents the interfacial tension of the particles-liquid

γ_{sl} represents the interfacial tension of the solid-liquid.

The assumption following this condition is that if the surface tension of the solid and liquid are equal, then it leads to zero interfacial tension. The assumption stated has its limitation. More so, the acid base interaction in

interfacial tension between solids nullifies the belief that solid-liquid interfacial tension can only be zero or positive. This leads to the representation of the interfacial tension between two surfaces as follows:

$$\gamma_{12} = \gamma_{12}^{LW} + \gamma_{12}^{AB} \quad (2.38)$$

Where LW represents the London-Van der Waals interaction

AB represents the acid-base interactions respectively.

A further simplification of equation 2.38, leads to the following equation.

$$\gamma_{12} = \left(\sqrt{\gamma_1^{LW}} - \sqrt{\gamma_2^{LW}}\right)^2 + (\gamma_1^{AB} + \gamma_2^{AB} - \gamma_{12}^{AB}) \quad (2.39)$$

2.2.14.15 Donor-acceptor interaction at surfaces

Fowkes (1983), Bolger and Micheal (1969), sees the interaction between surfaces to consist of two major components: dispersion forces and acid-base interactions. Acid is described as a proton donor and base as a donor of a lone pair of electron. Chaundry, (1996) states that a quantitative estimate of Lewis acid-base interaction energy is got from Drago's formula. The Drago's formula stipulates that the enthalpy (ΔH) of acid-base interaction can be derived from parameter, which is expressed as bases or acids. This expression made with reference to surface and represented as follows:

$$-\Delta H = c_A c_B + E_A E_B \quad (2.40)$$

Where C represents the covalent interaction across the surfaces

E represents the electrostatic interactions.

2.3 Influence of Mechanical Properties of Pressure Sensitive Adhesive on Adhesion

Mechanical properties of pressure sensitive adhesive reveal their behavior under stress. Sun, et al, (2012), states that the mechanical properties of pressure sensitive adhesive are defined by tack, shear resistance and peel strength. These properties are deeply linked to the bulk viscoelastic properties

of adhesive. The enumerated adhesive properties alongside adhesive cohesive strength and adhesion strength affect the mechanical properties of the adhesives .The listed viscoelastic properties define the rheology of an adhesive. The rheology of an adhesive measures its response on the application of stress and deformation. It explains the intrinsic pressure sensitive adhesive micro structural constitution. The behavior of pressure sensitive adhesive under stress predicts the relationship of the adherent tack and strength (Mokhtari, et al, 2017). The behavioral analysis of the adhesive analyzes the stress distribution in an adhesive/ substrate interface, during bonding. Tsai, et al, (1995) held that the variation of mechanical and geometrical properties of a bond influences adhesive durability. Adhesive durability affects bond performance and quality, which is part of the investigation, this research seeks to address.

Engineers require information on mechanical properties of pressure sensitive adhesive, to stipulate the conditions for use. The mechanical properties reveal adhesive strength, stiffness, brittleness, hardness, softness. It explains the adhesive behavior when subjected to cyclic stress and repeated loading. Fuentes, et al, (2015), stated that physical adhesion evaluated between single fibre and bamboo composites influenced the mechanical properties, at the matrix interface. The ultimate tensile strength and interfacial shear force posited poor performance for the bamboo. The single fibre glass experienced a high performance for the two parameters. The result showed a low stress transfer capability when two materials are held in a matrix. Thus the mechanical properties of the pressure sensitive adhesives are discussed below.

2.3.1 Tensile Strength

Tensile strength is the amount of stress required to break an adhesive bond, when it is stretched. It is measured in Pascals or Pound per square inch. The tensile strength is measured with a tensile tester such as testomeric tensile machine, Instron. The applied force is the tensile stress made on the bonding material measured over the area of the substrate under bonding. Tensile strength of a bond is measured in the load- displacement graph by two parameters, the maximum load and bond energy (Al-Qadi, et al, 2008). These two parameters can be regarded as indications of adhesion. Nevertheless the bond tensile strength can be obtained from a tensile test, which measures the engineering stress-strain curve. The stress-strain curve works on the principle of Hooke's law. This law measures the stress as being proportional to the strain with a constant of proportionality Young Modulus. (Royalance, 2001).

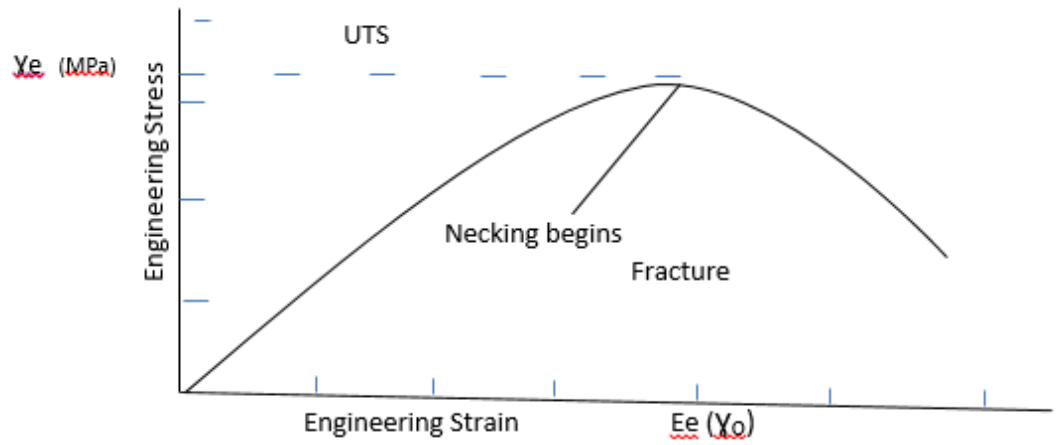

Figure 2.2. Engineering Stress – Strain Curve.

When a bond is subjected to a strain it moves out from the linear proportion. This range where the linear proportionality is felt is called the elastic limit. Beyond this limit, there is an intermolecular misalignment of the molecules across the interface from its initial position. At this region plastic deformation is induced and dislocation ensues. Brittle materials break up at this point, while ductile materials persist. Further application of stress beyond the

proportional limit increases the strain, leading to a continual strain. This phenomenon is called strain hardening. As the strain hardening increase it diminishes. It arrives at the ultimate tensile strength. This point marks the point of maximum tensile strength. When the strain goes beyond the ultimate tensile strength it leads to soft strain. This position is where little increment in stress leads to a higher strain. Beyond this point is the necking region where there is fibrillation (or necking) and eventual debond fracture.

2.3.2 Modulus Of Elasticity.

Pressure sensitive adhesives are viscoelastic in nature, and the elastic deformation influence the modulus. The adhesive modulus of elasticity is a measure of how its elastic deformation reacts to an extension on application of load. The elasticity of a pressure sensitive adhesive is applicable to a limit, which is called the Yield Strength. When the applied stress exceeds its limit, the bond goes into plastic deformation. Plastic deformation is a region where the material (adhesive) losses it shape from the original. It cannot come back to its initial position. According to Xiaocong, (2010), the mechanical properties of an adhesive affect the stress distribution across the bond interface. This is demonstrated in a single- lap cantilever beam, where the adhesive Young Modulus and Poisson's ratio strongly affects stress distribution across the bond in the beam. Hence the stress distribution is demonstrated to affect the strength of the bond, quality of adhesion at interface. Bonding makes an adhesive to undergo deformation which leads to adequate wetting of the substrate. The elastic modulus helps the adhesive to secure areas of contact, penetrate through cervices and stick to adherent. Low modulus is responsible for good wetting. The strength of adhesive bond is measured by itsdebond resistance, while the bond strength rises with high modulus (Bendek, 2004). The flow limit of an adhesive is correlated to the value of the modulus. The

elastic modulus at low frequency improves wettability and bonding behavior. When it (elastic modulus) is at high frequency it favors debonding. The adhesive stickness is improved by lowering the elastic modulus at the plateau region in a viscoelastic curve. The modulus is lowered by measuring the molecular weight of the pressure sensitive adhesive. During the process of debond of a pressure sensitive adhesive from a substrate, cavitation, fibrillation, crack propagation takes place. These processes occur with the release of elastic energy through the adhesive modulus. Pressure sensitive adhesives which demonstrate a decrease in creep improves wettability by increasing modulus. This leads to lowering of the tack and peel adhesion. The modulus of elasticity of an adhesive is affected by chemical composition structure, environment and experimental conditions. The modulus of elasticity of an adhesive helps to distinguish between permanent adhesives and pressure sensitive adhesives. This is because the material rheology is influenced by its elastic components, thereby storing the bond rupture energy. Bendek, (2004) held that this leads to a higher peel and tack properties in the pressure sensitive adhesive. The stored energy consists of energy dissipated to overcome drag and manifests in kinetic energy and potential energy. The potential energy is the region of elastic modulus.

2.3.3. Glass Transition Temperature.

Glass transition temperature is the point at which an amorphous material transit from a brittle solid to a viscous liquid with a rise in temperature. Glass transition or vitrification is a discontinuity in the second derivative of Gibbs free energy. According to (Glass transition temperature, polymer data base, 2015), it involves parameters such as expansion coefficient and heat capacity. The amorphous solid turns into a soft vicious material with a rise in temperature and reverts to a brittle material on cooking.

Stiffer adhesives emanate from higher glass transition point, leading to decreased wettability, and a reduction in adhesive properties (Bendek, 2004). Contrastingly, low glass transition temperature favors wettability and intimacy between adherent and adhesives. Adhesion bonding proceeds in a fluid material (adhesive involved). Adhesion in polymeric adhesive is influenced by diffusion of chain elements across the interface between adhesive and adherent. This process is influenced by glass transition temperature. The adhesive bonding is favored by modulus mobility of the pressure sensitive adhesive across the interface. This bonding is influenced by fluidity of the adhesive which proceeds at glass transition temperature functioning below the reaction temperature. Thus the molecular motion needed for interface adhesions influenced by the glass transition temperature.The glass transition temperature is influenced by the polymer molecular weight. The mobility of the polymer chains of the adhesive is needed to achieve adhesion at an interface. Thus an increase in the molecular weight of the adhesive results in decrease of chain mobility of an adhesive. This prior indicates the role of molecular weight in the effectuality of the glass transition temperature.

The chemical structure and composition of the adhesive affects the glass transition temperature. The mobility of the polymer chain, depends on internal forces acting within the adhesive bulk. This internal movement affects the composition of the adhesive which increases the tack. This increase in tackiness is accomplished by a low transition temperature. The nature and arrangement of the adhesive chain affects its morphology. The forces acting across the molecules of the adhesive influence crystallization. Crystallization results in reduced chain mobility and increase in the glass transition temperature.

2.3.4 Formulation of Pressure Sensitive Adhesives.

The formulation of a pressure sensitive adhesive is the blending of its material component. The blending of the components is needed in an adhesive recipe to arrive at a specified end use property for technological application. Formulation enables the improvement of adhesive properties of an adhesive. This is the reason why tackifying resins are introduced to a natural rubber based adhesive to improve tack. High tackification is specifically meant for the improvement of the peel adhesion. Peel performance is enhanced by tackification which improves bonding, yet improves cohesion which is needed to resist for peel. Fujita, et al, (2000) described the effects of miscibility and viscoelasticity on shear creep resistance of natural- rubber based pressure sensitive adhesive. The system holding time decreased as the tackification rise for the miscible natural rubber based pressure sensitive adhesive. This is due to a decrease in plateau modulus.

2.3.5 Degree of Crosslinking.

Crosslinks involves the process of chemically joining polymer chains by covalent bonding. This limits the sliding of polymer molecules, thus making the pressure sensitive adhesive, on application tougher, less flexible. Crosslinking helps to imbue high cohesive strength in a polymer, make it more chemical resistance. In addition it raises the melting point of the adhesive and promotes its adhesion ability. Benedek, (2004), stated that crosslink follows a post-modification of the elastic network vital to regulate the adhesive-cohesive balance in a pressure sensitive adhesive. Crosslinking can be done through a classic polymerization technology or a radiation-induced reaction.

2.3.6 Surface Properties.

Substrate surface properties are vital in the determination of adhesion. The adhesive viscoelastic properties and surface morphology affects the adhesion at interface. Sun, et al, (2012) explained that for softer adhesives an enhanced adhesion is observable on rough surfaces, comparative to debonding energy applicable on smooth surfaces. The rise in debonding energy is list with regards to materials with high stiffness or high surface roughness value. Cavity growth mechanisms on both lateral and omnidirectional are influenced by surface roughness.

2.3.7 Selection of monomers.

Monomers built up to comonomers which lay the foundation for polymer formation. The comonomers affect the physical characteristics of the final pressure sensitive adhesive. Benedek, (2004), stated that the synthesis of the main polymer affect the chemical composition of adhesive through a process of built in-reactivity subject to a later activation. Thus monomer such as t-butyl styrene improves tack, methyacrylate hardens adhesives, octyl vinyl ether softens adhesives and acrylonitrile influences the hardness and solvent resistance. The incorporations of functional groups, through crosslinking on polymers impact on its chemical reactivity. This affects the adhesive film thermoplasticity and raises its tensile properties. Acrylic acid component, in acrylic copolymer according to (Benedek, 2004) increases adhesion and adhesion copolymers hysteresis. Furthermore the acrylic acid incorporation in acrylic copolymers slows the rate of crack propagation Monomers like biocides, antioxidant increases removability and flame resistance. According to Zbigniew, et al, (2012), in the report of the “Influence of residue monomers on selected properties of acrylic pressure sensitive adhesive”. Free monomers content of solvent-based acrylic pressure sensitive adhesives decreased the

mechanical properties of self-coated adhesive film. These properties include tack, peel adhesion, shear strength, and shrinkage.

2.3.8 Nature of Substrates.

Peel adhesion is influenced by the nature of substrate. Benedek, (2004), held that this condition affect the removability of the pressure sensitive adhesive label. The flexibility of a substrate, elasticity/ plasticity balance, and adhesive anchorage on the substrate surface impact on pressure sensitive adhesive removability. The capacity of substrate surface to exhibit deformation affects the distribution of stress across the bond. Adhesive and substrate interface sets the adhesive into tensional and compressive force. The stiffness of the adhesives/ substrate and the thickness of the system affect the tensile strength of the adhesive. Whan-Tong and Wen-Hua, (1995) in a study on interfacial adhesion of poly (vinyl fluoride) with substrate in a multilayer structure held as follows: peel force of PVDF film/ substrate joint depends on many factors such peel rate, substrate pretreatment. Others are film thickness, concentration of coupling agent on the substrate. The substrate pre-treatment and the treatment time of the coupling agent impact on the elasticity/ plasticity balance, thus the substrate flexibility. The film thickness, and peel rate influence the adhesive anchorage and removability.

2.3.9 Relaxation Phenomena.

Relaxation phenomena are dependent on stress- softening. Stress softening in pressure sensitive adhesive is a network of mechanisms which affect the structural properties of a polymer. It also affects the interaction of the polymer (adhesive). It impacts on the re-adhering of pressure sensitive adhesives, Bendek, (2004) stated that it influence the compressive-yield-shear stresses at adhesion interface between adhesive and substrate. The peel force

and peel rate in adhesive/substrate interaction depend on frequency of bonding and accompanying debond. This places a sort of memory effect on the adhesive which is needed at re-adhering adhesive on substrate such as in masking tapes. The mechanism properties of pressure sensitive adhesive are influenced from the point of balance between elastic and viscous properties. Applying the relaxation phenomenon affect fibrillation, while the cohesive strength of the fibrils increase with chain relaxation. Bendek, (2004) showed that area of contact of an elastic film on a rough surface is influenced by the relaxation properties of the pressure sensitive adhesive.

2.3.10 Mechanical Resistance

The mechanical resistance of a pressure adhesive refers to its ability to resist sudden applied load. This resistance makes the adhesive capable of absorbing energy at plastic deformation. The ability of an adhesive to react to the rheological and viscoelastic changes refers to its mechanical resistance or impact strength. The impact strength is determined by the modulus of elasticity E, tensile strength and the elasticity of the adhesive.

2.4 Role of Thermodynamic Work of Adhesion in Bonding.

The thermodynamic work of adhesion is the bonding energy existing at the interface. The interface with regards to this research refers to the bonding between aluminum plate (bearing the emergency signs), the various substrate surfaces, and the different pressure sensitive adhesives. Qi, (2000) described adhesion as a process through which two materials in contact form a region of adhesive bond that sustains and transmits stresses.

The bond formation at the interface is characterized by material exchange at both macro and molecular interactions. The result of which is the formation of a bond particularly when an adhesive is used to join the bond. The energy at

this bond is governed by the Vander Waals bond, inter-diffusion of polymer chain and chemical bond at the interface.

2.4.1. Interaction between the Surface Free Energy and Thermodynamic Work of Adhesion.

Surface free energy is the amount of energy needed to generate a thermodynamically reversible unit area across a surface. The energy present at the interface of two substrates is called the interfacial energy. A synthesis of the interaction energy and the surface free energy generates the thermodynamic work of adhesion, which varies according to materials propagation. The thermodynamic work of adhesion for two dissimilar surfaces is given as follows:

$$W_{adh} = \gamma_1 + \gamma_2 - \gamma_{12} \quad (2.41)$$

Where γ_1 represents the surface free energy of surface 1

γ_2 represents the surface free energy of surface 2

γ_{12} represents the interfacial energy between surface 1 and 2.

W_{adh} represents the thermodynamic work of adhesion

Conditions for the thermodynamic work of adhesion between two similar surfaces reverses the trend to thermodynamic work of cohesion. The interaction at the interface is given as follows;

$$W_{coh} = 2\gamma \quad (2.42)$$

Where γ represents the surface energy of the surface involved

Good – Van Oss Chaundry theory stipulates an acid- base theory for analyzing the surface free energy of materials. This involves the division of the surface free energy into three components namely;

Lifshitz- Van der Waals represented as γ^{LW}

Monopolar acid represented as γ^{+}

Monopolar basic represented as γ^{-},

Thus the surface free energy of the given material is as follows,

$$\gamma = \gamma^{LW} + 2\sqrt{\gamma^{+}\gamma^{-}} \quad (2.43)$$

Using Good-van Oss Chaundry principles the adhesion between two surfaces are sustained across interface. More so, debonding across interface can be through the adhesive bulk or along the interface. According to Howson, (2011) in "Relationship between Surface Free Energy and Total Work of Fracture of Asphalt binder and Asphalt binder-Aggregate interface"; there are two possible location for crack initiation. They are through the asphalt binder or along interface between the asphalt binder and aggregate. Thus for this research works there are two possible point of debond namely:

1 Within the pressure sensitive adhesive bulk used.
2 The interfaces between the aluminum (emergency sign) and the adhesive or between the adhesives and the substrate surface. The energy need to initiate a debond through the pressure sensitive adhesive bulk called the cohesive bond energy or work of cohesion. This is stipulated as follows

$$\Delta G_{coh} = 2\gamma = 2\left(\gamma^{LW} + 2\sqrt{\gamma^{1}\gamma^{-1}}\right) \quad (2.44)$$

Where ΔG represents the cohesive bond energy

The energy needed to initiate a debond at the interface between the aluminum plate (emergency signs) and the pressure sensitive adhesives is called the adhesive bond energy. The adhesive bond energy is applicable to the interface between the various substrate surfaces and the different pressure sensitive adhesives used. The interaction at the interface is as follows:

$$\Delta G_{adh} = 2\sqrt{\gamma_1^{LW}\gamma_2^{LW}} + \sqrt{\gamma_1^{+}\gamma_2^{-}} + \sqrt{\gamma_1^{-}\gamma_2^{+}} \quad (2.45)$$

Where ΔG_{adh} represents the adhesive bond energy

γ_1 represents the surface free energy of the pressure sensitive adhesive

γ_2 represents the surface free energy of the aluminum plate or the various substrates surfaces

Howson, (2011) demonstrated that the amount of energy required for water to displace asphalt binder from an aggregate is as follows:

$$\Delta G_{123}^{a} = \gamma_{13} + \gamma_{23} - \gamma_{12} \quad (2.46)$$

Comparatively, the amount of energy needed to initiate a debond at the interface between aluminum (emergency sign), the various pressures sensitives, and the different substrates surfaces is similar to Equation 2.46. Thus it is written as follows:

$$\Delta G_{123b}^{b} = \gamma_{13} + \gamma_{23} - \gamma_{12} \quad (2.47)$$

Here 3 component are involved, aluminum (emergency sign), pressure sensitive adhesives, substrate. Furthermore, the bonding component are represented as follows:

γ_1 represents the surface energy of the aluminum

γ_2 represents the surface free energy of each substrate surface

γ_3 represents the surface free energy of each pressure sensitive adhesive

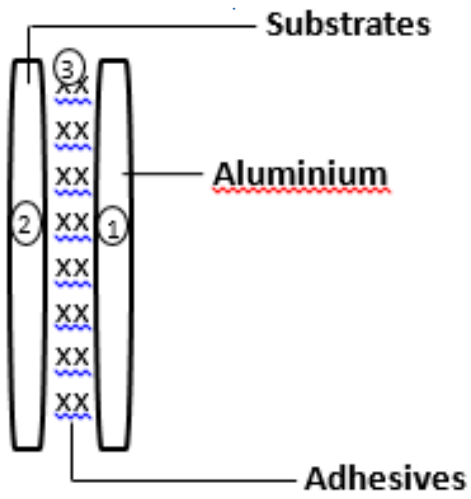

Figure2.3 Bonding Components at Interface Boundary

Equation 2.47 shows the various components at the bond interface, and the interfacial energies present. The interfacial energies present are as follows:

γ_{13} represents the interfacial energy between aluminum plate and pressure sensitive adhesives.

γ_{12} represents the interfacial energy between aluminum plate and the substrate surfaces

γ_{23} represents the interfacial energy between the various substrate surface and the various pressure sensitive adhesives

The interfacial energy between two materials can be calculated by the use of Good-van Oss Chaundry principle. It is represented as follows:

$$\gamma_{ij} = \gamma_i + \gamma_j - 2\sqrt{\gamma_i^{LW}\gamma_j^{LW}} - \sqrt{\gamma_i^{+}\gamma_j^{-}} - \sqrt{\gamma_i^{-}\gamma_j^{+}} \qquad (2.48)$$

The thermodynamic work of adhesion is based on fundamental material properties, as such is independent of external experimental factors (Howson, 2011). This means that intrinsic material characteristics determine the thermodynamic work of adhesion. Characteristics such as surface energy, contact angles, interaction energies are peculiar to particular material. During the interactions between two materials, the thermodynamic work of adhesion describes the tack energy across the parallel surfaces. However the surface

energy of a substrate can be derived from the contact angles. The thermodynamic work of adhesion between the substrate and the liquid (contact angles) is derived as follows:

$$W_{adh} = \gamma_{lv}(1 + \cos\theta) \quad (2.48)$$

2.4.2 Role of Intrinsic forces in Interfacial adhesion.

Phattanarudee, (1998) prescribed some conditions for good bonding or adhesion to proceed at an interface. There are as follows:

- Adhesive must maintain flow-ability to provide room for molecular contact across the material interface. This will establish intrinsic adhesion forces between substrates and adhesives.
- Adhesive must harden to enable it transmit stress and withstand strain at interface
- Adhesive must possess capacity for plastic deformation, to dissipate energy at interfacial crack tip.

The intrinsic force at interfacial adhesion is expressed through the surface free energies of the substrate and adhesive.

Fowkes, (1964) demonstrated that the surface free energy of a material is a sum total of the surface free energies of the components of the material. This is as follows:

$$\gamma = \gamma^d + \gamma^i + \gamma^p + \gamma^h \quad (2.49)$$

Where d represents the London dispersion interaction

P represents the Keeson dipole- dipole interaction

I represents the Debye dipole interaction

Furthermore these components can be categorized into 2 components, γ^d and γ^p where d exponent symbolizes the London dispersion interaction and p is the polar interaction.

Drupe equation relates the surface free energy to the thermodynamic work of adhesion. (Similar to equation 2.41). This is as follow:

$$W_{12} = -\Delta G_{12}^{a} = \gamma_1 + \gamma_2 - \gamma_{12} \quad (2.50)$$

Where W_{12}represents the thermodynamic work of adhesion

ΔG_{12}^{a}represents the Helmholtz free energy per unit area

$\gamma_1$andγ_2 represent the surface free energies of substrate 1 and 2

γ_{12} represents the interfacial surface free energy

The free energy of adhesion per unit area between two phases in a non- polar system is represented as a geometric mean of their surface free energies of each phase. Thus the interaction is represented as follows;

$$-\Delta G_{12}^{a} = 2(\gamma_1 \gamma_2)^{1/2} \quad (2.51)$$

Where Wa is the work of adhesion.

The work of adhesion for each component of the two phases are represented as follows:

$$W_a = W_a^d + W_a^i + W_a^p + W_a^h + \cdots \quad (2.52)$$

Where d is the London dispersion interaction

p is the Keesom dipole- dipole interaction

i is the Debye dipole interaction

h is the Hydrogen bonding

According to Fowkes, the work of adhesion is a geometric mean of the dispersion components of the work of adhesion. The result is as follows;

$$W_a^d = 2\left(\gamma_1^d \gamma_2^d\right)^{1/2} \quad (2.53)$$

Phathanarudee, (1998) demonstrated that the thermodynamic work of adhesion can predict the adhesion strength across interfaces in both inert atmosphere and wet environment. The study showed moisture effect on lead frame / adhesive interfaces for integrated circuit semi-conductor devices. The

moisture effect predicted the decrease in adhesion strength at interfaces, while dry samples maintained higher adhesion strength. Invariably lower thermodynamic work of adhesion suggests low adhesion strength, while the higher thermodynamic work of adhesion suggests higher adhesion strength.

2.5 Fracture Energy in Adhesion.

Fracture energy is a measure of practical adhesion. It is linked to chemical and mechanical interactions across bond interface. The estimate of the interactions by the chemical and mechanical constituents at the interface is measured by a destructive mechanical test. Such tests include peel test, pull-off test hemispherical probe tack test, and micro-indentation.

Fuentes, et al (2015), found out that micro mechanical test measure both surface interactions and inter dependence in interface. The researchers found out that in analyzing the mechanical behavior and practical adhesion at a bamboo composite the following happens:

- The adhesion strength is the work needed to separate the matrix from the fibre under loading perpendicular to fibre surface,
- There is a load transfer between the fibre and matrix which is affected by local stress and matrix residual stresses.

The practical fracture toughness (fracture energy) of an adhesive bond is usually quantified as critical strain energy release rate Gc (Qi, 2000). The fracture energy depends on the thermodynamic work of adhesion, fracture mechanics and rheology. Fracture energy measures the energy differential between adhesive bond, surface energy and the total of the surface energies generated by newly formed surfaces in a debond. Fracture energy measures the Griffith energy criterion of fracture.

Al- Quadi, et al, (2008), illustrates that the Griffith criterion is an axiom of the principle of energy balance. This is because cracks propagate if the energy

available is higher by quantification or equivalent to energy needed to increase the crack by a unit surface area. The Griffith criterion prescribes that stored energy in the bond must be quantifiable to initiate an increase in crack surface area.

Elastic material which evolves into new surfaces, have a fracture energy which is equivalent to the critical strain energy. The process leading to this position is represented as follows:

$$G_C = 2\gamma \tag{2.54}$$

Where G_C is Griffith Critical strain energy release rate.

When Griffith criterion is applied to a purely elastic material, the crack propagation under this condition is represent as follows:

$$G_C = \gamma_1 + \gamma_2 - \gamma_{12} \tag{2.55}$$

Where γ_1 and γ_2 represent the surface free energy of the two materials

γ_{12} represent the surface free energy at the interface.

Howson, (2011) showed that a plane stress condition representing an infinitely long sheet with an elliptical crack has a length of 2c, and has a diminished minor axis. The crack propagation along the plane proceeds in a direction perpendicular to the applied load. The stress applied in the material is represented as follows:

$$\sigma \leq \sigma_C = \left[\frac{2E\gamma}{\pi c}\right]^{1/2} \tag{2.56}$$

Where σ_C is the Critical stress, at which the crack between unstable.

E is the Young modulus of the material

γ Is the Surface free energy of the material.

Griffith demonstrated that the theoretical tensile strength computed based on the adhesive surface free energy is 10 times more than the measured tensile strength of the adhesive. This development is adduced to presence of

flaws sites on the material surface. This stress sites consists of high stress agglomeration.

Considering the effect of fracture energy in inelastic material, there is an irreversible energy dissipation. This dissipation leads to the condition where the fracture energy is extremely greater than the thermodynamic work of adhesion. The plastic energy dissipation during debond is traceable to cohesive fracture within the adhesive. This leads to the modification of the Griffith Criterion to the followings:

$$\mathrm{Gc} = 2\gamma + W_{PL} \quad (2.57)$$

Where W_{PL} represents the plastic deformation energy.

Irwing theory substitutes equation (2.57) into equation (2.56). This is to accommodate crack and geometry for the adhesive. This results into the following;

$$\sigma \leq \sigma_C = \frac{1}{\alpha}\left[\frac{E(2\gamma + W_{PL})}{\pi c}\right]^{1/2} \quad (2.58)$$

Fracture energy depends on external factors. The factors include loading, sample geometry, loading rate for time dependent material, adhesive thickness.

Considering the concept of fracture energy in an adhesive/ substrate interface, the effects of crack and crevices on material surface need be examined. The fracture phenomenon is examined through two processes, namely; (1) Stress analysis (2) Energy analysis. Shao-Yun, et al, (2008), state that the stress intensity process of fracture mechanics analysis describes the fracture energy (fracture toughness) as K_c. This value K_c relates the crack size to fracture strength. The energy analysis process utilizes the critical energy release rate G_c. The value G_c is the work dissipation needed to induce a crack of unit area. Furthermore, the researchers showed that the stress analysis value K_c and the energy analysis value G_c are related when applied to particle-

filled composites. The application of these values on the particles filled composites is prevalent under the condition of heterogeneities among the particles of the composites. These conditions connect the two values K_c and G_c as follows for the particle filled composites.

$$G_c = \frac{K_{2c}}{E_c} \quad (2.59)$$

Where E_c is the effective composite modulus.

The macroscopic measurement for the fracture energy through G_c and K_c shows that particle size, interfacial adhesion, particle loading affects it.

2.5.1. Impact of wetting and deformation on Fracture Energy.

Fracture energy occurs at the point of maximal interfacial contact between an adhesive and substrate surface. Fracture energy is dependent on viscoelastic energy, dissipation energy and complies with the temperature rate super position principle (Howson, 2011).

The capacity of an adhesive to withstand shear deformation decreases with an increase in adhesive spread. This leads to formation of stronger bond as contact time and pressure increases. Furthermore the fracture energy capacity remains constant at this point as more deformation of the adhesive does not affect it.

Wetting of a substrate by a pressure sensitive adhesive is a function of difference in the surface energies of both materials. The substrate here which allows wetting of its surface exhibits higher surface energy than the pressure sensitive adhesive applied. Contrarily dewetting occurs if the pressure sensitive adhesives have a higher surface free energy than the substrate surface. The tack of the adhesive is favored by an even wetting of the surface with regards to the Dalhiquist Criterion.

The ability of any of the pressure sensitive adhesives used in this study to wet the surface of each substrate adequately will determine it adhere ability. The pressure sensitive adhesives, each when applied to the surface and wet each surface according to the value of its surface free energy. The wetting and adherence reaches a maximum where it attains maximum interfacial contact. During the period of maximal interfacial contact, increase in applied pressure or contact time between substrate/adherent proves invalid. This is the point where maximal force is required to induce a stress/ stain that facilitate the formation of a fracture across the bond interface. The energy expounded to induce this practical deformation between the aluminum plate (emergency sign)/ adhesive/ substrate bond is the fracture energy. Inducing the debonding goes with deformation in the viscoelastic quality of the bond, generation of a dissipation energy. Fracture energy is measured in J/m^2 while thermodynamic work of adhesion is measured in mJ/m^2

2.5.2 Relationship between the Thermodynamic Work of Adhesive and Fracture Energy.

The thermodynamic work of adhesive is related to the fracture energy as follows;

$$W_T = W_a(1 + \emptyset) \quad (2.60)$$

Where W_T represents the total work of adhesion or the fracture energy

W_a represents the thermodynamic work of adhesion

$\emptyset$represents the dissipation factor

However, (Gent and Schultz, 1972) posit that the fracture energy and the thermodynamic work of adhesion are related as follows;

$$G_C = W_{adh}[1 + \emptyset(v, T)] \quad (2.61)$$

$G_C$represents the fracture energy

W_{adh} represents the thermodynamic work of adhesion

Øepresents the viscoelastic energy dissipation factor

v represents debonding rate

T represents the testing temperature

2.5.3 Measurement of Fracture Energy.

Fuentes, et al(2015) demonstrated the use of micromechanical experiments to measure practical adhesion. This micromechanical test view purely physical and chemical interaction at the interface. The interface involved consists of a bamboo and optical glass held in a composite matrix. The exact micromechanical test used was a pull out test, to evaluate the shear stress (τ_d) and ultimate stress (σ_{ult}) as point of crack interaction at the interface.

The results obtained showed that both shear stress and ultimate stress when independently analyzed for either glass fibre or bamboo remained in agreement with W_{adh}.

W_{adh} represents the thermodynamic work of adhesion. However when bamboo and glass systems are compared, both the shear stress and ultimate stress showed poor performance for bamboo composite. Meanwhile bamboo showed a higher thermodynamic work of adhesion than glass, while maintaining a lower shear stress if compared to glass system. Friction also played a role in the pull out test. Results showed that friction played a major role in a bamboo fibre system, where debond occurs at relatively low force, while friction keeps rising. This mean that the ultimate stress value obtained for bamboo is higher than glass. Evidently, fracture energy value and performance is influenced by the role of the shear stress acting on the interface; while friction across interface affects the ultimate stress.

Peel test uses a measured force value to separate two surfaces and evaluate the energy dissipation between the bond surfaces. It depends on variables such as peeling speed, peeling angle, peel thickness, and adhesive thickness.

The model of a peel process which contains a damage criterion shows the material properties of the entire peel arm. The damage criterion represents the mode of fracture. The mode of fracture might be cohesive failure or adhesive failure.

Examples of failure criterion include: Cohesion Zone Mode, Virtual Crack Closure, peel test is conducted with the aid of single peeling speed and thick metal peel arm (Mohammed, et al,2016).

Du, et al, (2004) demonstrated peel test using rubber based pressure sensitive adhesives, which the researcher modeled through the Finite Element (FE) software, Abaqus. Abaqus Version 6.13 HabbittKarlsson and Soresen, alongside an elastic energy- density failure criterion was used to describe the interfacial bebond. The result showed that numerical and experimental values gave the same shape for the force- speed master curve. However, the predicted peel force was lower than the measured value as the rate of peel increased. The difference was attributed to small strain characterization of rheological data.

Probe Tack test was used to monitor the mechanical response of a polyester backing membrane, (Mohammed et al, 2016), and a pressure sensitive adhesive. The test utilized the rate- dependent cohesive parameters (Fracture Energy and Maximum Stress) to arrive at numerical and experimental value for the Cohesive Zone Model and Finite Element Analysis. The results indicated that for a relatively thin pressure sensitive adhesive film, rate dependency observed for the probe tack test was due to rate dependency of the cohesive zone model properties. This is contrary to the expectation of the

effect of strain rate on the deformation of the adhesive bulk with regards to the cohesive zone model properties.

2.6 Mechanismof Debondingbetween Dissimilar Surfaces.

Joining the aluminum plate (emergency signs) to the substrates (different walls) with the aid of pressure sensitive adhesive is a quasi-probe tack experiment. Here the substrate deposited with the pressure sensitive adhesive film takes the role of the rigid planar. The aluminum plate takes the role of the probe which is brought to stick with the substrate under little applied pressure, contact time, and recorded traction. However, the inability of some of the signs to stick to the substrate and eventual fall off is similar to debond. Thus to study the role of debond in adhesion, factors affecting it, relative to interfacial parameters need be examined.

Debonding can be described as joint failure at an interface between adhesive and applied surface resulting in failure, energy dissipation and bond degradation. It is a process which permits use of linear viscoelasticity, large strain behavior, molecular rheological properties to explain rupture of adhesion between adhesive and substrate.

Deplace, et al, (2009), describeddebond as condition when the shear resistance of an adhesive bulk exceeds the adhesive strength at the substrate. This leads to degrade of joint mechanical durability. Geiss and Vogts, (2007) stated that such degradation results from a combination of moisture rate and mechanical stress. During debond applied energy extends fibrillation, (Connor and Willenbacher, 2004), till it exceeds adhesion between adherent and pressure sensitive adhesive. The result is an adhesive fracture or separation of the adhesive from the probe. Debond is a morphological change leading to failure in cohesion strength of an adhesive (Patil, et al, 2012). This results in bulk failure, and decrease in energy dissipation. Furthermore, it lowers the

work of adhesion. Later it is followed by fingering, cavitation, fibrillation both in the elastic and viscoelastic adhesion. According to (Zbigniew, et al, 2013), debond is in influenced by degree of cross link in the pressure sensitive adhesive.

2.6.1. Failure Mechanism in Debond

Failure in adhesion occurs in the bulk of the pressure sensitive adhesive, adhesive - substrate interface and as a mix of both failures.

The points of failure in an adhesive bond are as follows;

- Substrates
- Adhesives
- Interface.

The observable fracture modes at the failure points are as follows;

1. Substrate Fracture: This occurs at the substrate due to its inability to withstand applied load, chemical or acid attack. It can be the result of an adhesive bond which has a lower strength than the substrate resistance.
2. Adhesive Fracture: This occurs at interface between adhesive and substrate. It exhibits a complete or partial demerge from substrate surface. Adhesion failure takes place in either one or on both surfaces. This is as a result of the listed factors;
    - Improper surface preparation before administration of adhesive.
    - Poor wetting of the substrate by the pressure sensitive adhesive.
    - Use of improper adhesive which does not generate adhesion on substrate surface.
    - Poor or inadequate thickness of the applied adhesive.
    - Ageing phenomenon between and substrate.

3. Cohesive Fracture: This occurs at adhesive bulk, and accompanied by traces of adhesive on both surface of the substrates. This is as a result of the listed factors;
    - When the theoretical tensile strength of the adhesive is equivalent to the real breaking stress of the adhesive.
    - When the applied load on the bond is greater than the adhesive bond design limit
    - Pressure of bubbles and pores.
    - Ageing of the adhesive bonding.
    - Inability to adhere to adhesive curing times.
4. Interface Fracture: This occurs as a result of specific problem such as hydrolysis at the interface. Interface fracture can be the result of polymers phase separation or crack depth misalignment. Crack depth misalignment takes place when crack occurs at a region very slightly below the interface. Cross linking of polymer in excess, leads to a situation where the polymer becomes tightly attached to the substrate. The polymer lacks the ability to remain integrated in the polymer network. Debonding is characterized by cavitation, crack propagation, fibrillation, fingering, nucleation etc.

2.6.2 Evaluation of Adhesive Performance.

The performance of a pressure sensitive adhesive is derived from the graphical relation between the force-displacement curve. The evaluation curve enumerates:

1) The maximal nominal stress

2) The maximal strain

3) The adhesion energy.

Furthermore these parameters adjudged on a stress- strain probe tack curve defines the adhesion energy as the area under the graph (stress-strain)

(Deplace, et al, 2009). There are four principal types of Stress- Stain curve with regards to polymers.

They are represented as follows

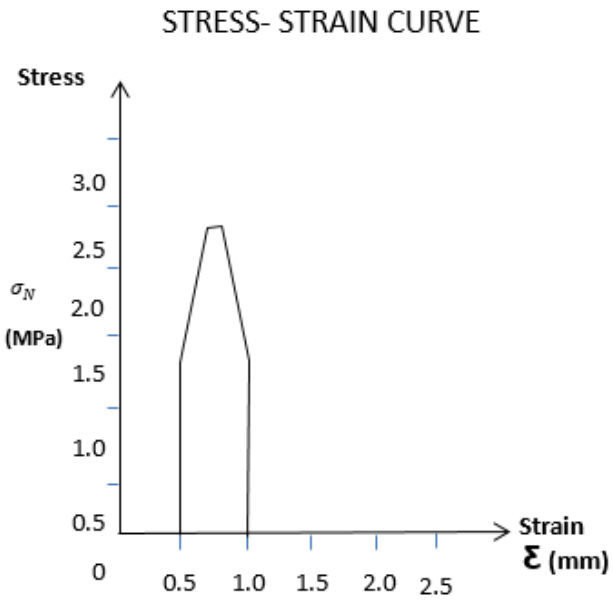

Figure. 2.4a Brittle Failure.

Figure 2.4a shows a brittle fracture. It is characterized by a sharp maximum and accompanied by low strain. There is a very small area under the stress-strain curve representing the adhesion energy.

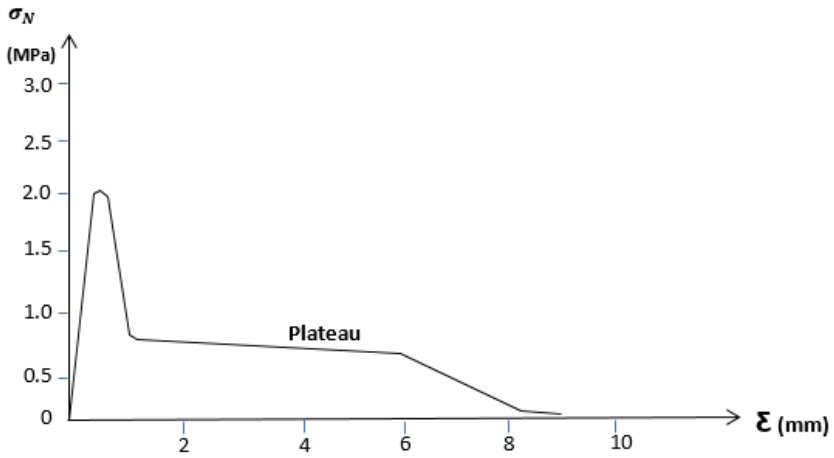

Figure2.4b Adhesive Debond.

Figure 2.4b shows a stress-strain curve depicted by a maximum stress and pronounced shoulder. And later the stress drops to zero. This graph shows typical case of adhesive debond. Here the detachment occurs at interface between the probe (aluminum plate) and the adhesive layer. The result is a non- residue at the probe after test.

STRESS- STRAIN CURVE

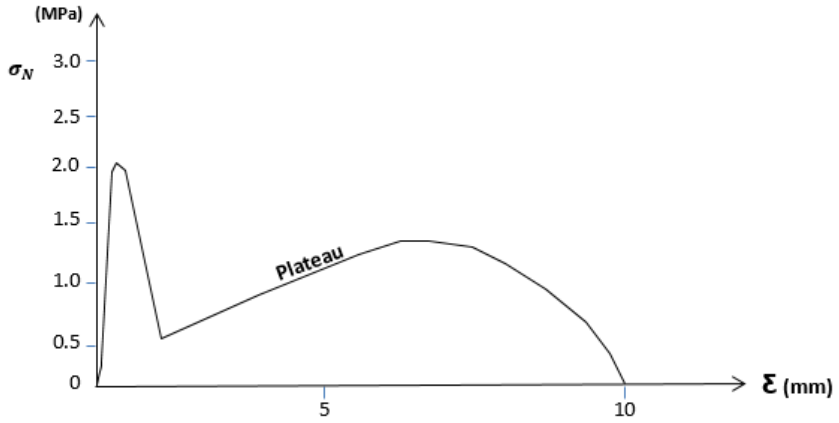

Figure2.4c Adhesive Debond With Strain Hardening.

Figure 2.4c shoes a stress- strain curve which occurs when the adhesive undergoes strain hardening just before final detachment. This process undergoes slightly higher stress as well as a second peak.

STRESS- STRAIN CURVE

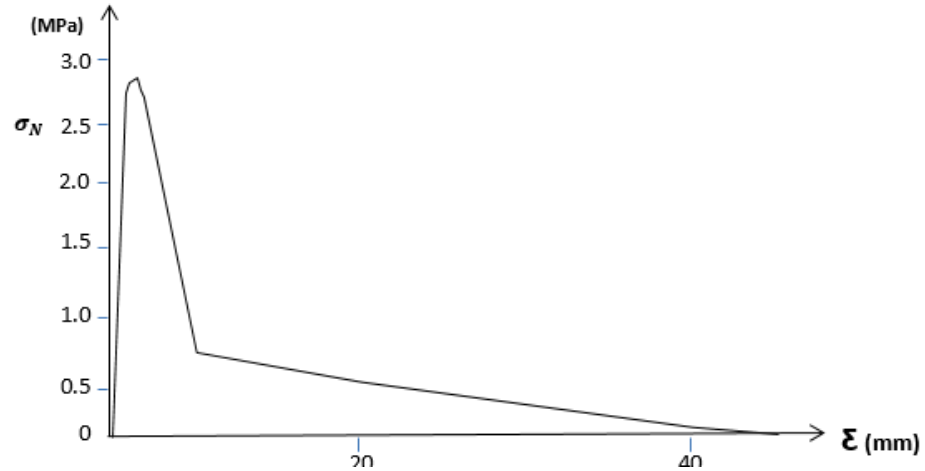

Figure 2.4d Cohesive Debond.

Figure 2.4d shows a stress-strain curve which occurs when the adhesive is highly viscous. The adhesive joint breaks by cohesive fracture within the adhesive. This leads to debond, accompanied by a viscous flow. Cohesive debonding shows residue of the adhesive left on the probe at the end of the traction.

2.6.3 Mechanism of Crack Propagation and Cavitation

Crack propagation and cavitation are usual phenomenon experienced by adhesive films undergoing traction. Crack propagation between an adhesive and substrate is influenced by applied stress, elastic modulus, separation energy and atmospheric pressure. Cavitation is a reflection of elastic resistance of an adhesive to bubble growth.

Cavitation and cracks appear as a result of failure. Thus this study shall use the force curve to interpret both cohesive and adhesive failures. Teisseire, et al, (2006) demonstrated that plateau region is a common phenomenon in both crack propagation and cavitation. Plateau existence for cavitation in the adhesive bulk is a result of very low pressure inside the bubbles and the atmospheric pressure outside the bulk. The drop in force plateau was interpreted as the penetration of air into the cavities. Cracks do not have any appreciable amount of gas and the adhesive bulk shields the interior from air. However, Figure 2.5 shows a description of debond along an adhesive/ substrate interface.

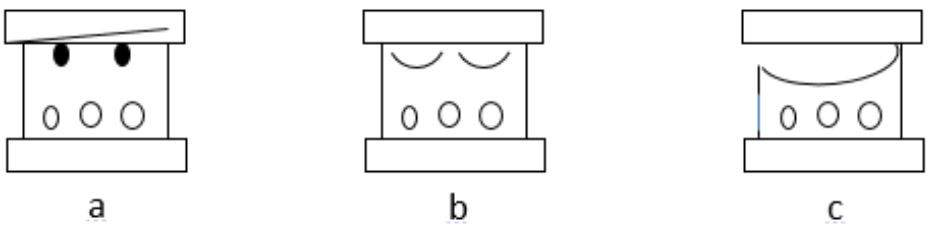

Figure2.5Stages of Debonding.

Figure 2.5a.shows the appearance of small cavities with small air bubbles within the adhesive bulk.

Figure 2.5b shows the emergence of small interfacial cracks

Figure 2.5c shows the quick propagation of cracks and merging of adjacent cracks. Here the tensile stress around the cavities relaxes and shrinks back.

During debond there is a drop in the plateau which signifies the break in the pressure difference at the interface. The cavity is formed by the breaks, while the force applied drops. The force drop affects the traction velocity, leading to a rise in traction velocity. The traction velocity affects the plateau length and determines the failure at the adhesive/substrate interface. Adhesive failure occurs at region of crack propagation while cohesive failure is observed in region of cavity. Teisseire, et al (2009) observed that the increase in traction velocity for a highly viscous G20m silicone oil resulted in crack propagation beyond fingering and cavitation. This infers a cohesive failure which gradually evolved into a purely adhesive failure as the velocity of traction rises. Thus there is a drop in the plateau length, showing cavitation before crack propagation. This is peculiar to debonding mechanism.

2.6.4 Predictionof Debonding Mechanism from Linear Rheological Properties

Debonding is a complex microscopic deformation mechanism. Deplace, et al, (2009), observed that it consists of interfacial failure, cavitation, and fibrillation. Interfacial failure is the process of crack propagation, while cavitation involves bulk fingering, and fibrillation evolves with serve deformation in the adhesive. The linear viscoelastic properties of pressure sensitive adhesive are certified by two major conditions namely; Dahlquist Criterion and Growth of a defect at interface. The Dahlqist criterion requires that each pressure sensitive adhesive must exhibit a shear modulus of 0.IMPa

at bonding frequency, and within contact time. This basic requirement from the pressure sensitive adhesive, alongside the interaction of the bulk and material interface properties determine the debonding process. The growth of a defect at a bond interface is controlled by interfacial crack growth and bulk deformation. The interfacial crack growth is determined by the critical energy-release rate (G_c). The bulk deformation is derived by the average stress within the layer, which depends on the adhesive elastic modulus (E). Thus an analytical comparism between the linear elastic fracture mechanics and cavitation describes the growth of a defect at adhesion interface. Weber, et al, (2003) demonstrated that the ratio of the critical energy-release rate to the elastic modulus of an adhesive (G_c/E) can be used to predict debonding. However, Deplace et al, (2009) showed that the ratio needs be compared to two nomenclature namely: the thickness of the adhesive (h) and the size (r) of a defect. Thus the theory holds that when G_c/E is less than r, interfacial crack propagation manifest. When ratio G_c/E is larger than h, the result is a non-linear deformation in the bulk, followed by fibrillation. This relationship between the critical release energy rate and elastic modulus along interface is represented in figure 2.6

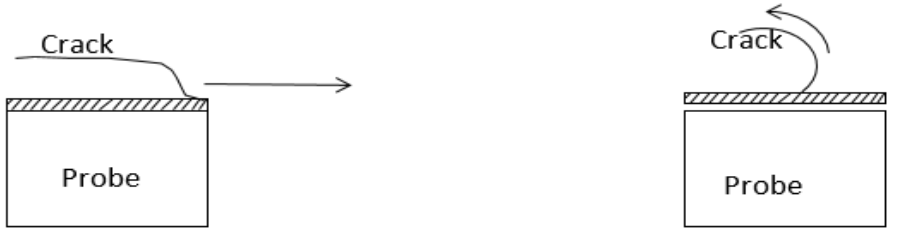

(a) Crack propagation (b) Crack blunting

Figure 2.6 crack propagation and crack blunting at adhesive/probe interface

Figure 2.6a shows a low value for G_c/E which portends crack propagation but controlled by G_c.

Figure 2.6b shows a high value for G_c/E which portends bulk debonding but limited by E

Figure 2.6 shows an assumption of a linear elastic adhesive layer with dissipative properties confined to the region of crack propagation. This relationship when considered for a rubbery material (adhesive) and solid surface G_c is represented as follows:

$$G_c = G_o(1 + \emptyset\,(a_T v) \qquad (2.63)$$

Where G represents the restraint to the crack propagation at low crack velocity.

$\emptyset\,(a_T v)$represents the dissipative factor for adhesive.

When Equation 2.63 is considered along Van der Waals force particularly in elastomers, the results is as follows:

$$\emptyset\,(a_T v) = k tan\, \mathcal{S}\,(w) \qquad (2.64)$$

Where K is an experimental constant.

According to Sauliner, et al, (2004) for adhesion of a linear viscoelastic material on solid; the Young modulus E replaces the frequency dependent shear elastic modulus. Then equation (2.64) transforms as follows:

$$\frac{G_o}{E} \approx G_o \frac{(1+\emptyset\,(\alpha_T v)}{G'(w)} = G_o \frac{\left(I + k tan\ \mathcal{S}\,(w)\right)}{G'(w)} \approx k\, \frac{Gotan\ \mathcal{S}\,(w)}{G'\,(w)} \qquad (2.65)$$

2.6.5 Impact of Dissipative Properties of Pressure Sensitive Adhesive onDebonding.

Higher elastic modulus for pressure sensitive adhesives signifies more dissipation of energy, while low elastic modulus causes more elasticity. Deplace, et al (2009), demonstrated that latex based hard shell-soft core particles differ in their linear rheological properties. This is due to the effect of the glass transition temperature and chain transfer agent constituting the pressure sensitive adhesive. To this effect tack experiment were performed

on the material across polyethylene substrate and stainless steel substrate. The results showed that at variable debonding speeds, the fibrillation plateau across the stress-strain curve varies. At lower debonding speeds both samples of the adhesives HS4 (latex based hard shell-soft core particle 4) and HS5(latex based hard shell-soft core particle 5) had varied nominal strains, and fibrillation plateau. The analysis showed that frequency of oscillation of the various samples (measured against the Dahlquist criterion) causes variation in the bulk properties of the adhesive. This lead to differences in elastic modulus, variation in the values of $G_c/E(or\ {}^{tan\sigma}/_{G})$. As a result of these

varying viscoelastic properties two types of failure occurred at the interfaces of the samples and substrates. They are brittle failure for the HS5 characterized by a sharp decrease in stress after the initial peak at higher debonding velocity. HS4 exhibited a lower nominal strain at debond for both substrates indicating adhesive debond, for lower debonding velocity. Linear viscoelastic properties determine the hardness and adhere ability of the pressure sensitive adhesive. It does not influence the adhesive shear resistance since it primarily does not involve cohesive strength test. The dissipative properties are particularly examined in tack experiments. The hardening or softening of pressure sensitive adhesive on performance determines its softness/ hardness, thus the usage. Dissipative properties of pressure sensitive adhesive are similar to its viscoelastic properties. Yana, et al (2012), discussed the role of nature of substrate on the adhesive properties of acrylate copolymer. The research exhibited the dependency of debonding mechanism on polymer deformation, rate of cavitation, stress distribution at interface. Furthermore the study showed that polymer cross linking, glass transition, surface roughness determine the kind of failure occurring in a bond as well as its deformation at interface.

2.6.6 Prediction of Debonding Mechanism from Nonlinear Rheological Properties.

The formation of cavity is favored when the ratio of critical release energy is greater than the adhesive thickness. This process, leads to the eventual collapse of cavities into fibrils when the applied strain is extended. More so at higher application of strain across the bond the rate of cavitation competes with crack propagation. Fibrillation leads to thinning in the absence of strain hardening across the bond which leads to eventual cohesive failure, in the bulk. When the pressure sensitive adhesive is crosslinked, the fibrils store elastic energy on application of stress. The result of the collapse of the elastic energy stored by the fibrils as a result of crosslink is an adhesive failure. This point is marked by an immediate detachment of the fibrils from the probe when the fibrils elastic energy exceeds the adhesion energy. Thus higher elastic energy stored in fibrils, leads to the detachment. Higher adhesion energy is accompanied by maximal deformation of the fibrils (Deplace, et al, 2009), leading to fibril elongation and energy dissipation. The energy dissipation is caused by relaxation of polymer chain as a result of extension.

Figure 2.7 shows a non-linear behavior of an adhesive when subjected to a tensile experiment. It shows an observable softening at intermediate strain and strain hardening at large strain.

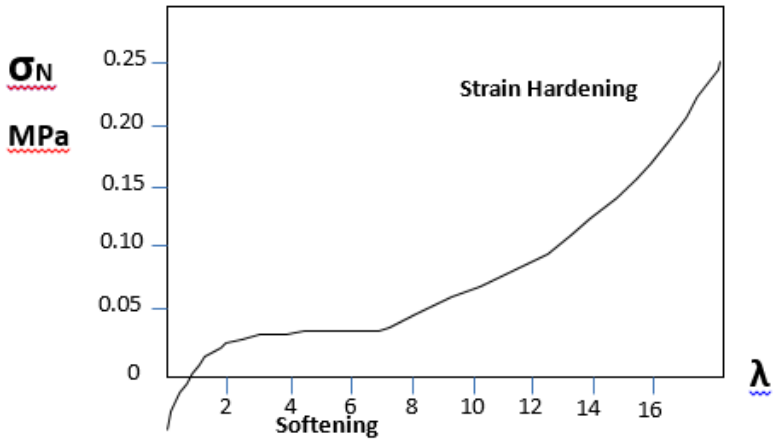

Figure 2.7: Non-linear behavior of a pressure sensitive adhesive.

2.6.7 Debonding Mechanism of Soft Adhesives

Soft adhesive refers to viscoelastic polymer layers applied between two or more rigid bodies to hold the together (Creton, 2003). Debonding between a soft adhesive and substrate depends on interfacial interactions and rheological properties of the adhesive. During debonding, the energy dissipated depends on applied contact pressure and contact time. However, the popular Dahlquist's criterion demands that a pressure sensitive adhesive maintains an elastic modulus of 0.1MPa at maximum at a frequency of 1Hertz. When the compressive force applied at the substrate/adhesive interface is withdrawn often one second contact it affects the stored elastic energy. During withdrawal of the compressive force, if the elastic energy of the adhesive at interface rise beyond the work of adhesion, spontaneous contact breakdown occurs, even at application of no force. Considering the macroscopic analysis of debond between the pressure sensitive adhesive and the two interfaces:

- aluminum (emergency sign) and pressure sensitive adhesives and
- substrates (ceramic wall tile, mild steel etc.) and pressure sensitive adhesives.

There is need to analyze the mechanism of debond across the interfaces as follows:Interface debond to bulk deformation, Interfacial crack propagation and Bulk deformation to fibrillation

1. Interfacial debond to bulk deformation: Considering the asperities existing across surfaces, there is bound to be pockets of voids between interfaces in contact. This leads to the formation of localized deformation (Creton and Ciccotti, 2016), points at the interface. The application, of tensile stress across the adhesive/substrate interface leads to crack propagation, cavitation and fibrillation. The zones of void forming localized deformation facilitates this transition from interfacial debond to bulk formation. When an external force is applied (probe force) to initiate a debond at the bond interface, the average nominal stress rises. This process when it reaches a particular critical value of local stress makes the trapped air pockets at the substrate/ adhesive interface expand in size, and the result is expressed in figure 2.8

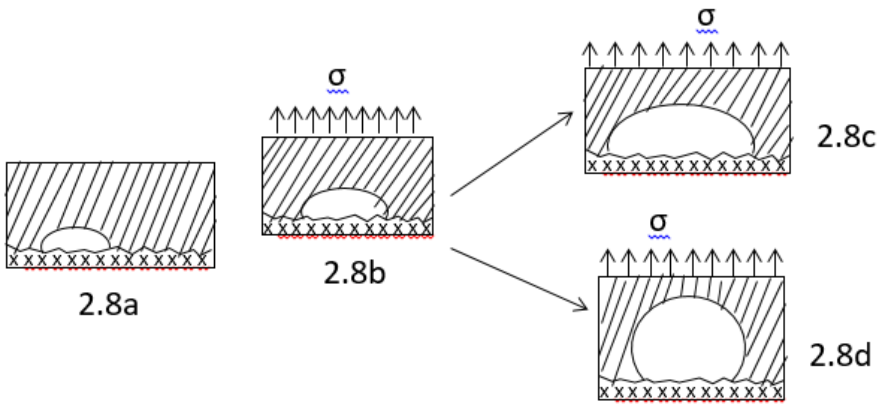

Figure 2.8 Early stage debond: Cavity growth from defect to hemisphere and macroscopic stress field rise to create nucleation of cavities along the surface.

Figure 2.8 displays two mechanism at the start of debond namely: Interfacial growth of cavities into crack and bulk mechanism with cavity growth in direction parallel to tensile. Yamaguchi, et al, (2007), compared debonding mechanism across 3 differently crosslinked acrylic pressure sensitive

adhesives. The result showed that less crosslinked adhesives formed nearly spherical cavities (Figure. 2.8d), while the more crosslinked adhesives formed disk like cracks (Figure. 2.8c). The disk like cracks for the high crosslinked acrylic never evolved into large growth in the bulk; it coalesce at low level deformation. The less crosslinked acrylic pressure sensitive adhesive forms a nucleated cavity which is marked at the interface. Meanwhile the change in mechanism can be adduced to changes in the surface morphology of the substrate. Interfacial propagation mechanism gives rise to an amalgamation of different cracks at the interface, while the bulk adhesive remains mainly underformed. The transition from interfacial debond to bulk deformation can be predicted by the relationship between the fracture energy, elastic modulus and the adhesive thickness. This relationship is writing as follows:

$$\frac{\Gamma}{Eh} = I \qquad (2.66)$$

Where Γ representthe fracture energy

Erepresents the elastic modulus.

$h$represents the adhesive thickness.

(a) interfacial crack propagation: The reversible separation between two surface is represented as follows:

$$\Gamma_o = w \qquad (2.67)$$

Where w represents the reversible work of adhesion.

Equation 2.67 shows the strength of the interaction at adhesive/substrate interface. However the fracture energy is higher than the work of adhesion due to extraction of interdiffused chains. Zhang, et al, (1995) demonstrated that the influence of the interface on dissipation is not only dependent on the fracture energy. It can be influenced by frictional forces between surfaces sliding relative to each other, thereafter leading to failure. Friction is reducing by the application of lubrication such as the application of low glass transition

polymer. Lubrication reduces adhesion but also promotes interfacial slippage. Interfacial slippage is overcome across the level of interface by the application of polymer chain interdiffusion which increases the level of interfacial interaction. These interactions are called entanglements and it promotes the fracture energy. High fracture energy depicts high adhesion, while good interfacial interaction signifies greater Van der Waals bond. Thus it can be inferred that interfacial entanglement promotes fracture energy and high debond velocity. This affects energy dissipated during debond, at the interfaces, while the application of external force triggers debond. The value of the fracture energy rises, as the size of the interface widens leading to debonding mechanism which exceeds crack propagation.

2. Bulk deformation to Fibrillation: Beyond the crack propagation, is the deformation in the adhesive bulk. At this stage nucleation and cavity growth spreads across the bulk. When a tensile force is applied at this point the cavities tend to enlongate in the tensile direction. It further spreads across the adhesive bulk, and depends on the viscoelastic properties of the bulk and substrate roughness. The growth of cavities with the evolution of changes in shape accompanying it, in an adhesive bulk leads to energy dissipation across the bulk. The growth of these individual cavities transforms to a wider growth in number of cavities, leading the formation of a foam structure at the interface. Tanguy, et al (2014), demonstrated three typical situation that arises as a consequence of measuringtrue tensile stress experienced by materials, in walls between cavities. Such is shown in figure 2.9

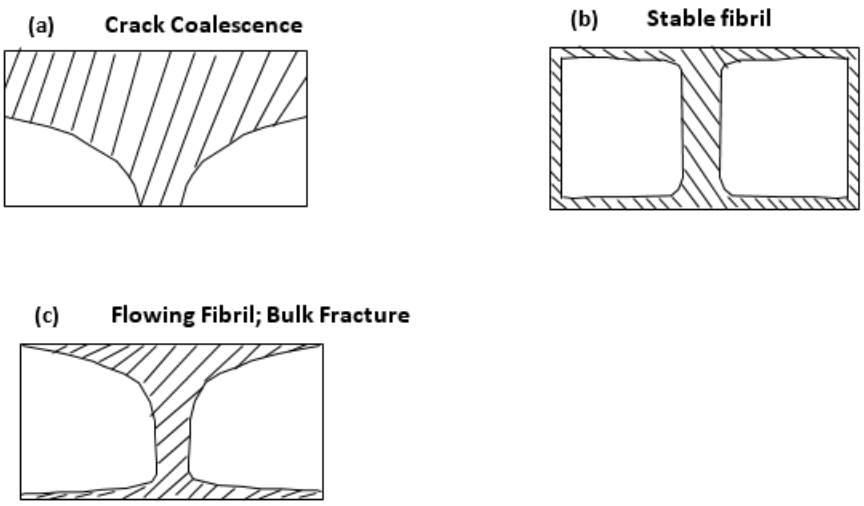

Figure 2.9 Three phases of Bulk Deformation during Debonding

Figure 2.9a, shows a very elastic material, where stress across the cavity rises with minor bulk deformation. The result is an increase in stress concentration at cavity edges, leading to crack propagation along interface, finally to debond.

Figure 2.9b, shows an optimized viscoelastic process. Here there is strain hardening as a result of fibril stabilization. The real stress marginally rises with stretch and fibril stretch rises proportionally with nominal stretch. The stable fibrillation leads to strain hardening until final debond from surface.

Figure 2.9c, shows an insufficient elastic material. Here, the average stress remains stable with strain. The cavity ligaments diminish resulting in failure. Creton, et al (2016), stated that non-linear elastic behavior explains the fracture of fibrils in large strain, which leads to deposit of residue on substrate at debond. In addition fibril can detach from the substrate surface without leaving deposit on it. This makes the analysis of the process of bulk deformation to fibrillation more discreet as rigours persist in giving details. This is unlike linear viscoelastic properties which are limited to prediction of debonding mechanism during transition between interfacial crack propagation and bulk deformation.

2.6.8 Debonding within a Pressure Sensitive Adhesive Bulk.

Debonding is not exclusive to interface between the adhesive and a substrate it occurs within the adhesive bulk, yet it is similar to the former. Greensmith, et al, (1960), demonstrated polymer network fracture; the research determined the tear energy (fracture energy) as superlatively dependent on crack propagation rate and temperature. This is similar to the variation of linear viscoelastic properties noticed with rate and temperature. Lake and Lindley, (1965) determined that the threshold value of polymer network fracture energy represented as F, and was three times higher than the Drupe work of adhesion represented as W. This assertion is meant to proceed in the absence of viscoelastic dissipation. The factor that influence debonding within a pressure sensitive adhesive bulk are as follows:

(a) Threshold Fracture Energy: This is the minimum amount of energy required to initiate a crack propagation across a stretch of chain bonds within an adhesive bulk. The minimum energy required to break the chain is proportional to the length of that chain (Creton and Ciccotti, 2016).

(b) Finite Crack Propagation Velocity: When the temperature around the bonds of a pressure sensitive adhesive decrease to a value near the glass transition temperature it increase the fracture energy. Fracture energy is also influenced by the rate at which the networks are broken; broken networks increase the fracture energy. However, the force required to break a highly increase energetic covalent bond remains constant with a deformation rate. The rise in fracture energy expressed with rate is as a result of energy transfer from loading point to the fracture point.

2.7 Review of Related Literature

Adhesion between substrates and pressure sensitive adhesives are influenced by interfacial parameters. These parameters play significant roles on the potency of micromolecular and macromolecular interactions at substrate/ adhesive boundaries. The ability to predict bond performance through non-destructive processes remains vague. Thus a background review of works, researches, ideas, concepts, generalization, conclusions arrived by various authors, organizations, researchers with regard to interfacial adhesion need be reviewed.

2.7.1 Surface Properties

The potential of any adhesion process is influenced by the substrate or adhesive parameters. Parameters such as surface energy, wettability, work of adhesion, interfacial energy determine adhesion ability at interface. Achebe, et al, (2012) established that the process of prognosis for interaction between two particles is consequent upon their surface properties. The study considered the potential for infections between lymphocyte CD 4 cells by Human immunodeficiency virus (HIV) as largely based on adhesion. The adhesion yields a potential for surface interaction between healthy cells and HIV with a resultant infection. However the basis of interaction is influenced by a Lifshitz Van der waals constant called Hamaker. The Hamaker measures dielectric interaction across interface. Omenyi, et al, (1983) posited that interface energy between surfaces played a vital role in microcirculation of blood across the blood vessels, adsorption of proteins, cell adhesion, phagocytosis and antigen-antibody interaction. The result showed that in the midst of high surface tension liquids, adhesion to solid surface by the cells diminished. The reverse was observed for low surface tension liquids. Chukwuneke, (2016) used surface energetic tool to determine interaction across particles suspended in serum. The interaction centered on potentials of

monitoring mycobacterium tuberculosis on host cells and penetration of HIV virus into particular cells, through cellular surface interfacial energy. Hamaker constant, was used to determine the scope of this interaction. Zbignew, et al, (2013) assessed the tackability of model acrylic pressure sensitive adhesive cross-linked with aluminiumacetylacetomate across substrates. Substrates investigated are stainless steel, glass, polyethylene, poly(methy(methacrylate). Results from the study shows that at larger difference between the value of each substrate surface free energy and the adhesive surface free energy a higher tack is experienced. Rudeneaur, (2013) assessed the role of interfacial parameters on adhesion using statistical acrylate copolymer model pressure sensitive adhesive. The adhesion was tested cross rough and smooth substrates surfaces. Substrate surface free energy and surface roughness influenced debond with the model adhesive. Zbigniew, et al, (2013) observed that improvement in the crosslink of pressure sensitive adhesives enable tack performance, as well improves shear capacity. The impact is better adhesion when applied at interface due to moderate viscosity and improved peel adhesion. Yana, et al, (2012) observed that a steady rise in value of substrates surface energy is accompanied by a decrease in cavitation and cavity growth across interfaces. The interface is between substrates si-water, stainless steel, polyethylene and uncrosslinkedbutylacrylate-methylacrylate. Paper surface interfaced with adhesive tapes when subjected to peel test 180^0 and varying speed showed that paper chemistry, internal bond strength, surface roughness leads to interfacial failure (Boxin 2004).

2.7.2 Adhesion Rheology

The capacity of an adhesive to withstand stress and strain is expressed by its rheology. Adhesion is promoted at interface with lower elastic modulus and

viscoelastic properties. The adhesion relaxation phenomenon within bulk was traced to be responsible for the inability of pressure sensitive adhesive release liner to adhere with polyvinyl(N-alkylarbonate) (Li, et al, 2001). The study held that pressure sensitive adhesive had a surface free energy of 245mJ/m^2. The substrate had a surface free energy of 20mJ/m^2. The result is a poor wetting of the surface by the adhesive, which portend poor work of adhesion. Sun et al, (2015) reviewed various research works involving mechanical properties of pressure sensitive adhesives. It concluded that tack, peel and shear properties of pressure sensitive adhesive are influenced by its viscoelastic properties. Moreso, the quality of interfacial bond was found to be affected by adhesive rheology. Tangy, et al, 2004 showed that various adhesives exhibited varying degrees of nucleation, cavity growth when subjected to probe tack test. This development was traced to the variation in adhesive mechanical molecular weight and branch chain. The result also showed that kinematics deformation at adhesive/ substrate interface was influenced by its rheological properties under same boundary conditions. Bulk fingering is a phenomenon caused by failure within fibril or adhesives entanglements. This is a rheological challenge which Abdelhaye, et al, (2012) expressed in result of experiments carried out on ten different pastes prepared by mixing crushed quartz sand with varying degrees of water and cellulose derivative. The rheological properties of each paste was traced to debond conditions and varying failure modes when subjected to simple power law $\tau = K\gamma^{\alpha}$. In the law shear stress is K and α represents adjustable parameters. Zbignew, et al, (2012) observed that mechanical properties of synthesized free monomer blend of acrylic pressure sensitive adhesive influenced its rheology. The properties which are tack, shear, peel and shrinkage showed optimum performance at coating weight range of 30g/m^2 - 60g/m^2. This is particular when used as polymeric films and

with maximum weight of 0.3wt% for residue monomer. Rudeneaur, (2013) found out that at interface between substrate and adhesive, cavitation was influenced by rise in shear modulus of the pressure sensitive adhesives. For smooth surfaces, it remained insensitive to increase in shear modulus. These characters of the adhesives are influenced by its chemical composition, crosslink. These characters influence debonding. Xiacong, (2010) stated that on bonding adhesives distribute stress across interface. The capacity for stress distribution is determined by the adhesive mechanical properties. The adhesive viscoelastic behaviour on subjection to finite element analysis shows that the mechanical properties of adhesive determine its Young modulus and Poisson's ratio. Kovacevic, (2008) states that the wetting thermodynamics of an adhesive, is determined by its rheological behaviour. Hence it determines its intermolecular interactions with substrates. Yang, (2006), explained that thin layer administration of pressure sensitive adhesive across interface boundary functions to distribute stress at interface.

2.7.3 Adhesion Prediction

Engineers need to know the strength of each adhesive to determine its use and application. The strength of adhesive defines its quality and durability when used across any interface. Deplace, et al, (2009) showed that monitoring elastic modulus of pressure sensitive adhesives along a rigid surface aids to predict transition from interfacial cracks to cavitations and fibrillation. According to the study monitoring strain procedures at adhesion interfaces aids to predict the on-set of fibrillation through tensile test. Bernardes, et al, (2012) explained that the work of adhesion of different dairy products can be predicted by monitoring the influence of the diary protein components. The surface energy, contact angles of various adhesives were used to derive work of adhesion along interface between stainless steel and

different dairy products. Fuentes, et al, (2015) showed that high thermodynamic work of adhesion is influenced by surface roughness across Bamboo – PVDF matrix, and Glass – PVDF matrix. This is because higher surface roughness promotes better mechanical interlocking at interface of composite components. A correlation between interfacial fracture energy and thermodynamic work of adhesion was rarely found by (Phattanarudee, 1998) this was done in a bid to predict adhesive strength using thermodynamic work of adhesion, for lead frame-die adhesive attachment for IC packages. However the study ascribed the discrepancy in the correlation between the two parameters to unverifiable method of assessing viscoelastic dissipation at interface between the lead and adhesive. According to Howson, (2011) a congruity exists between bond energy (thermodynamic work of adhesion) and total work of fracture (fracture energy) during a pull- out test. This is when the interface between asphalt binder and asphalt binder aggregate for paving industry was examined. Later bond energy was agreed to be a useful process of assessing quality and performance of asphalt mixtures. Antuness, (2015) showed that it was not feasible to obtain an objective metal to composite adhesive bonded joint. This is because of failure in finding a correlation between experiments conducted for adhesive modulus, peel resistance and computationally derived finite element analysis of the adhesive bonded joint. The adhesive joint used in the experiment is a double cantilever beam bonded by Epoxy 3N9323BA. Al-Qadi et al, (2008) investigated the development of an approach for predicting adhesion debond at interface. The interface consists of bituminous crack sealants and hot asphalt at service temperature of 4^0c to 40^0c. Three tests were recommended for measuring adhesion across asphalt and crack sealant. They are surface energy approach, direct adhesion test, and interfacial failure energy and modulus test. Surface energy measurement was

found to be a vital tool in analyzing thermodynamic work of adhesion across interface. Parreidt, et al, (2017) developed a novel technique to evaluate the surface free energy of irregular shape object. This is with the aid of Drop Snake based Image J program. It measures the contact angle across irregular surface. Results derived showed a high correlation with contact angle derived from conventional methods. This validates the new technique.

2.7.4 Surface Modification

Surface modification is a way of promoting adhesion at interface between substratesand adhesive. Wolf and Sparavinga, (2010) demonstrated the use of plasma treatment to promote the value of surface free energy for polyester (PET). The research involved 3 models of surface treatment for the substrate polyester. Surface treatments applied include corona, and atmospheric plasma. A control model had no pretreatment. The post treatment results showed a rise in the surface free energy for the material as follows: (1) Corona treated polyester - 46mN/m (2) Atmospheric plasma treated polyester – 54mN/m (3) Non treated polyester – 4mN/m. This posts a high wettability and potential for high adhesion for polyester on plasma treatment. Ashley, et al, (2014) investigated the impact of surface treatment on nylon peel using atmospheric pressure plasma. The aim was to improve the adhesion ability of the nylon surface. Nylon surface was characterized by contact angle and Fourier transforms infrared spectroscopy (plasma treatment). A control model which remained untreated with the plasma was setup and double cantilever mechanism was adopted to test the fracture energy across the 2 model surface. Results showed that fracture energy for the plasma treated surface was 3 times higher than for the untreated surface. Gutowski and Sherry, (2014) used corona treatment and surface grafting to study the effect of

surface modification for polymer substrates. The substrate includes EVA/PPblems, PPand HDPE. Graphing was performed on the substrate surfaces treated with the corona, using organic functional silane. Adhesives such as silicon, silicon 7004/Rhone poulnec and elastomeric acrylic pressure sensitive adhesives were used to conduct shear strength, peel strength, fracture energy test and X-Ray photo electron spectroscopy test. Two models were set up which include ungraftted and untreated substrates, and grafted and treated substrate surface. Results showed interfacial adhesion; fracture energy performance at polymeric/adhesive interface can be promoted and monitored using surface grafting.

2.7.5 Debonding Mechanism

Debonding is simply failure at interface in a joint. Rudenaeur, (2013) observed debonding mechanism between statistical acrylate copolymer pressure sensitive adhesive and a stainless steel probe tack, with emphasis on cavitation. Results showed that at interface between probe and adhesive substrate, surface roughness affected cavity growth, nucleation and tack value. Polymer crosslinking and molecular weight also affected tack value, shear strength of the adhesive and promoted work of adhesion at interface between adhesive and probe. Creton et al, 2015 describes two mechanism of debond present in probe tack test. They are namely interfacial crack propagation and bulk deformation. The bulk deformation occurs at the adhesive bulk, while the interfacial failure mechanism occurs as crack propagation between adhesive and substrate. The research stipulated that the transition from crack propagation to bulk deformation at debond depend on the following: (1) Fracture energy represented as Γ (2) Adhesive thickness represented as H (3) Module of elasticity of the adhesive represented as E

(4)Crack defect size represented as R. Evaluating the relationship between these variables shows that when the ratio of fracture energy Γ to the elastic modules E is less than the crack defect R. $\left[\Gamma/_E < R\right]$, interfacial propagation is favored when the ratio of the fracture energy Γ to the elastic module E is greater than H $\left[\Gamma/_E > H\right]$ adhesive bulk cavitation is favored. Furthermore (Creton et al, 2015) stated that energy dissipation at interface between substrate and adhesive can occur through the routes of microscopic and and macroscopic scale dissipation. The microscopic scale energy dissipation influenced activities at interface or bulk. Both routes depend on size of surface defect and crack propagation. However the microscopic scale dissipation is independent of surface geometry. According to Julia, et al, (2010), the measurement of the receding contact angle at interface between adhesive and rigid surface is vital for monitoring debond as well as adhesive energy. The research involved evaluating the performance of model adhesive DOW Corning's Sylgard 184 PDMS elastomer under probe tack test. Results showed that the contact angle between the adhesive and probe receded under confined condition. It also observed adhesion occurred for cross linked material at contact angle close to 90^0. Tip blunt, interfacial crack was also observed for weakly cross linked material.

2.7.6 Interfacial Adhesion

Adhesion takes place at an interface between an adherent and an adhesive. It takes place at particular condition such as substrate surface wettability, viscoelastic deformation and energy dissipation. Piltonen, (2013) examined, detail mechanism of surface fouling of paper machine surface by recycled

papers. Fouling is a consequence of adhesion between contaminants found in recycled papers and paper machine surfaces. The mechanism of adhesion at the interface paper machine and recycle paper were carried out in both wet and dry environments. Models used are Polyacrylates and SB-Latex. Results showed that low surface energy materials are less susceptible to fouling in dry environment. More so high surface materials are less susceptible to fouling in dry environment. Howson, (2011) examined the use of bond energy and energy ratio parameters to appraise the impact of modification (addictive to asphalt binders) on asphalt binders at interface with aggregates. Energy ratio is a function of surface energy for both asphalt binders and the aggregate components. The study used 37 polymer modified asphalt binders and 11 aggregate samples. Results show that at interface between asphalt binders and aggregates, cohesive energy of the asphalt binders and its surface energy components proved effectual. They proved a vital tool in comparing asphalt binders against each other. The comparison is used to determine the asphalt binder aggregates combination which best resists fracture and moisture damage. Creton, et al, (2015) explained that at interface between pressure sensitive adhesive and substrates, energy is dissipated. Energy dissipated during debond depends on applied contact pressure and time. The work stated that interfacial cohesion involving pressure sensitive adhesive takes place at a contact time of 1 second. Accordingly the bond is established when the work of adhesion resulting from applied force overcome the elastic energy stored per unit area across the interface. Phattanarudee, (1998) examined the impact of moisture on the thermodynamic work of adhesion at interface of IC package (between die attach adhesive and lead frame substrate). Two models were set up for the IC package, one was place in inert air, the other in the presence of moisture. Result showed that the interface expose to moisture

generated lower thermodynamic work of adhesion. Thus decrease adhesion strength (against inert air). Kovacevic, (2008) in “Surface and interface phenomenon in polymer” posits that knowledge of surface and interface phenomenon helps determine the outcome at interface between polymer multiphase systems. According to the paper, interfacial adhesion is described as a processing of wetting across the interface (substrates/ adherent). This interaction produces interfacial bond. Wetting of the substrates are held to depend on kinetics such as liquid viscocity and substrate roughness. Clean surface are specified to promote intimate molecular contact which initiates interfacial contact. Deplace et al, (2009) focused on microscopic improvement of adhesion using a synergy between particles structure and polymer structure. The reports show that monomer composition of adhesive and setting the glass transition Tg, between 50^{0}c and 70^{o}C is vital for maximum interfacial adhesion. The application rheological measurements such as a shear elastic modulus G of less than 100kpa, and critical release energy G to meet criteria for fibril formation are vital for tack. Tack is essential for interfacial adhesion.

2.8 Summary /Knowledge Gap

The study intends to fill the gap of knowledge on the comparative performance of both synthetic and nature sourced pressure sensitive adhesive with the substrate surfaces mentioned. Previous literatures consists of the study of a single polymer adhesive source (crosslinkedor un-crosslinked) tested on a specific interfacial parameter across a single or multiple surfaces. The study enhances the possibility of opening research on the multiple applications and performance of different background of pressure sensitive adhesives for varied use.Furthermore, it hopes to postulate a system of measuring bond quality and adhesive bond strength without

destroying the bond. Available literature shows that the quality and strength of bond is only measurable upon destruction of the bond (Ashley, et al, 2014). The bond destruction is hinged on measuring the fracture energy. (Howson, 2011) demonstrated a relationship between the interfacial energy and fracture energy for asphalt-blinder and its aggregate. Phattanarudee, (1998) observed that thermodynamic work of adhesion in presence of moisture predicts decrease in adhesion for lead frame/ adhesive interface. Moore and Mckenne, (1993) observed a good relationship between the work of adhesion and adhesion strength from peel strength.

Thus this study seeks to explore the prediction of the adhesive bond / adhesive strength without destruction, by utilizing the thermodynamics work of adhesion.

The thermodynamic work of adhesion is obtained by the measure of physical adhesion, while the fracture energy is derived by the measure of practical adhesion. Each of the variables (fracture energy or the thermodynamic work of adhesion) gives its own measurement. The result of the measurement obtained from the thermodynamic work of adhesion is tested for a correlation with the measurement obtained from the fracture energy. The measurements are done with the aid of interfacial parameters, and these parameters help to achieve expectations in the derived direction.

CHAPTER THREE

MATERIALS AND METHOD

3.1. Materials Collection and Preparation

The materials used for this study were substrates, pressure sensitive adhesives, and probe and surface liquids.

3.1.1. Substrates

The substrates used in the study were exactly the same as the vertical walls in the company. The substrate samples were sourced from the local stores: GEM- Hearts Food and Chemicals, No 5 Station Road Enugu, Enugu State, Nigeria.

The substrates are as follows:

(a) Flat Aluminum plate, of 1mm thickness and 30 gram weight (bearing the emergence signs)
(b) Mild steel plate of 3mm thickness and 150 gram weight
(c) Rubber tile of 2mm thickness
(d) High density fiberboard of 15mm thickness
(e)Ceramic wall tile of 0.5mm thickness

3.1.2. Probe and Surface Cleaning Liquids:

The probe liquids used for the study were sourced from the local chemical stores. They are as follows:

(a) Ethylene glycol

(b) Glycerol

(c) Ethanol

The surfaces prior to use for the experiment were considered contaminated. Thus petroleum ether (PET) which was sourced from the chemical store was used to clean the substrate surface. This removes dirt, grease, dust and other contaminants.The various pictures of the test liquids drop on the substrates were captured with the aid of camera. The camera model used in the study was Nikon D80 with production capacity D80, LEN=18 to 135mm, and made in Japan. It is a quality high definition camera HD.

Hypodermic syringe of 2mls capacity was used to release the test liquid drops on the substrate surface. It was sourced from the local store. The low bond axisymmetric drop shape analysis software (LSADSA) with plug in was used to calculate the contact angle of each test liquid droplet, on the substrate. The image the test liquid droplet formed on the substrate surface was captured with the software Image J.

3.1.3 Adhesives

Different varieties of pressure sensitive adhesives were used in this research. They all share basic peculiar characteristics of slight pressure application for optimum performance and contact time. The pressure sensitive adhesives are obtained from the public mall at Portharcourt. They are as follows:

(a) Abro- 200, RTV Silicon sealant with multipurpose application. The application range from adhering to glass, wood, metals, porcelain, ceramics, painted surface and rubber. It is manufactured by ABRO,

industries incorporated, South Bend, IN6624, and United States of America. Part No 55200, White color.

(b) Abro Epoxy Steel, Kwik-set, consists of an epoxy resin and hardener. It is for multipurpose work ranging from industrial, household application. It is manufactured by ABRO Industries Incorporated United States of America. The net weight for each (hardener/resin) is 57gramm (202, 0z), Part No ES-507.

(c) AB-Adhesive Ever-King, multipurpose acrylic adhesive. It is manufactured by Celez Global Resources Limited, People Republic of China.

(d) Cow Skin, animal based pressure sensitive adhesive. It is specially manufactured for the research, by GEM-Hearts Food and Chemicals, No 5 Station Road Enugu, Enugu State, Nigeria.

(e) General Purpose natural rubber based pressure sensitive adhesive. Specially manufactured for the research by GEM- Hearts Food and Chemicals, No 5 Station Road Enugu, Enugu State, Nigeria.

3.2 Material Preparations

Under this subsection, the substrates and pressure sensitive adhesives will be discussed.

3.2.1 Substrate Preparation and Characterization

The substratesamples used in the research have flat surfaces. The substrates are as follows:

- Aluminum plate
- High density fibre wood
- Ceramic wall tile
- Rubber tile

The substrates surfaces were cleaned with cotton wool soaked in petroleum ether (PET). This is done to clean the surface from dust, grease. Thereafter the substrates were left to dry at room temperature, to ensure that the PET does not mix with the test liquids. This is because it will affect the result of the contact angle measured asa result of mixing with the cleaning agent (PET).

The characterization of the various substrates was done with anOxford instrument X-Met 700 XRF-Spectrometer. The X-ray fluorescent analyzer (XRF-spectrometer), gives a non-destructive material test which helps to give information on the positive elements contained in each of the substrate. This report gives the chemical composition of each substrate material used in the research. The information of material chemical composition will enable the research track the performance of each substrate with each adhesive at every particular interface. It will help identify the material and the type of substrate surface treatment applicable to promote adhesive if need be.

Procedure:

The hand held XRF-Spectrometer works on the principle of illuminating the substrate surface by an X-ray incident beam resulting in scattered incident beams. The XRF- Spectrometer is placed in contact with each substrate for at least 15 seconds. The machine with the aid of the advanced software inside it gives information on the chemical composition of each substrate.

Plate 3.1 characterizing the substrate surfaces with XRF-Spectrometer

3.2.2 Pressure Sensitive Adhesive Film Preparation

3.2.2.1Production of Plant (Natural rubber) based pressure sensitive adhesive.

Sample Collection:

The natural rubber based pressure sensitive adhesive used for the experiment was specially designed for research using the following specification, as seen in table 3.1.

Table 3.1: Material Composition for Preparation of Pressure Sensitive Adhesive.

RAW MATERIALS	QUANTITY APPLIED IN GRAMMES (gm)
Chlorinated Natural Rubber	1000
Phenolic Resin	250
Light Magnesium Carbonate	125

Table 3.2: Solvent composition for Preparation of Pressure Sensitive Adhesive

SOLVENTS	QUANTITY APPLIED IN MILLILITRES (ml)
Toulene	1000
Acetone	300
Premium Motor Spirit	150

Sample preparation:

The sample preparation is divided into samples, A, B, and C.

For sample A:

1000grams of chlorinated natural rubber is added to 150ml of acetone, and 500ml of toluene. The mixture is well agitated till there is complete dissolution of the components.

For sample B:

250gram of phenol resin is differently mixed with balance of 150ml of acetone and 500ml of toluene. The mixture is well agitated till complete dissolution of the components. The mixture (phenol resin, acetone and toluene) is further treated with 125gram of light magnesium carbonate. The resulting mixture is the agitated, till complete dissolution is achieved.

For sample C:

The sample A and B are mixed together and agitated to ensure complete dissolution. Later 150ml of premium motor spirit is added to the mixture of sample A and B. This is sample C. The new sample C is as well agitated properly and the mixture (sample) is stored in a tight container ready for use.

The light magnesium carbonate accelerates the dissolution of chlorinated natural rubber. The phenolic resin increases the tack of the adhesive. The premium motor spirit is used as a general solvent to increase the quantity of the new natural rubber based pressure sensitive adhesive. The entire

experiment is carried out at room temperature of 20^0C, since all components (raw material/ solvents) are inflammable.

3.2.2.2 Production of Animal based pressure sensitive adhesive (From Fresh Cow Skin)

Sample Collection: The raw materials for the production of animal based pressure sensitive adhesives are as follows:

Table 3.3: Raw Materials Composition for preparation of animal pressure sensitive adhesive (From Fresh Cow Skin) with quantity applied.

RAW MATERIALS	QUANTITY APPLIED (gram)
Sodium Thioglycolate	75
Strontium Sulphide	15
Calcium Thioglycolate	25
Wet Cow Skin	10,000
Dry Cow Skin	8,000

Sample Preparation:

The fresh cow skin is dehaired by the use of chemical depilatories such as sodium thioglycolate, strontium sulphide and calcium thioglycolate. The exact amount of the samples used is expressed in the sample collection. The raw cow skin is cut into small pieces and put on boiling water to simmer for 4 hours or more, depending on the hardness of the water. The end of the

simmering process leaves a residue of very soft hide, and the residual liquid thickness. The cow skin liquid is sieved with a stainless steel sieve to remove unwanted materials. Thereafter a rubbery mass results and is allowed to dry in a cool place with high degree of aircirculation. The preparation is heated till a dry mass results and the adhesive is set for use.Meanwhile excessive heating destroys tack, while tack properties can be tested with thumb.

3.3 Chemical Composition of Plant based Pressure Sensitive Adhesive

The various recipes for samples of Abro-2000 RTV Silicon sealant, AB-Adhesive Acrylic Ever-King and Abro Epoxy steel kiwi set will be discussed.

3.3.1 The Abro -2000 RTV Silicon Sealant

The Abro -2000 RTV Silicon Sealant consist of the components stated in table 3.4.

Table 3.4: The Recipe for Abro-2000 RTV Silicon Sealant

COMPONENTS	**Amount(%)**	**PURPOSE**
Methyltriacetoxysilane	2	Cross linking agent/Adhesion promoter
Alkyltriacetoxysilane	2	Cross linking agent
Ethyl trace to tail end	2	Solvent
Amorphous Silica	10	Plasticizer
Decamethylcyclopentasiloxane	34	Anti oxide
Silicon dioxide	28	Thickener
Calcium Carbonate	5	Filler/Opacity
Methyl Ethyl Ketone	5	Solvent

Titanium Dioxide	12	Filler
Total	100	

3.3.2 The AB- Adhesive Acrylic Ever- King

TheAB- Adhesive Acrylic Ever- King consists of the components stated in Table 3.5.

Table 3.5: The Recipe for Acrylic Ever-King adhesive

COMPONENTS	**AMOUNT IN (%)**	**PURPOSE**
Acrylic Polymer	25	Resin
Dichloropentanyl Methacrylate	20	Monomer
Thioglycolic Acid	1.5	Antioxidant
Azobisisobutylronitrile	0.5	Thixothropiv
Precipitated Amorphous Silicon dioxide	30	Plasticizer
Toulene	23	Solvent
Total	100	

Sample Preparation:

The reaction took place in a four neck flask under a Nitrogen atmosphere at 70^{o}c for one hour. Then 0.5% of Azobisisobutylrontrile was placed in the resin

as a thermal polymerization initiator to react with the other components at 70^{o}c for two hours.

3.3.3 The Abro-Epoxy Steel Kwik set adhesive

The Abro-Epoxy Steel Kwik set adhesive consists of the resin components stated in table 3.6 and Hardener component stated in table 3.7.

Table 3.6: The Recipe for resin component of Abro-Epoxy steel kiwi set

COMPONENTS	**AMOUNT IN %**	**PURPOSE**
Polycarbonate	42	Plasticizer
Dichloromethane	2	Organic solvent
Methyl Ethyl Ketone	22	Solvent
Epoxy Resin	20	Resin
Fumed Silica	14	Viscosity adjustment
Total	100	

Table 3.7The Recipe for hardener component of Abro Epoxy, steel kiwit set

COMPONENTS	**AMOUNT (%)**	**PURPOSE**
Triethylenetetamin	13	Chelating agent
Isophronefiamine	8.7	Curing agent (Crosslinking agent)
Diaminodiphnylsulfone	8	Antioxidant
Amorphous silica precipitate	32	Plasticizer
Bisphend A	38.3	Raw material in Epoxy Resin

Sample preparation: The ingredients enumerated in the Resin were all added into the polycarbonate solution. Then the liquid was continuously stirred for 11minutes. Thereafter a clear liquid was obtained.

There after the Hardener part was mixed with the resin part for 15minutes at 60^{o}C. However for the experiments the thickness of each adhesive film used was 40±4µm. The films were spread on clean glass. The glass was cleaned

with petroleum ether to remove contamination. These samples were used for the derivation of the contact angle for each adhesives, and further necessary calculation.

3.4 Confirmatory Test on the Products.

In the subsection, the various confirmatory test performed on the products are discussed.

3.4.1 Contact Angle Measurements

The contact angles are measured for each substrate and each pressure sensitive adhesives. The test liquids used are (i) Ethylene Glycol (ii) Ethanol (iii) Glycerol

Method

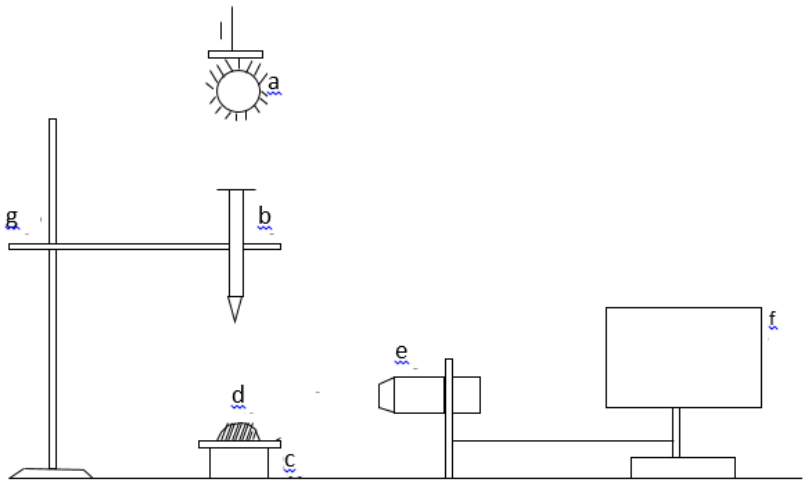

Figure 3.1: Experimental set up for the measurement of contact angle

Figure 3.1 is a representation of a set up to measure the contact angles of eachtest liquid,with the different substrates. The alphabetically labeled parts of figure 3.1 are as follows:

a. represents the light source

b. represents the syringe

c. represents the block

d. represents the test liquid droplet

e. represents the high definition camera

f. represents the computer

g. represents the clamp stand

Flat substrate surfaces are mounted on the block, while the adhesive film is spread on a flat glass and mounted on the block. The light is to illuminate the place in order to obtain a bright image of the droplet. The syringe is brought close to the flat substrate while the test liquid is released to the substrate/film surface. The test liquid drops of 1micro litrevolume is released unto the substrate surface. The frozen drop images of the side views of the test liquid were taken by the high definition camera. The snap shots were taken at a rate of 10 frames per second, while the distance between the syringe needle and substrate was reduced. This is to minimize the effect of air current distortion of the drops. The contact angle is measured 7 times for each substrate, with the average and standard derivation calculated. The frozen image is transferred to a computer as shown in Figure 3.2. The computer is fitted with a software called Image J, and assisted by the low bond axisymmetric drop shape analysis. The contact angle is derived as follows:

- Load an image into Image J and ensure that is on gray scale.
- Launch the plug-in low bond axisymmetric drop shape analysis (LBADSA)
- Ensure proper setting of the image scale under the icon (means)
- Choose the liquid capillary constant

- Make adjustment of the drop profile with the first step of positioning the drop height and radius of curvature at the apex.
- Utilize the optimization using gradient energy by pressing the energy gradient
- Add the optimization result to the drop properties into the table.
- The value of the contact angle is determined.

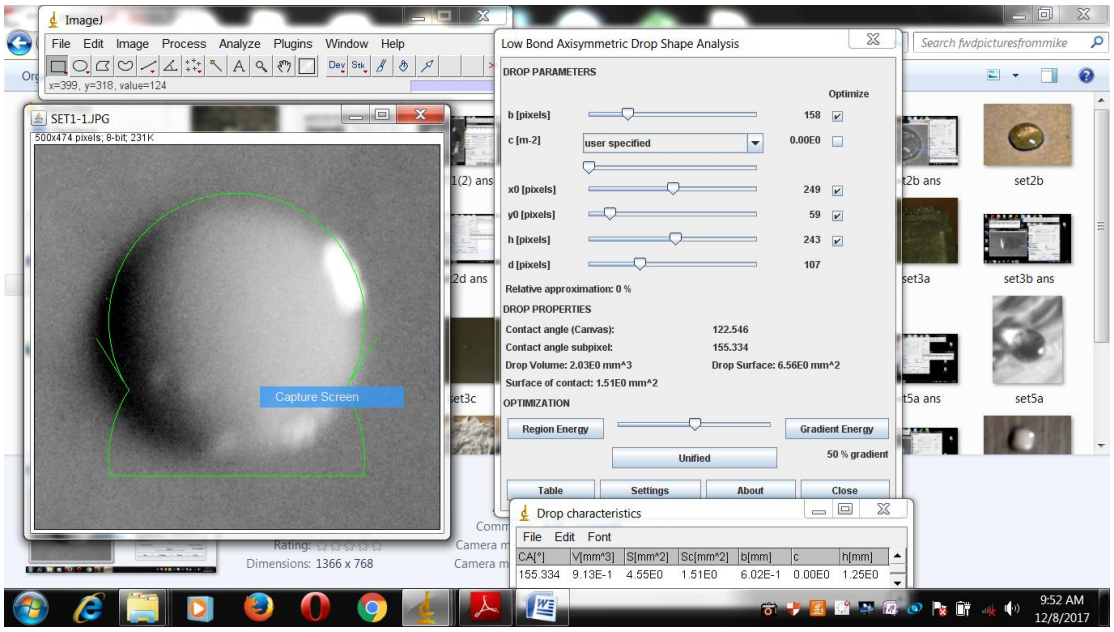

Figure 3.2 Sample of Drop shape analysis and measurement

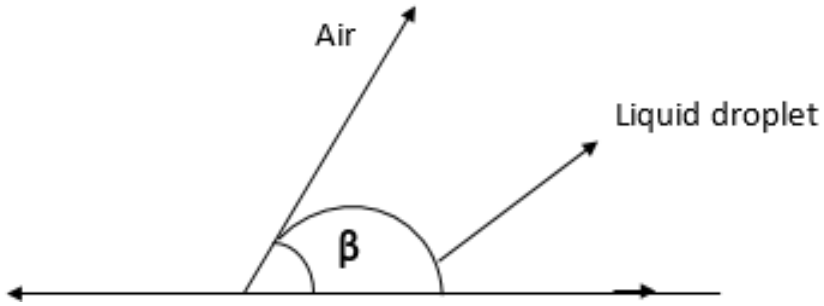

Figure. 3.3 Contact angle of liquid droplet

βrepresent the contact angle.

3.4.2 Determination of Surface Energy

The determination of the surface energy of either substrate or adhesive film is dependent on the contact angle. The average values of the contact angle measured were used to calculate the polar and dispersive component of the surface free energy.

The surface energy is calculated by the use of equation 3.1. (Flinn and Ashley, 2010)

$$\frac{\gamma_{lv}(\cos\theta+1)}{2\sqrt{\gamma_{lv}^{p}}} = \sqrt{\gamma_{sv}^{d}}\left[\sqrt{\frac{\gamma_{lv}^{d}}{\gamma_{lv}^{p}}}\right] + \sqrt{\gamma_{sv}^{p}} \qquad (3.1)$$

Where the variables are represented as follows:

γ_{lv} represents the total surface energy between the liquid and the vapour

γ_{lv}^{p} represents the polar component of the surface energy between the liquid and vapour.

γ_{lv}^{d} represents the dispersive component of the surface energy between the liquid and the vapour.

γ_{sv}^{p} represents the polar component of the surface between the solid and the vapour.

γ_{sv}^{d} represents the dispersive component of the surface energy between the solid and vapour.

Equation 3.2 and 3.3 are components of equation 3.1. They are represented as follows:

$$\frac{\gamma_{lv}(\cos\theta+1)}{2\sqrt{\gamma_{lv}^{p}}} \qquad (3.2)$$

$$\sqrt{\frac{\gamma_{lv}^{d}}{\gamma_{lv}^{p}}} \qquad (3.3)$$

The Kaelble plot for each test liquid was plotted. The Kaelble plot shows the relationship between the contact anglesmeasurements got from each test

liquid. To this effect, equation 3.2 is plotted as Y coordinate while equation 3.3 is plotted as X- coordinate. The polar component of the surface energy was calculated as the Y-intercept of the plot squared. The dispersive component of the surface energy was the slope of the plot squared.

Table 3.8: Surface free energy values for test liquids used for the study

Test liquids	Surface Free Energy Values (mJ/m^2)	Dispersive Component of (mJ/m^2) Surface free energy Values δ^d	Polar Component of Surface Free energy values δ^p(mJ/m^2)
Ethelene Glycol	48.8	32.8	16.0
Glycerol	64	34	30.0
Ethanol	21.40	18.8	2.60

Source:Accue Dyne Test Chart, 2017.

The surface energy of the test liquid components were derived from the literature ACC Dyne Test Manual, as shown in table 3.8. However the surface free tension of each adhesive film or substrate was calculated by the summation of the surface free energy of components.

$$\gamma_{sv} = \gamma^{d} + \gamma^{p} \quad (3.4)$$

3.4.3 Determination of the Interfacial Surface Energy

The interfacial energy exists across two boundaries. The first is between the pressure sensitive adhesive and aluminum. Second is between the pressure sensitive adhesive and substrate. Fowke's law is used to derive the relation as follows;

$$\gamma_{sl} = \gamma_{sv} + \gamma_{lv} - 2\left(\gamma_s^d \gamma_l^d + \gamma_s^p \gamma_l^p\right) \quad (3.5)$$

Applying the Owendts Wendt law to obtain the interfacial surface energy isrepresented as follows:

$$\gamma_{sl} = \gamma_{sv} + \gamma_{lv} - 2\left(\gamma_{sv}^d \gamma_{lv}^d\right) - 2\left(\gamma_{sv}^p \gamma_{lv}^p\right)^{1/2} \quad (3.6)$$

Where equation 3.6.is further simplified with regards to the contact angle as follows:

$$\gamma_{sv}(\mathbf{1}+\boldsymbol{cos\theta}) = \mathbf{2}\left(\gamma_{sv}^{d}\gamma_{lv}^{d}\right) + \mathbf{2}\left(\gamma_{sv}^{p}\gamma_{lv}^{p}\right)^{\mathbf{1/2}} \quad (3.7)$$

3.4.4 Determination of Thermodynamic Work of Adhesion

The thermodynamic work of adhesive refers to the fundamental adhesion. It deals with the forces actingamong atomsacross an interface. The thermodynamic work of adhesion shall be calculated across boundaries. The boundaries are between the pressure sensitive adhesive and aluminum or pressure sensitive adhesive and substrate surface. This is stipulated as follows;

$$W_a = \gamma_{sv} + \gamma_{lv} - \gamma_{sl} \equiv \gamma_{lv}(\mathbf{1}+\boldsymbol{cos\theta}) \quad (3.8)$$

3.4.5 Determination of Fracture Energy

Fracture energy is measured using the “Pull-off test”. The pull-off test regards the amount of displacement generated by an applied force. It shows the stress-strain relation of each particular adhesive for each bond pair.

The bond pair represents the interaction among the Aluminum/Pressure Sensitive Adhesive/ Substrates and the interfaces across each joint. The various adhesives bonds, the different surfaces with the Aluminum (emergency sign) plate. The pull-off test is conducted with the aid of a Testomeric Universal testing machine, Model M500- 25CT, computerized and 27KN capacity. The type of tensile test conducted was PWG25W and the test conducted at test speed of 50millimeters/minute (50mm/min.).

The substrates are all cleaned with Petroleum ether (PET), to remove grease, dirts and other contaminants. The environment for the test is at 20^0C and room humidity. Strips of length 120mm, thickness range of 1.25mm-15mm, width range of 23.30mm-26.50mm, were cut from larger piece of the

substrates. The substrate samples were labeled as well as the different pressure sensitive adhesive used in the study to facilitate precision and avoid ambiguity in selection. To this effect the researcher developed a matrix. The matrix helps to select the adhesive and the substrate at each test, and this eliminated error from repetitions. Each bond pair consists of an aluminum plate bond to any substrate with any of the selected pressure sensitive adhesives. The adhesives thickness ranged from 100µm-500µm for the test. The adhesive thickness was measured using the Dry Film Thickness gauge (DFT-gauge), by placing it on the adhesive after they have been spread on surface of the substrate. Each bond pair is mounted on the tensile testing machine which is computer controlled. It measures force at ranges of pre-determined cross head speed. The mounted bond pair is gripped in the vice of the tensile machine for the pull-off test. The test is conducted at speed of 50mm/min. During the tensile test the computer visual display unit records the stress-strain relationship of the pressure sensitive adhesive with regards to the substrates in the bond. The stress- strain graph gives in information on the failure mode for the bond such as (1) Adhesive failure (2) Cohesive failure (3) Interfacial failure or Brittle failure. Furthermore the stress-strain graphical relationship helps to identify the adhesive Young Modulus; the peak stress the bond can bear, the yield stress, break strain, Energy at break (Fracture energy), elongation at yield and break, plastic strain etc. The type of failure involved in the bond indicates the bond quality, while the peak stress, (Fracture energy) energy at break, helps to identify the bond strength. The tensile machine was put to zero, before each test. The enumerated variables are measured for each bond pair and this aided in the analysis.

Plate 3.2: Substrate bond pair mounted on a tensile machine

Plate 3.3: Substrate bond pairat break on a tensile

. .

3.4.6 Determination of the Surface Finish of the substrates.

The substrates surface roughness were measured with the aid of Surface Roughness Tester Model No. SRT-6100, 4 digits, 10mm, LCDwith blue light. It has a measurement range Ra 0.05-10.00 µm, Rz 0.1-50.0µm.

The surface roughness tester is placed on surface of each substrate. The in-built in sensor underneath helps to derive the value of the surface roughness via inductance. The value of the surface finish for each substrate surface is thus derived and recorded.

3.4.7 Prediction of Adhesion through non-destructive method

The adhesion at each bond type can be predicted using the combination of interfacial parameters vital to enforce tack. These include thermodynamic work of adhesion, work of cohesion, workof spreading and total work of adhesion. The combination of these parameters is used to derive adhesion ratio. The adhesion ratio is used to measure the bond performance and

quality across each bond type. The force at peak derived from the tensile test is established as the tack from practical adhesion test (fracture energy). The value from adhesion ratio of each bond type was found to be in the range of -1 to +1 for each bond type. The following equations express how the interfacial parameterssuch as adhesion, cohesion and spread were used to derive the adhesion ratio.

Thermodynamic work of adhesion W_A

$$W_A = \gamma_{sv} + \gamma_{lv} - \gamma_{sl} \quad (3.9)$$

Work of cohesion

$$W_A = 2\gamma_{lv} \quad (3.10)$$

Work of spreading

$$W_S = W_A - W_C \quad (3.11)$$

Total work of adhesion at bond W_{AC}

$$W_{AC} = W_A + W_C \quad (3.12)$$

Adhesion Ratio is ratio of work of spread to Total work of adhesion and represented as A.R.

$$\text{A.R.} = {}^{W_S}/_{W_{AC}} \quad (3.13)$$

CHAPTER FOUR

RESULTS AND DISCUSSION

4.1Contact Angle of Different Substrates and Pressure Sensitive Adhesives

Table 4.1 showed contact angles which each test liquid formed with respective substrates surfaces used in the study. Ethylene glycol drop spontaneously wetted the surface of the rubber tile. This showed that the

rubber tile surface has extreme affinity for the ethylene glycol. This behavior is termed spontaneous wetting or hyperhydrophilicity (Jennisen, 2012). The spontaneous wetting indicates that the contact angle between the test liquid and rubber is zero or less than 3^{o}, making it difficult for an image of the contact to be collected.

Contact angles less than 90^{o} indicate complete wetting over time and are termed hydrophilic (Kock-yee, 2014). This is the case of 81.662^{o} for ethanol/ceramic wall, 73.542^{o} for ethanol/rubber tile, 74.542^{o} for glycerol/rubber tile, 64.099^{o} for ethanol/high density fibre wood and 73.466^{o} for glycerol and mild steel. Contact angles greater than 90^{o}but less than 140^{o} ($90^{o}<\theta< 140^{o}$),indicate negligible or non-wetting (Kanwoo et al, 2019; Sara et al 2020; Kock-Yee, 2014). This is the cases of 102.715^{o} for ethanol/aluminum, 118.867^{o} for ethylene glycerol/high density fibre wood, 122.815^{o} for ethylene glycol/mild steel, 102.889^{o} for ethanol/mild steel and 131.265^{o} for ethylene glycerol/high density fibre wood. Contact angles greater than 140^{o} indicate complete non-wetting as is the cases of 163.598^{o} for Ethylene glycerol/aluminum and 156.820^{o} for ethylene glycerol/ceramic wall tile. Surfaces exhibiting such characteristics are termed super hydrophilic surfaces (Chengchun-Zang et al, 2019; Baruch et al, 2020; Hauschwitz et al, 2020).

Table 4.2 shows the contact angles between the test liquids and the pressure sensitive adhesives. Ethanol drop on the surface of acrylic pressure sensitive adhesive showed spontaneous wetting indicating a high attraction between molecules of the test liquid and acrylic pressure sensitive adhesive. The spontaneous or hyper hydrophilic wetting indicates a zero or less than 3^{o} contact angle. Contact angles of 89.619^{o} for ethanol/natural rubber, 78.687^{o}

for glycerol/natural rubber and 89.7^{o} for ethanol/silicon being less than 90^{o}, depict hydrophilic or complete wetting phenomena (Piltomen, 2013; Knock-Yee, 2014).

Hyper hydrophilic phenomena (contact angles greater than 90^{o} but less than 140^{o}) were recorded by contact angles of 114.81^{o} for ethylene glycol/cow skin, 136.689^{o} for ethanol/cow skin, 137.689^{o} for glycerol/cowskin, 119.628^{o} for ethanol/natural rubber, 130.083^{o} for ethylene glycol/acrylic, 120.128^{o} for glycerol/acrylic, 128.128^{o} for ethanol/silicon, 111.315^{o} for glycerol/silicon, 130.293^{o} for ethylene glycol/epoxy and 96.41^{o} for glycerol/epoxy. The conditions of complete non-wetting was seen in contact angles of 181.852^{o} for ethanol/epoxy

Table 4.1 Solid substrate average contact angle and standard deviation for each test liquid.

Solid Substrates / Test Liquids	**Average CA (0) Rubber Tile**	**Standard Deviation (0) Rubber Tile**	**Average CA (0) Aluminium**	**Standard Deviation (0) Aluminium**	**Average CA (0) High Density Fibre Wood**	**Standard Deviation (0) High Density Fibre Wood**	**Average CA (0) Mild Steel**	**Standard Deviation (0) Mild Steel**	**Average CA (0) Ceramic Wall Tile**	**Standard Deviation (0) Ceramic Wall Tile**
Ethylene Glycol	-	-	163.598^0	0.558^0	118.676	0.722	122.815	0.767	156.820	0.962
Ethanol	73.542	0.704	102.715^0	0.873^0	64.099	1.8055	102.887	1.029	81.662	0.913
Glycerol	74.542	0.729	118.897^0	1.109^0	131.265	1.054	73.466	0.989	55.736	0.635

Solid Substrates / Adhesive Substrate / Test Liquids	Average CA (0) Cow Skin	Standard Deviation (0) Cow Skin	Average CA (0) Natural Rubber	Standard Deviation (0) Natural Rubber	Average CA (0) Acrylic	Standard Deviation (0) Acrylic	Average CA (0) Silicone	Standard Deviation (0) Silicone l	Average CA (0) Epoxy	Standard Deviation (0) Epoxy
Ethylene Glycol	114.810	0.964	89.619	1.083	130.083	1.017	128.025	1.058	130.293	0.923
Ethanol	136.689	1.330	119.628	1.223	Nil	Nil	89.703	1.488	181.852	1.134
Glycerol	137.138	1.184	78.687	1.417	120.128	1.364	111.315	1.065	96.410	0.623

Table 4.2 Pressure Sensitive Adhesives Average Contact AngleData and StandardDeviation for each Test Liquid.

The acrylic surface is spontaneously wetted by the drop of ethanol. The test liquids exhibit different degrees of contact angles on the drop of each test liquid ranging from less than 90^0 which Is indicative of wetting. Contact angles beyond 90^0 indicate no wetting or negligible wetting. The pressure sensitive adhesives are viscoelastic solids. In the research work they presented higher contact angles than the solid substrates. This can be attributed to the arrangement of particles at the interface between the adhesives and the test liquid. The viscoelastic nature of the pressure sensitive adhesive, likely led to a low interaction between the adhesive and test liquid. The low interaction is traceable to differences in chemical composition, which leads to passivity at the interfacial boundary. This poor interaction results in the high contact angle. The high contact angle depicts hydrophobicity while low contact angle depicts hydrophobicity. High contact angle are contact angles higher than 90^0, while lower contact angles are less than 90^0.Thus the test liquid with high contact angles did not wet or barely wetted the surface of the pressure sensitive adhesive. The low contact angles points to good wetting or partial wetting by the test liquid.

4.2 Result of the thermodynamic work of adhesion at interface between substrate and pressure sensitive adhesives

The thermodynamic work of adhesion in a 3 component system such as the present work is evaluated through the following equation:

$$\Delta G^{a}_{123=} \gamma_{13} + \gamma_{23} - \gamma_{12} \quad (4.1)$$

The interfacial energy across the interfacial boundaries is evaluated in line with the Fowkes Law. This law is represented as follow:

$$\gamma_{sl} = \gamma_s + \gamma_l - 2\left(\gamma_s^d \gamma_l^d + \gamma_s^p \gamma_l^p\right)^{1/2} \quad (4.2)$$

For the current study, the application of the Fowkes law is simplified as follows:

$$\gamma_{13a,b,\ldots\ldots} = \gamma_1 + \gamma_{3a,b,\ldots\ldots} - 2\left(\gamma_s^d \gamma_{l3a,b,\ldots.}^d + \gamma_s^p \gamma_{l3a,b,\ldots.}^p\right)^{1/2} \quad (4.3)$$

Where:

$\gamma_{13a,b,\ldots\ldots}$ Interfacial energy between substrates and pressure sensitive adhesive.

$3a, b, \ldots.$ Various pressure sensitive adhesive at the substrates and pressure sensitive adhesive interface.

$\gamma_s^d \ldots.$ Dispersive component at the solid substrate.

$\gamma_{l3a,b,\ldots.}^d$ Dispersive component at the various pressure sensitive adhesive.

γ_s^d Polar component at the solid substrate.

$\gamma_{l3a,b,\ldots.}^p$ Polar component pressure sensitive adhesive.

Table 4.3shows the values of the dispersive and polar components of the surface free energy of each material used in the research. The surface free energy value for each material was derived from the summation of the dispersive and polar components of the surface free energy.

Table 4.3: Dispersive and Polar Components of Surface Free Energy

Materials	**Polar Component of Surface Free Energy γ^p (mJ/m^2)**	**Dispersive Component of Surface Free Energy γ^d (mJ/m^2)**	**Surface Free Energy $\gamma_T = \gamma^p + \gamma^d$ (mJ/m^2) approximately**
Aluminum	205.3489	14.3315	220
High Density Fibre Wood	112.5508	1.5623	114
Mild Steel	27.1191	1.7916	28.91
Ceramic Wall Tile	58.8688	1.6742	60.54
Rubber Tile	19.8167	16.6823	36.50

It is observed that all materials showed an inclination towards the polar component.Fowkes described the interfacial energy between two surfaces as the sum of the polar and dispersive components. The dispersive component is inclined to the London – dispersive forces present in the materials. The polar force is a summation of the dipole forces, hydrogen forces and ionic forces present at the material surface. Furthermore Liftshitz described the interfacial tension between two surfaces as the sum of the London-Van der Waals forces and the acid-base interaction energy components. According to Liftshitz, the London Van der Waals interfacial energy component is positive. This is akin to the dispersive component. The acid – base component is negative which is akin to the polar component of the interfacial energy.Thus the materials (solid substrates) can be graded as acting as the negative components of the interfacial energy in the bond.

Table 4.4 Show the values of the dispersive and polar components of the surface free energy of each pressure sensitive adhesive. The surface energy of each pressure sensitive adhesive is the sum of the polar component and dispersive component for each pressure sensitive adhesive.

Table 4.4 Pressure Sensitive Adhesives Polar and Dispersive Component Surface Free Energy values.

Materials	**Polar Component of Surface Free Energy** $\gamma^p\ (mJ/m^2)$	**Dispersive Component of Surface Free Energy** $\gamma^d\ (mJ/m^2)$	**Surface Free Energy** $\gamma_T = \gamma^p + \gamma^d\ (mJ/m^2)$ **approximately**
Cow Skin	54.0710	0.1295	54.20
Natural Rubber	0.5309	15.1913	15.72
Epoxy	0.4348	9.6926	10.13
Acrylic	6.6352 58%	4.7437 42%	11.39
Silicone	2.7579 37%	4.7241 63%	7.48

Epoxy, natural rubber pressure sensitive adhesive shows extreme inclination to dispersal component of the surface free energy. The silicone pressure sensitive adhesive has a high inclination to the dispersive component. The cow skin pressure sensitive adhesive is inclined to polar component of the surface free energy more than the dispersive component.The polarity of the components of the pressure sensitive adhesive or the solid substrate determines the level of interaction at the interface. This means that the interfaces will develop electrostatic attraction dependent on the ratio of dispersive and polar components. The level of attraction between these components across the interfaces will determine the level and strength of adhesion across the interface.

4.3 Effects of Surface Free Energy Component on the Interfacial Energy

The surface free energy consists of polar and dispersive component. The interaction of these components affects interfacial interaction, thus the interfacial energy across the bond. Table 4.5 represents the surface free energy of substrates and the surface free energy of the various pressure sensitive adhesives. The interfacial energy accompanying each substrate at the boundary with each pressure sensitive adhesive is as well represented. The polarity of each substrates and each pressure sensitive adhesive is also shown.

Table: 4.5 Interfacial Free Energies of Substrates/Pressure Sensitive Adhesives and Accompany Interfacial Energies.

S/N	SUBSTRATES	COWSKIN	INTERFACIAL ENERGY γ_{sl} mJ/m^2	ACRYLIC	INTERFACIAL ENERGY γ_{sl} mJ/m^2	EPOXY	INTERFACIAL ENERGY γ_{sl} mJ/m^2	SILICON	INTERFACIAL ENERGY γ_{sl} mJ/m^2	NATURAL RUBBER	INTERFACIAL ENERGY γ_{sl} mJ/m^2
1	Mild Steel (polar)	Polar	6.52	Moderate Polar	12.98	Dispersive	28.23	Moderate Dispersive	18.13	Dispersive	31.73
2	Ceramic Wall Tile (polar)	Polar	1.90	Moderate Polar	32.00	Dispersive	57.74	Moderate Dispersive	21.96	Dispersive	61.20
3	High Density Fibre Wood (polar)	Polar	12. 18	Moderate Polar	70.46	Dispersive	108.12	Moderate Dispersive	85.80	Dispersive	111.48
4	Aluminium (polar)	Polar	64.50	Moderate Polar	154.48	Dispersive	197.27	Moderate Dispersive	177.12	Dispersive	198.18
5	Rubber Tile (Moderate polar)	Polar	25.17	Moderate Polar	27.34	Dispersive	20.53	Moderate Dispersive	18.12	Dispersive	19.90

In table 4.5, the substrates exhibit polar properties. Table 4.3, expressed that each substrate had a very low dispersive component despite their high polar component. This is with the exception of Rubber tile, which shows an almost equivalent value for both dispersive component and polar component. This led to designation of the Rubber tile substrate as moderately polar substrate. Here (Table 4.5.), at the interface boundary between each substrate with a polar component and each pressure sensitive adhesive with same polar component, interfacial energy is low. During the interaction, at interface boundary between each substrates with a polar component and each pressure sensitive adhesive with a moderate polar component, interfacial energy rises. It rises more than the interfacial energy between, substrate with polar component and pressure sensitive adhesives with polar component at interface boundary. However at the interface boundary between polar substrates and moderately dispersive pressure sensitive adhesive, the interfacial energy rises higher.

The interfacial energy here is higher than the amount (interfacial energy), existing at the polar substrate and moderately polar pressure sensitive adhesive interface boundary. The interfacial energy existing between a polar substrate and dispersive pressure sensitive adhesive is the highest value, shown on Table 4.5. Rubber tile substrate (moderate polar component) exhibited the highest interfacial energy at interface boundary with acrylic (moderate polar) pressure sensitive adhesive. The value of interfacial energy exhibited at the rubber tile/ acrylic adhesive interface is followed by interfacial energy at rubber tile/ cow skin adhesive interface. The dispersive pressure sensitive adhesives namely epoxy and natural rubber exhibited lower interfacial energy at the rubber tile interface. Silicone exhibited the least interfacial energy at the interface boundary with rubber tile. This is despite its moderately dispersive component.

Deductions from Table 4.5,showed that a high interfacial energy evolved at interface boundary interaction between dissimilar components (polar and dispersive). This is with the exception of rubber tile. The high interfacial energy exhibited at the interface boundary can be attributed to interactive forces. These interaction forces are forces of repulsion and attraction at the interface boundary between the adhesive and substrates. When substrates and pressure sensitive adhesives with similar surface components (such as polar to polar) interact, low interfacial energy occurs. This is traceable to repulsive forces at such interface, thus resulting in weak attraction and the low interaction energy. Substrates which possess dissimilar polarity components, (polar and dispersive) attract each other often, and exhibit high interfacial energy. This is due to the high interaction at the interface boundary. When the substrate has a polar component with a moderate dispersive pressure sensitive adhesive at interface boundary; there is moderate repulsion. This leads to the medium interfacial energy recorded in the experiment. This same process occurs at interface boundary between a polar substrate and moderate polar pressure sensitive adhesive.

The latter when compared with the former has a slightly lower value of interfacial energy compared with the former. This can be traced to the polar arrangement at the interface boundary (except rubber tile). The marked difference in the differential between the rubber tiles with each pressure sensitive adhesive is traceable to the component compositions, (Table 4.3.). Thus the atomic/electron cloud for polar-polar interaction seems to evolve higher interfacial energy. Rubber tile and acrylic pressure sensitive adhesive exhibited the highest interfacial energy at the interface boundary. The rubber tiles as well as the acrylic both possesses moderate polar components. This

behavior can be attributed to a balance competitive electrostatic attraction and repulsion at the interface boundary. The interfacial boundary interaction between rubber tile substrate and cow skin pressure sensitive adhesive, presents a condition between high polar interaction and moderate polar interaction. Here, there is also the second highest interfacial energy recorded (for Rubber Tile). This is also traceable to a high attraction of the polar molecules of the cow skin adhesive to the pronounced dispersive components in the rubber tile. Natural rubber and epoxy adhesives each maintain a narrow differential in the interfacial energy with rubber tile. This indicates that since both share dispersive components in profound proportion, they are both attracted by the near average polar components of the rubber tile. The silicone adhesive with rubber tile interfacial boundary exhibited the lowest interfacial energy. This can be attributed to a near balance of the attraction and repulsion (components polar and dispersive) at their interfacial boundary.

4.3.1 Effect of Surface Free Energy Components on the Thermodynamic Work of Adhesion.

The thermodynamic work is the energy needed to break the force of attraction between the intermolecular forces holding the pressure sensitive adhesive and solid substrate in bond. Table4.6. enumerates the effect of the surface free energy components on the thermodynamic work of adhesion at the substrate/pressure sensitive adhesive interfacial boundary.

Table: 4.6 Substrate/Pressure Sensitive Adhesive Bond, Interfacial Free Energy Components and Thermodynamic Work of Adhesion

S/N	SUBSTRATES		PRESSURE SENSITIVE ADHESIVE	THERMODYNAMIC WORK OF ADHESION (WA) (J/m^2)	PRESSURE SENSITIVE ADHESIVE	THERMODYNAMIC WORK OF ADHESION (WA) (J/m^2)	PRESSURE SENSITIVE ADHESIVE	THERMODYNAMIC WORK OF ADHESION (WA) (J/m^2)	PRESSURE SENSITIVE ADHESIVE	THERMODYNAMIC WORK OF ADHESION (WA) (J/m^2)	PRESSURE SENSITIVE ADHESIVE	THERMODYNAMIC WORK OF ADHESION (WA) (J/m^2)
1	High Density Fibre Wood (polar)	Aluminium (polar)	Natural Rubber (Dispersive)	282.91	Epoxy (Dispersive)	275.62	Acrylic (Moderate Polar)	195.17	Silicon (Moderate Dispersive)	163.64	Cow Skin (polar)	46.86
2	Ceramic Wall Tile (polar)	Aluminium (polar)	Natural Rubber (Dispersive)	199.49	Epoxy (Dispersive)	195.12	Acrylic (Moderate Polar)	126.59	Silicon (Moderate Dispersive)	159.19	Cow Skin (polar)	6.64
3	Mild Steel (polar)	Aluminium (polar)	Natural Rubber (Dispersive)	130.60	Epoxy (Dispersive)	126.19	Acrylic (Moderate Polar)	58.15	Silicon (Moderate Dispersive)	96.11	Cow Skin (polar)	-28.33
4	Rubber Tile (Moderate polar)	Aluminium (polar)	Natural Rubber (Dispersive)	158.19	Epoxy (Dispersive)	92.58	Acrylic (Moderate Polar)	56.60	Silicon (Moderate Dispersive)	70.02	Cow Skin (polar)	-35.60

In Table 4.6, the performance of each pressure sensitive adhesive when used to bond to solid substrates and accompanying thermodynamic work of adhesion generated are expressed. In table 4.6, natural rubber pressure sensitive adhesive generated the highest amount of thermodynamic work of adhesion. This is indicative of the high dispersive component of the material. Dispersive component are positively charged and natural rubber adhesive used in the research expresses this concept. Table 4.6. Epoxy pressure sensitive adhesive exhibited the second highest value for the thermodynamic work of adhesion behind the natural rubber adhesive sensitive adhesive. Table 4.4 shows that next to the natural rubber adhesive, epoxy has the second highest dispersive component. Thus when placed between two highly polar (negative) substrates induces a high attraction favoring the formation of a strong bond. This condition is accompanied by the evolution of the second highest value for thermodynamic work of adhesion. Across the table 4.6 cow skin pressure sensitive adhesive shows the lowest value for the thermodynamic work of adhesion. When cow skin adhesive is used to bond any of the substrate, there is a possible electrostatic repulsion.

This is likely because the polar substrate will repel similar charges from a polar pressure sensitive adhesive like cow skin. This electrostatic repulsion leads to the formation of very low and negative values for the thermodynamic work of adhesion involving the cow skin adhesive. More so, from the table cow skin adhesive bond between Mild Steel and Aluminum, then between Rubber Tile and Aluminum indicates negative thermodynamic work of adhesion. It can be inferred that the negative thermodynamic work of adhesion, which indicates very poor adhesion is traceable to the values of surface free energy. Table 4.3 and Table 4.4 show that the surface free energy of the cow skin adhesive is

higher than those of mild steel and rubber tile. The resulting situation will be inability of the cow skin adhesive to wet both material and these results to improper bonding. Acrylic pressure sensitive adhesive exhibited higher thermodynamic work of adhesion for bond between high density fibre wood and aluminum compared to silicone adhesive. Across all other bonds among other substrates silicone had higher thermodynamic work of adhesion value. This behavior for silicon adhesive can be adduced to presence of silicon in the ceramic tile, rubber tile and mild steel (chemical similarity of substrates and adhesive). Thus behavior of acrylic in the bond between high density fibre wood and aluminum can be linked to the acrylic flow. Polyacrylates have higher flow ability than silicone. This makes inter atomic interaction more possible. Thus, this condition promotes mechanical interlocking, which in turn generates higher amount of energy needed to be break the bond. The higher value of thermodynamic work of adhesion for silicone pressure sensitive adhesive among other bonds is traceable to its lower surface free energy when compared with acrylic. This means silicone spread flowed across the surface than acrylic which has higher surface energy

4.3.2 Relationship between Interfacial Energy and Thermodynamic Work of Adhesion

Thermodynamic work of adhesion is derived by the use of Young Drupe Equation (Equation 4.1). This consists of the interfacial energy acting on surfaces between the adhesive/ substrate, adhesive / substrates respectively. The thermodynamic work of adhesion is a sum total of interfacial energy acting within a space.

Table: 4.7a Interfacial Energy between Substrates/ Aluminum and between Substrates/ Pressure Sensitive Adhesives (mj/m^2)

	SUBSTRATES				
Pressure Sensitive Adhesives	**High Density Fibre Wood**	**Ceramic Wall Tile**	**Mild Steel**	**Rubber Tile**	**Aluminum**
Natural Rubber	111.43	61.21	31.93	19.93	198.18
Epoxy	111.45	57.74	28.23	20.53	197.27
Cowskin	12.18	1.90	6.52	25.12	64.45
Silicon	85.83	41.96	18.13	18.12	177.12
Acrylic	70.46	32.00	12.98	27.13	125.22
SUBSTRATES/ ALUMINUM					
	29.79	59.89	99.31	125.22	-------

Table 4.7b Thermodynamic Work of Adhesion for various Pressure Sensitive Adhesives across Bond Surfaces

Natural Rubber Pressure Sensitive Adhesives		**Epoxy Pressure Sensitive Adhesive**		**Acrylic Pressure Sensitive Adhesive**		**Cow Skin Pressure Sensitive Adhesive**		**Silicon Pressure Sensitive Adhesive**	
BOND SURFACES	**THERMODYNAMIC WORK OF ADHESION (J/m^2) (W_A)**	**BOND SURFACES**	**THERMODYNAMIC WORK OF ADHESION (J/m^2) (W_A)**	**BOND SURFACES**	**THERMODYNAMIC WORK OF ADHESION (J/m^2) (W_A)**	**BOND SURFACES**	**THERMODYNAMIC WORK OF ADHESION (J/m^2) (W_A)**	**BOND SURFACES**	**THERMODYNAMIC WORK OF ADHESION (J/m^2) (W_A)**
High Density Fibre Wood-Natural Rubber-Aluminum	282.91	High density Fibre Wood-Epoxy-Aluminum	275.62	High Density fibre Wood-Acrylic-Aluminum	195.17	High Density Fibre Wood – Cow Skin – Aluminum	46.86	High Density Fibre Wood –Silicon - Aluminum	163.64

Ceramic wall tile -Natural Rubber - Aluminum	199.44	Ceramic Wall Tile- Epoxy- Aluminum	195.10	Ceramic Wall Tile – Acrylic – Aluminum	126.59	Ceramic Wall tile – cow Skin – Aluminum	6.64	Ceramic Wall tile –Silicon - Aluminum	159.19
Mild Steel –Natural Rubber - Aluminum	130.60	Mild Steel- Epoxy- Aluminum	126.19	Mild Steel – Acrylic - Aluminum	58.15	Mild Steel –Cow Skin - Aluminum	-28.33	Mild Steel –Silicon - Aluminum	96.11
Rubber Tile -Natural Rubber - Aluminum	158.19	Rubber Tile – Epoxy - Aluminum	92.58	Rubber Tile – Acrylic -Aluminum	56.60	Rubber Tile –Cow Skin - Aluminum	-35.60	Rubber Tile – Silicon - Aluminum	70.02

Natural Rubber Pressure Sensitive Adhesive shows a decrease across Table 4.7a with regards to interfacial energy value. The decrease in values is viewed from High Density fibre wood, Ceramic wall tile, mild steel then Rubber tile (viewing from left to right). Correspondingly in Table 4. 7b, there is similarly a decrease in the value of the thermodynamic work of adhesion value with exception of Rubber tile. The rubber tile has an interfacial energy value of 19.93mJ/m^2 but with a thermodynamic work of adhesion value of 158.19mJ/m^2. This value of thermodynamic work of adhesion is higher when compared to Mild steel which is the nearest in value; with a thermodynamic work of adhesion value of 130.60mJ/m^2. In the contrast,mild steel exhibited a higher interfacial energy with Natural rubber pressure sensitive adhesive as shown in Table 4.7a. The higher work of adhesion value for Rubber tile can be attributed to higher interfacial and inter molecules interaction between similar molecules. Rubber tile consist of predominantly silicone (67.36%). The Natural rubber adhesives is made of light magnesium. Silicone and Magnesium favorable combined to

produce a dense cross link. The decrease in the values of the interfacial energy across the boundaries of the substrate with natural rubber pressure sensitive adhesive shows the strength of the interfacial energy. This corresponds with the values of thermodynamic work of adhesion for same natural rubber pressure sensitive adhesive, but with the exception of rubber tile. The rubber tiles varies in value for reasons given above. Otherwise for Natural rubber pressure sensitive adhesive bonds, the interfacial energy strength takes the trend as follows: High density fibre wood > Ceramic wall tile> Mild steel> Rubber tile. Considering thermodynamic work of adhesion is for interfaces, involving natural rubber pressure sensitive adhesive, with the exception of rubber tile. The strength across the substrate is as follows: High density fibre wood> Ceramic wall tile> Rubber tile> Mild steel. The interfacial energy between the natural rubber pressure sensitive adhesive and aluminum is constant at 198.18mJ/m^2. This is because the aluminum and the natural rubber adhesive is always together for every bond while other surfaces vary.

Epoxy pressure sensitive adhesive, there is a decrease in the values of interfacial energy between it and substrates. This is as follows: High density fibre wood> Ceramic wall tile> Mild steel> Rubber tile. This is corresponding to the values of the thermodynamic work of adhesion for epoxy involving same substrate. The values are as follows: High density fibre wood> Ceramic wall tile> Mild steel> Rubber tile. The interfacial energy between Epoxy pressure sensitive adhesive and aluminum is constant at 197.27mJ/m^2. This is because the aluminum and the epoxy adhesive is always together for every bond, where other surfaces vary. Thus for bonds involving epoxy pressure sensitive adhesive, it can be inferred that a decrease in strength of thermodynamic work of adhesion corresponds with a decrease in the interfacial energy across each bond. High

density fibre wood with epoxy pressure sensitive adhesive can be inferred to exhibit the most excellent bond strength across all bond arrangement. This is followed by Ceramic wall tile, Mild steel and lastly, Rubber tile.

Acrylic pressure sensitive adhesive shows a decrease in interfacial energy across the substrate in Table 4.7a, with the exception of rubber tile. Rubber tile exhibited higher interfacial energy than Mild steel according to the table. However the values of thermodynamic work of adhesion for bonds involving epoxy adhesive decrease as follows: High density fibre wood> Ceramic wall tile> Mild steel> Rubber tile. The interfacial energy between the acrylic pressure sensitive adhesive and aluminum is constant at 125.22mJ/m^2. This is related to the position of aluminum and the acrylic in the bond pair. They are always together for every bond while the surfaces vary. The higher value for the interfacial energy for rubber tile (27.13mJ/m^2) with regard to Mild steel (12,98mJ/m^2) is suspected to be due to the difference in their rheological properties. The rheological properties involved here are related to their glass transition temperatures and damping factor. Cow skin pressure sensitive showed a decrease in the values of thermodynamic work of adhesion from High density fibre wood to Rubber tile in Table 4.7a. Contrarily for Table 4.7a. Cow skin adhesive does not follow the same trend. Here the interfacial energy between Mild steel/ Cow skin and Rubber tile/ Cow skin contradicts the trend. This difference in the behavior of these substrates with cow skin adhesive can be traced to their surface free energy values (Tables 4.3 and 4.4).

The cow skin pressure sensitive adhesive (54.20mJ/m^2) is higher than surface free energy for Mild steel (28.91mJ/m^2), and Rubber tile (36.50mJ/m^2). This surface energy differential determines the interfacial behavior of the adhesives. Thus the higher surface free energy of the cow skin adhesive prevented it from

wetting both substrates surface. There was a limitation of spreading of the cow skin adhesive due to this surface energy differential between the adhesive and the substrate. This phenomenon caused limited adhesion, which is indicated by the negative thermodynamic work of adhesion. Silicone pressure sensitive adhesive shows a decrease in the values of the interfacial energy from High density fibre wood to Rubber tile in Table 4.7a. Table 4.7b shows a corresponding decrease in the values of the thermodynamic work of adhesion across each bond pair. Thus it can be inferred than a decrease in the thermodynamic work of adhesion corresponds to the decrease in the interfacial energy for silicone adhesive. The interfacial energy between silicone pressure sensitive adhesive and aluminum is constant at 177.12mJ/m^2. Table 4.7a shows a rise in the interfacial energy between each substrate and aluminum (the emergency sign bearer), ranging from High density fibre wood to Rubber tile. The substrates are all dominated by the pronounced polar component except rubber tile. The high polarity across each substrate surface determines the level of electrostatic repulsion between substrate at interface boundary. Thus the interfacial energy and arrangement of the substrate can be traced to level of electrostatic repulsion strength across each substrate bond at interface.

4.3.3 Analysis of the relationship between Surface Finish among substrates and Thermodynamic work of adhesion for each bond surface

Surface finish measured the overall texture of the substrate (Wall) surface. It measured the surface Lay, surface roughness, waviness. It characterized the surface quality and measure itssynchronism with dissolved quality. The substrates used in the research work were earlier engineered to serve different needs. Each surface had its own distinct characteristic and peculiarity. For the

research the substrates with the exemption of Aluminium were considered as wall surfaces. Thus they were each tested for adhesion.

Table 4.7c: Result of Surface Finish Measurement for different Substrates

S/N	Sample Description	Sample Code	Surface Finish (μm)
1	High Density Fibre wood	A	0.0817
2	Ceramic Wall Tile	B	1.159
3	Carbon Steel (Mild steel)	C	1.657
4	Rubber tile	D	4.412
5	Aluminium	E	1.635

Aluminium was exempted in the Analysis as it was not considered a wall substrate/ surface. Comparison of data enumerated from the measure of surface finish

(Table 4.11) and Thermodynamic work of adhesion for various Pressure Sensitive Adhesives across bond surfaces (Table 4.7b) shows the following:

1. High Density Fibre Wood generated the highest Thermodynamic work of adhesion across bond surfaces (Table 4.7b). This corresponds to a surface finish measurement of 0.0817μm (Table 4.7c)
2. Ceramic Wall Tile generated the second highest Thermodynamic work of adhesion across bond surfaces (Table 4.7b). This corresponds to a surface finish measurement of 1.159μm (Table 4.7c)
3. Carbon Steel (Mild steel) generated the third highest Thermodynamic work of adhesion across bond surfaces (Table 4.7b). This corresponds to a surface finish measurement of 1.657μm. (Table 4.7c)

4. Rubber Tile generated the least Thermodynamic work of adhesion across bond surfaces (Table 4.7b). This corresponds to a surface finish measurement of 4.412µm. (Table 4.7c)

Thus it can be inferred that the surface finish or surface texture across the substrate influence the thermodynamic work of adhesion for each surface. Secondly for the substrate used in the research work, the higher the surface finish, the higher the thermodynamic work of adhesion.

Predictive models analyzed the relationship between substrates surface texture and thermodynamic work of adhesion. Results obtained, showed that higher surface texture produced higher thermodynamic work of adhesion. Figures 4.1, 4.2, 4.3, 4.4 and 4.5 illustrated scattered plot relationships generated between surface finishes of various substrate surfaces and thermodynamic work of adhesion at respective bond surfaces.

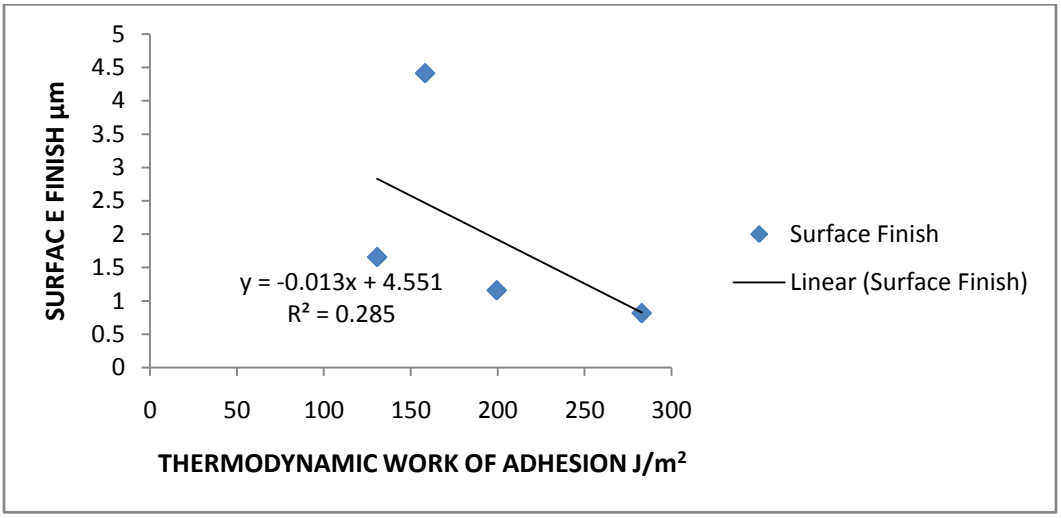

Figure 4.1: Scattered plot of surface finish against thermodynamic work of adhesion for natural rubber pressure sensitive adhesive

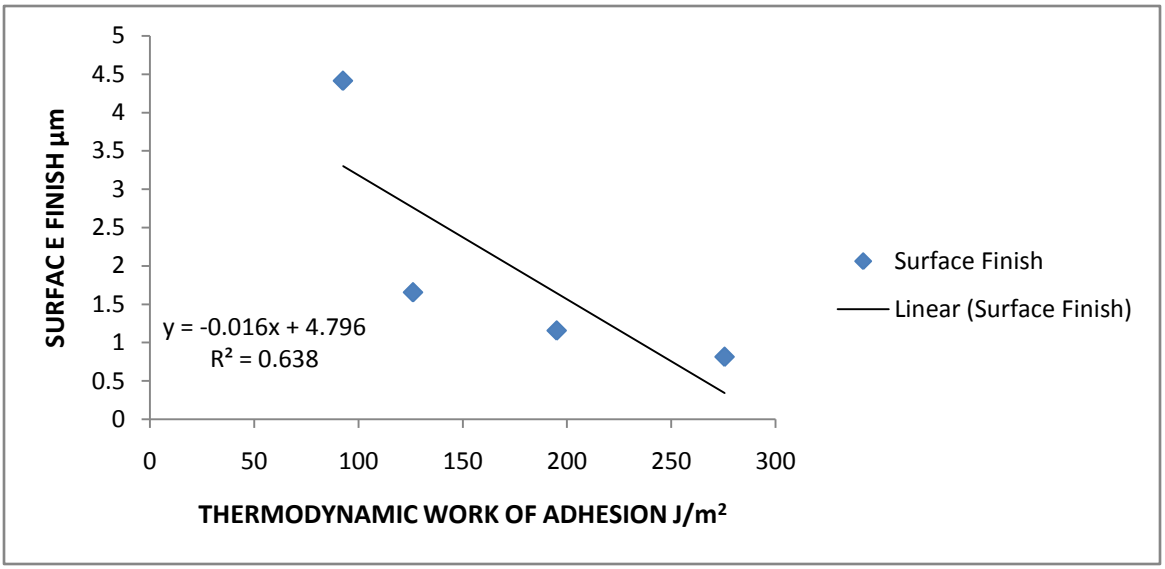

Figure 4.2: Scattered plot of surface finish against thermodynamic work of adhesion for epoxy pressure sensitive adhesive

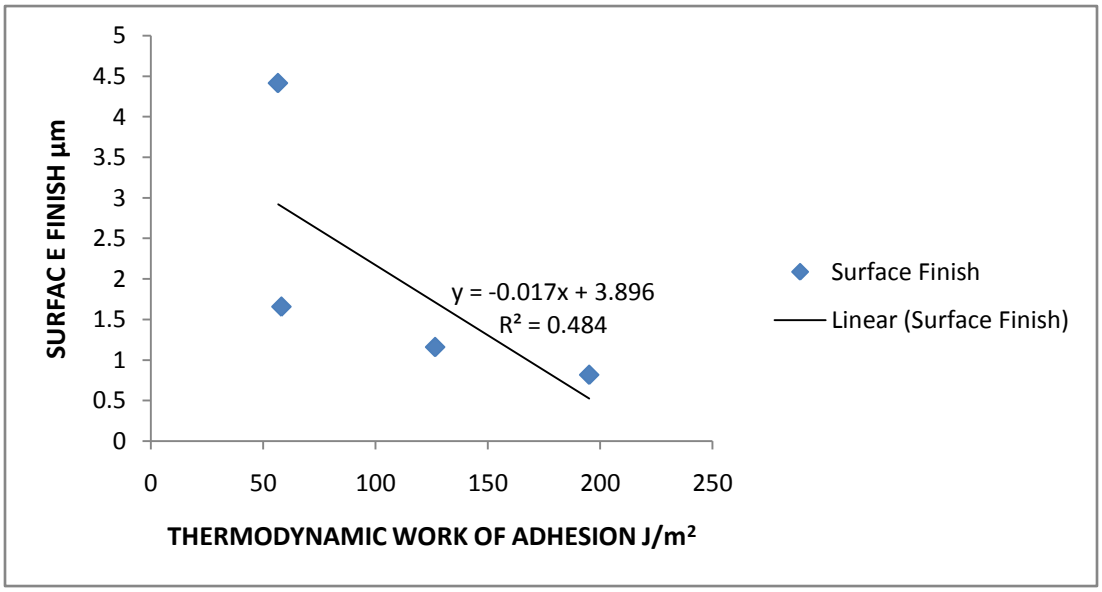

Figure 4.3: scattered plot of surface finish against thermodynamic work of adhesion for acrylic pressure sensitive adhesive

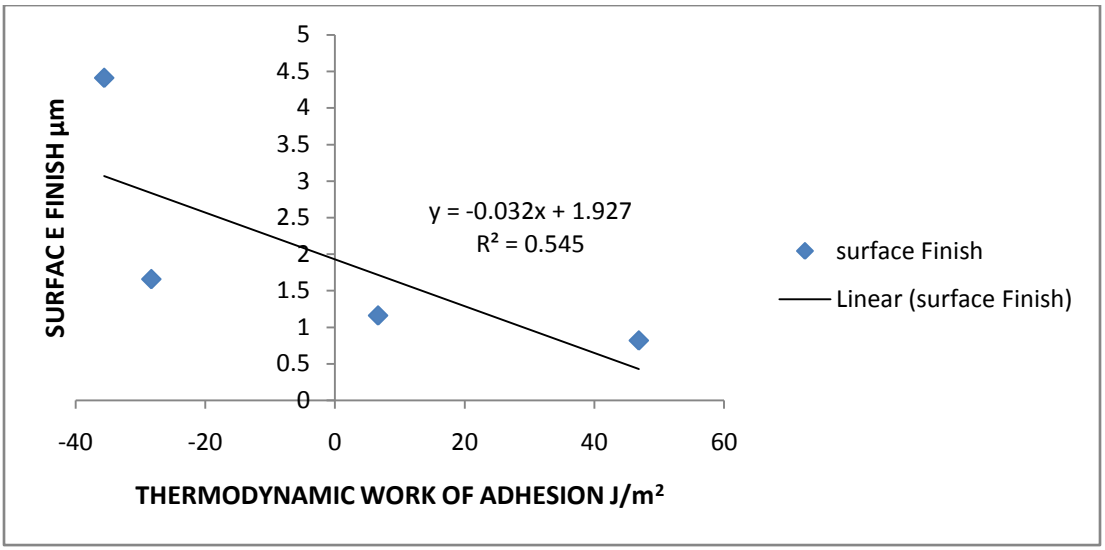

Figure 4.4: Scattered plot of surface finish against thermodynamic work of adhesion for cow skin pressure sensitive adhesive

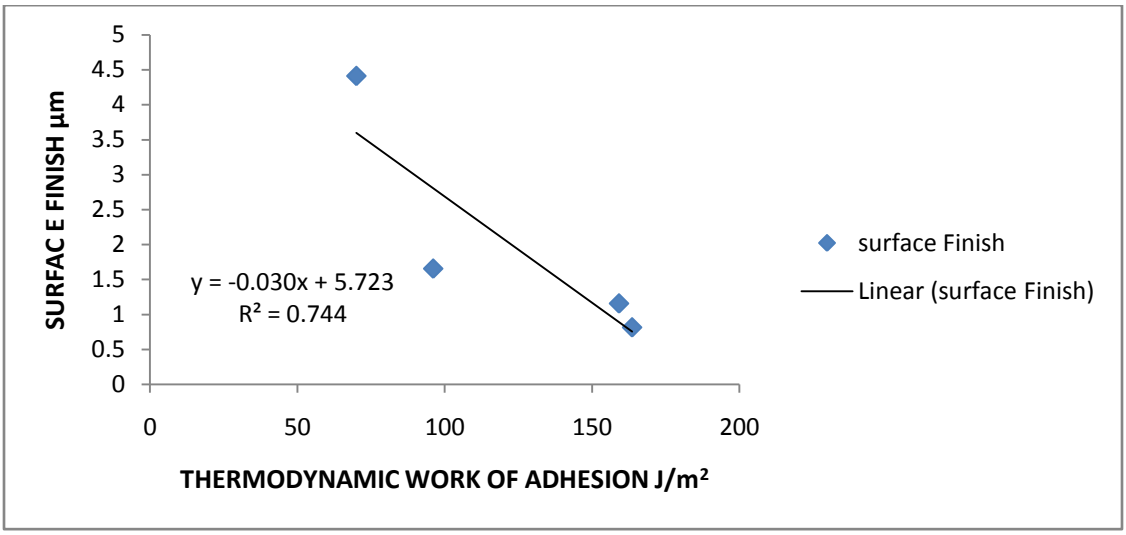

Figure 4.5: Scattered plot of surface finish against thermodynamic work of adhesion for silicon pressure sensitive adhesive

4.4 Result of Mechanical Test for Fracture Energy.

The fracture energy and accompanying information for each bond pair is expressed in stress-strain graph relation. Figure 4.6 gives an enumeration of the graphs and interpretation of particular interfacial parameters attached to it.

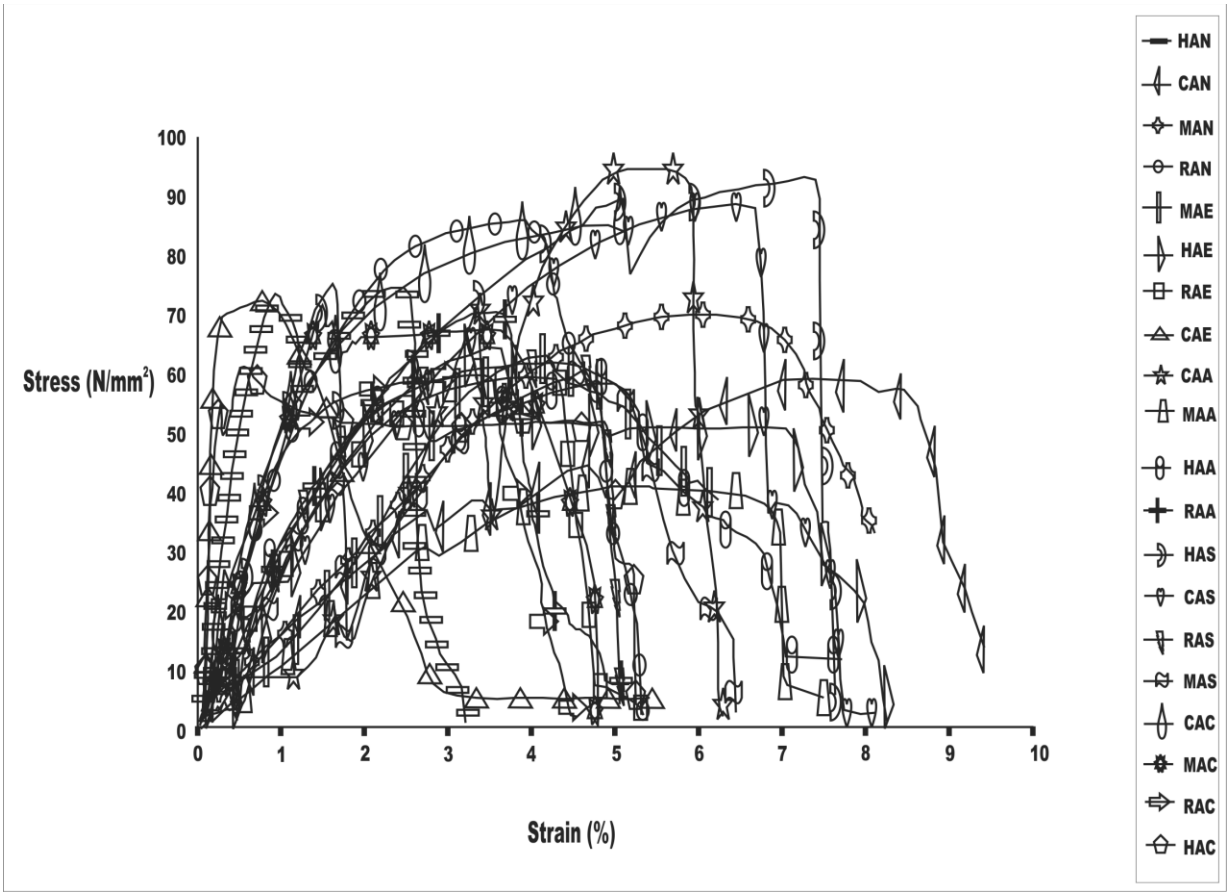

Figure 4.6 Stress-Strain Graph for Substrates and Adhesives

HAN represents, Stress-Strain between High Density Fibre Wood surface and Aluminum surface bond by Natural Rubber adhesive. This is a bond where a high density fiber wood surface and aluminum surface is bond with a natural rubber pressure sensitive adhesive. The stress-strain graph shows a homogenous deformation across the bond, which is accompanied by a plastic deformation. The plastic deformation marks the beginning of the crack formation, which continues till point of yield stress. At the yield stress there is an initiation of cavity formation. Thus crack formation is delayed because of cavity formation. From the point of peak stress there is a sudden drop at the shoulder, and a display of slight hardening. After the shoulder drop, fibrillation ensues, leading

to maximum extension and eventual break. The graph of the stress-strain graph indicates a Brittle Failure.

CAN represents, Stress-Strain between Ceramic wall Tile surface and Aluminum surface bond by Natural Rubber adhesive. This is a bond where a ceramic wall tile surface and aluminum surface is bond by a natural rubber pressure sensitive adhesive. There is no noticeable homogenous deformation across the bond. Contrarily, plastic deformation is spontaneously induced from point of origin. This is followed by the initiation of interfacial crack propagation, before the commencement of cavitation. Cavitation starts at the yield stress point. There is a strain hardening between the yield stress point and the point of maximum peak stress. The shoulder shown in the graph steeps to induce fibrillation; leading to eventual collapse of the bond without thinning and in the presence of limited extension. The failure observed is as a result of Adhesive Debond with strain hardening.

MAN represents, Stress-Strain between Mild steel surface and Aluminum surface bond by Natural Rubber adhesive. Here the bond is between a mild steel surface and aluminum surface, held by a natural rubber pressure sensitive adhesive. There is a lack of homogenous deformation across the bond. The bond undergoes an immediate plastic deformation where crack propagation starts. The growth of the cavity is triggered at point of yield stress (cavitation initiation) as a result of the crack propagation. The growth of the cavity is exacerbated because of the extremely low difference in the yield stress and peak stress. Beyond the point of peak formation, fibrillation occurs leading to a breakdown of the bond. Meanwhile the maximum extension proceeds at a moderate growth and an Adhesive Debond occurs.

RAN represents, Stress-Strain between Rubber Tile surface and Aluminum surface bond by Natural Rubber adhesive. The bond present is between a rubber tile surface bonds to an aluminum surface by a natural rubber pressure sensitive adhesive. The graph shows a non-homogenous deformation across the bond, accompanied by early plastic deformation (crack propagation). The crack propagation at the interface eventually leads to cavitation at the point of yield stress. This leads to rapid cavity growth, followed by formation of slight shoulder. Fibrillation starts from the point of shoulder and the process is prolonged to thinning and eventual bond failure. The extension is moderate and the bond failure is attributed to adhesive debond.

MAE represents, Stress-Strain between Mild Steel surface and Aluminum surface bond by Epoxy adhesive. This is a case where the mild steel surface is bond to an aluminum surface by epoxy pressure sensitive adhesive. The peak stress and yield stress have exactly the same value. There is no homogenous deformation, but an accelerated plastic deformation, while the crack propagation is initiated at the interface. Cavitation starts at the yield stress point lea2ding to early multiple cavity growth. The bond experienced a slight strain hardening, between the point of yield stress and peak stress. Beyond the peak stress, fibrillation starts and this leads to bond collapse, and there is moderate extension (strain) growth. The bond failure is indication of an Adhesive Debond.

HAE represents, Stress-Strain between High Density Fibre wood surface and Aluminum surface bond by Epoxy adhesive. Here, there is a bond between high density fibre wood surface and an aluminum surface held by an epoxy pressure sensitive adhesive. The stress-strain graph indicates slight homogenous deformation. The peak stress and the yield stress are extremely closed. This

leads to early cavitation, and the horizontal line signifies the presence of prolonged strain hardening. Fibrillation starts after the steep of the shoulder. The fibrillation bond prolonged leading to thinning, limited extension (strain) and eventual bond failure. The bond failure indicates an Adhesive Debond.

RAE represents, Stress-Strain between Rubber Tile surface and Aluminum surface bond by Epoxy adhesive. This shows a bond where the rubber tile surface and aluminum surface is held together by an epoxy pressure sensitive adhesive. The graph shows slight homogenous deformation, pronounced plastic deformation, and long crack propagation at the interface. The graph suggests a short time for growth of cavity, multiple cavity growth. Cavitation is spontaneous between yield stress and peak stress and the shoulder is pronounced, beyond the peak stress. The steep shoulder suggests prolonged fibrillation, leading to thinning out and bond failure. There is also a moderate extension. The bond failure suggests a Cohesive Debond.

CAE represents, Stress-Strain between Ceramic wall tile surface and Aluminum surface bond by Epoxy adhesive. This shows a bond between ceramic wall tile surface and aluminum surface bond together by an epoxy pressure sensitive adhesive. The graph shows a prolonged homogenous deformation across the bond. There is crack propagation along the interface, cavitation and steep shoulder. There is a close value between the yield stress and peak stress. This indicates a rapid growth of cavity. Beyond the shoulder there is a long steep which suggests a long thinning out, pronounced extension and eventual bond collapse. The bond failure suggests a Cohesive Debond.

CAA represents, Stress-Strain between Ceramic Wall Tile surface and Aluminum surface bond by Acrylic adhesive. The surfaces arebond together by an acrylic

pressure sensitive adhesive. Here, there is slight homogenous deformation across the bond. The yield stress and peak stress have a profound difference, alongside a pronounced strain hardening. At the point of plastic deformation the interfacial crack propagation is prolonged, and accompanied by a growth of cavity at the yield point. The bond exhibits a long fibrillation, thinning and eventual bond failure. The bond failure suggests an AdhesiveDebond, with strain hardening.

MAA represents, Stress-Strain between Mild Steel surface and Aluminum surface bond by Acrylic adhesive. This shows a bond between mild steel surface and aluminum surface bond by an acrylic pressure sensitive adhesive. The graph shows no homogenous deformation across the bond, and long interfacial crack propagation. There is a close value between the yield stress and peak stress. It shows a sharp shoulder, with prolonged fibrillation, long strain hardening, and slight thinning. The closeness between the peak stress and yield stress suggests a competitive cavity growth and cavitation initiation. At the bond break down the graph indicates an Adhesive Debond and moderate extension with strain hardening.

HAA represents, Stress-Strain between High density Fibre wood surface and Aluminum by bond by Acrylic adhesive. This bond between a high density fibre wood surface and an aluminumsurface bond by an acrylic pressure sensitive adhesive.The graph shows no homogenous deformation across the bond, with slight difference in the value of the yield stress and the peak stress. There is a competitive growth of the cavity and cavitation increase, probably for the nearness of yield stress and peak stress. The fibrillation is prolonged, thinning is pronounced with a limited extension. Meanwhile there is a plastic deformation

line which indicates Crack Propagation. The failure across the bond is in indicative of mixed debond (pronounced adhesive debond and slight cohesive debond).

RAA represents, Stress-Strain between Rubber Tile surface and Aluminum surface bond by Acrylic adhesive. This is an interface between a rubber tile surface and aluminum surface bond together by an acrylic pressure sensitive adhesive. The graph shows a non-existing homogenous deformation across the bond. The close nature of the yield stress and peak stress aids in the growth of the cavity at the yield stress point. There is a noticeable fibrillation, beyond the peak stress, pronounced thinning, limited extension. The plastic deformation process proceeds immediately from point of origin depicting resistance to flow. The failure across the bond is indicative of an Adhesive Debond.

HAS represents, Stress-Strain between High density Fibre wood surface and Aluminum surface bond by a Silicone adhesive. This is a bond between a high density fibre wood surface and aluminum surface bond by a silicone pressure sensitive adhesive. The graph shows a slight homogenous deformation, prolonged crack propagation at the interface. There is a good difference between the peak stress and yield stress. This favors cavitation, and delayed cavity growth, with moderate extension growth. The difference between the yield stress and peak stress aid in the formation of long strain hardening. The sharp shoulder is followed by long fibrillation and eventual bond failure. The bond failure here indicates an Adhesive Debond, with strain hardening.

CAS represents, Stress-Strain between Ceramic Wall Tile surface and Aluminum surface bond by a Silicone adhesive. This is a bond between a ceramic wall tile surface and aluminum surface held by a silicone pressure sensitive adhesive.

The graph shows slight homogenous deformation, prolonged crack propagation, good strain hardening as result of noticeable difference between the yield stress and peak stress. The graph shows the presence of delayed cavitation at the yield stress, then a moderate extension growth and good thinning. The sharp shoulder in the graph is followed by a long fibrillation and eventual bond failure. The bond failure indicates an Adhesive Debond, with strain hardening.

RAS represents, Stress-Strain between Rubber Tile surface and Aluminum surface bond by a Silicone adhesive. This is a bond between a rubber tile surface and aluminum surface held by a silicone pressure sensitive adhesive. The graph shows no homogenous deformation across the bond. The plastic deformation aids crack propagation. The close yield stress and peak stress values indicates a competitive cavity growth. Beyond the peak stress there is a pronounced shoulder, which steeps, and fibrillation accompanies the steep. Thereafter it leads to a breakup of the bond. The bond failure indicates an Adhesive Debond.

MAS represents, Stress-Strain between Mild Steel surface and Aluminum surface bond by Silicone adhesive. This is a bond in which a mild steel surface and aluminum surface held by a silicone pressure sensitive adhesive. The graph shows a slight homogenous deformation, and difference between the peak stress and yield stress. The plastic deformation helps the interfacial crack propagation while there is strain hardening, traceable to the difference in the peak and yield stress. There is a long-extension, subsequent thinning and bonding failure. Cavitation in the graph occurs after steep shoulder. The bond failure indicates an Adhesive Debond, with strain hardening.

CAC represents, Stress-Strain between Ceramic Wall Tile surface and Aluminum surface bond by a Cow Skin adhesive.This is a bond in which the ceramic wall tile

surface and aluminum surface is held together by a cow skin pressure sensitive adhesive. There is a remarkable difference between the value of the peak stress and yield stress, traceable to strain hardening. However there is poor extension, presence of plastic deformation leading to cavitation. At the yield stress cavitation develops accompanied by cavity growth fibrillation and eventual bond failure. The failure across the bond is indicative of an Adhesive Debond, with strain hardening.

MAC represents, Stress-Strain between Mild Steel surface and Aluminum surface bond by a Cow Skin adhesive. This is a bond in which a mild steel surface and aluminum surface is held together by cow skin pressure sensitive adhesive. The graph shows no homogenous deformation across the bond, slight difference between the yield stress and peak stress. Despite the slight difference between the yield stress and peak stress, there is noticeable strain hardening as an effect of suspected delayed cavitation. The shoulder is steep, leading to fibrillation and thinning. There is a crack propagation indicating a plastic deformation. The graph shows a noticeable extension and bond failure. The failure across the bond is indicative of an Adhesive Debond, with strain hardening.

RAC represents, Stress-Strain between Rubber Tile and Aluminum surface bond by a Cow Skin adhesive. This bond is between an aluminum surface and rubber tile surface held together by a cow skin pressure sensitive adhesive. From the graph the peak stress and yield stress are all most equivalent. There is a moderate extension, strain hardening as a result of suspected delay in cavitation. The plastic deformation accompanied the crack propagation. The break down in the bond is preceded by a thinning across the bond. The failure across the bond indicates an Adhesive Debond, with strain hardening.

HAC represents, Stress-Strain between High Density Fibre Wood Surface and Aluminum surface bond by a Cow Skin adhesive. There is a bond between an aluminum surface and high density fibre wood surface held by a cow skin pressure sensitive adhesive. The graph shows no homogenous deformation across the bond. There is a plastic deformation indicating crack propagation. Cavitation starts at the yield stress and cavity growth accelerates to peak stress. The graph shows a sharp shoulder after which shows a fibrillation, then thinning and eventual bond break down. The failure across the bond indicates an Adhesive Debond.

4.5 Analysis of relationships: between dispersive and polar components of surface free energy for substrates and pressure sensitive adhesives, thermodynamic wok of adhesion and fracture energy across different bond types.

Energy is consumed during the breakage of a bond. The thermodynamic work of adhesion measures the theoretical or physical adhesion. The fracture energy measures the practical adhesion. Energy consumed during the breaking of bond (fracture) is lost due to dissipation and viscoelastic deformation. The electrostatic model adhesion assumes that during adhesion, either the substrate or the adhesive is positive, while the other is negative. This model is particularly applicable where fracture or debond has taken place across a bond. Thus the inter-molecular forces of dispersive and polar forms built around dipoles-dipoles, Vander Waals and acid-base interaction exist at the adhesion interface. These forces play major roles in defining the adhesion behavior at any interface.

Table 4.8 Thermodynamic Work of Adhesion and Fracture Energy for each Bond type

	ACRYLIC/ALUMINUM		EPOXY/ ALUMINUM		NATURAL RUBBER/ ALUMINUM		SILICON/ ALUMINUM		COW SKIN/ ALUMINUM	
	FRACTURE ENERGY IN (Nm)	THERMODYNAMIC WORK OF ADHESION (J/m^2)	FRACTURE ENERGY IN (Nm)	THERMODYNAMIC WORK OF ADHESION (J/m^2)	FRACTURE ENERGY IN (Nm)	THERMODYNAMIC WORK OF ADHESION (J/m^2)	FRACTURE ENERGY IN (Nm)	THERMODYNAMIC WORK OF ADHESION (J/m^2)	FRACTURE ENERGY IN (Nm)	THERMODYNAMIC WORK OF ADHESION (J/m^2)
SUBTRATE										
HIGH DENSITY FIBRE WOOD	9.436	195.170	36.558	126.190	8.121	282.910	11.737	163.64	1.796	46.860
CEREMIC WALL TILE	7.035	126.590	7.154	275.620	4.489	199.490	5.316	154.19	4.148	6.640
MILD STILL	36.430	68.150	7.217	92.580	53.917	130.600	52.712	96.11	59.545	-28.330
RUBBER TILE	5.058	56.600	2.203	195.12	7.463	158.19	7.591	70.02	8.788	-35.600

Table 4.8 expresses the value of thermodynamic work of adhesion and fracture energy for each bond type. The bond type consists of each substrate and accompanying bond pairs. The bond pair is a collection of interfacial relation between each pressure sensitive adhesive and aluminum (the sign board). In the table, it is expressed that each fracture energy value is enormously larger than its corresponding thermodynamic work of adhesion for each bond type. However, the significant different in the value of the two interfacial parameters can be linked to observations made at tensile test. During tensile test there is a significant amount of viscoelastic energy generated due to deformation of pressure sensitive adhesive layers. The viscoelastic energy, though cannot be quantified by this research work consist of the thermodynamic work of adhesion and viscoelastic energy. Analytical tools such as Minitab plot, Microsoft Excel, Statistical Package for Social Science were employed to analyze data derived from the research.

4.5.1 Analysis of the relationship between Thermodynamic work of Adhesion and Fracture Energy

This was used to investigate the relationship between the Thermodynamic work of adhesion and Fracture Energy. Scattered Plots of thermodynamic work of adhesion and fracture energy showed predictive models for respective pressure sensitive adhesives used for the study. The predictive models showed that fracture energy across interfacial bonds decreased with decreasing thermodynamic work of adhesion. Figure 4.7, 4.8, 4.9, 4.10 and 4.11 showed scatter plots between fracture energy and thermodynamic work of adhesion for epoxy, acrylic, natural rubber, silicon and cow skin pressure sensitive adhesives respectively.

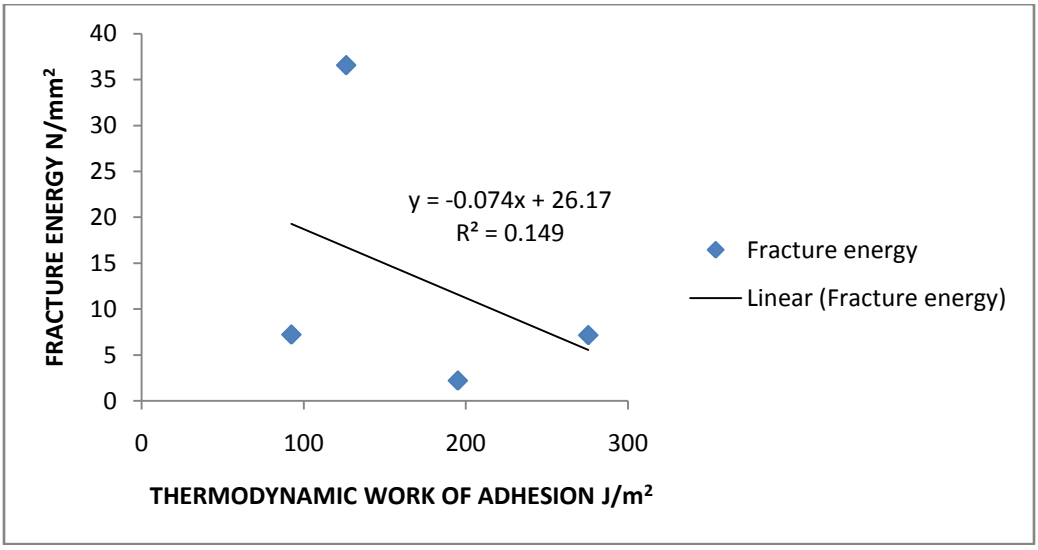

Figure 4.7: Scattered plot of fracture energy against thermodynamic work of adhesion for epoxy pressure sensitive adhesive

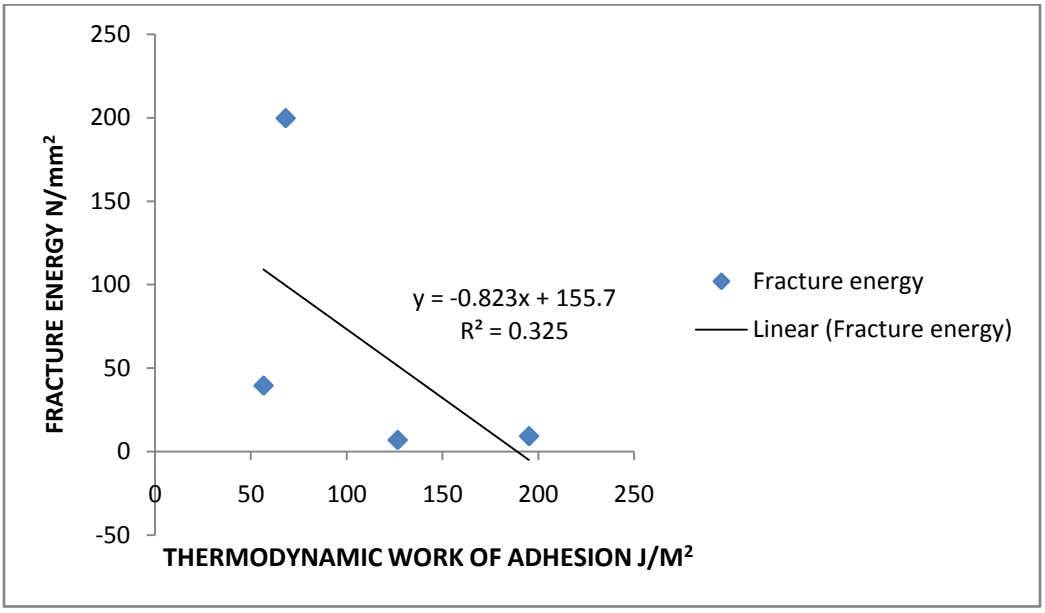

Figure 4.8: Scattered plot of fracture energy against thermodynamic work of adhesion for acrylic pressure sensitive adhesive

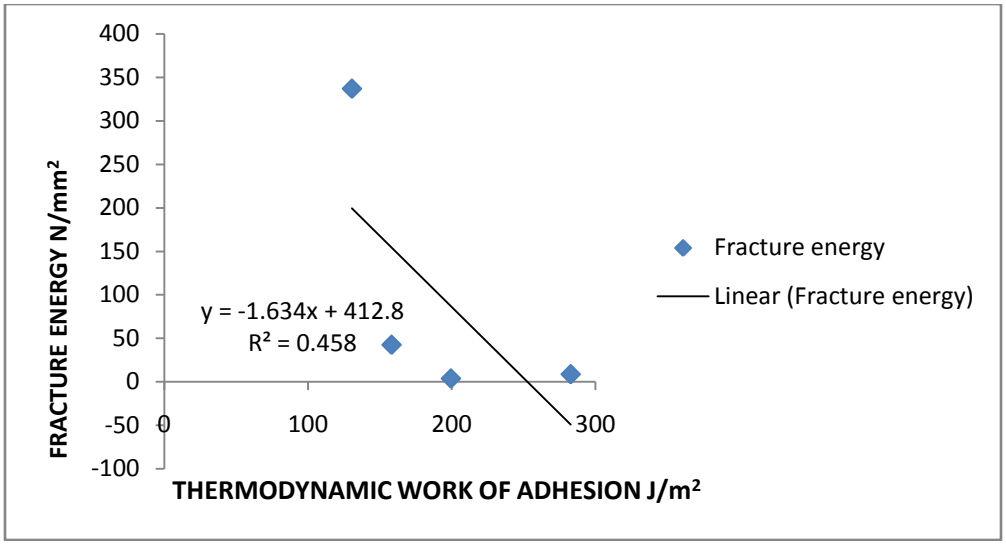

Figure 4.9: Scattered plot of fracture energy against thermodynamic work of adhesion for natural rubber pressure sensitive adhesive

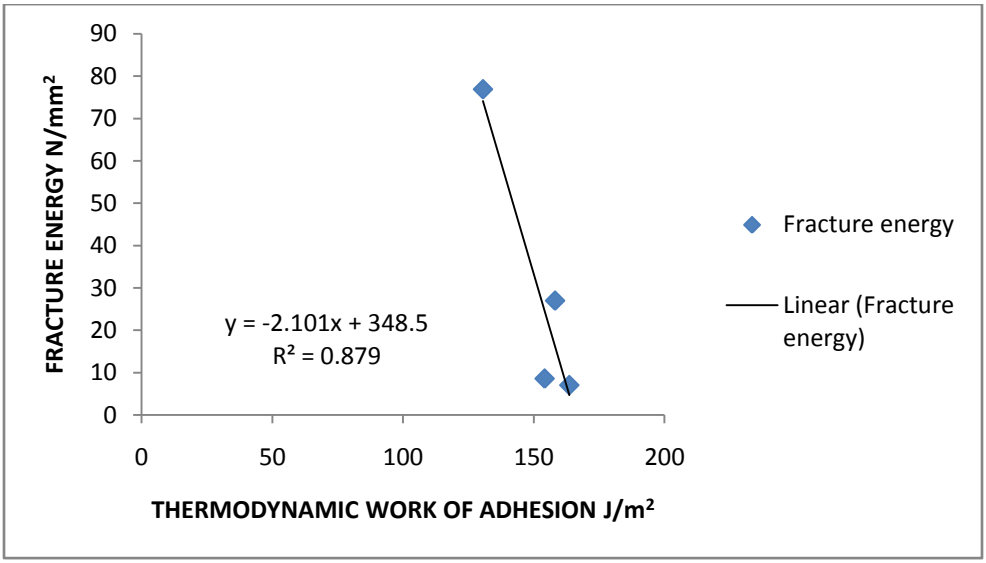

Figure 4.10: Scattered plot of fracture energy against thermodynamic work of adhesion for silicon pressure sensitive adhesive

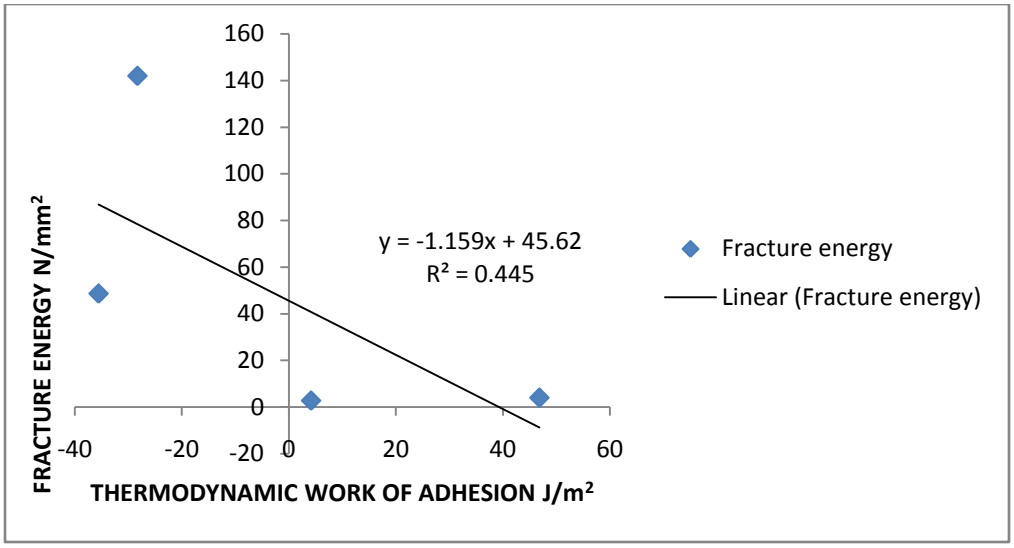

Figure 4.11: Scattered plot of fracture energy against thermodynamic work of adhesion for cow skin pressure sensitive adhesive

4.5.2 Analysis of the Relationship between Dispersive and Polar Component of

Surface Energy for both Substrates and Pressure Sensitive Adhesive

The relationship between the polar component and dispersive components of the surface free energy for both substrates and pressure sensitive adhesive, were used to derive surface free energy for both materials. This was done by the use and implementation of scatter plot of the Fowkes equation on both materials. These relationships were analyzed as follows:

(1) Microsoft Excel

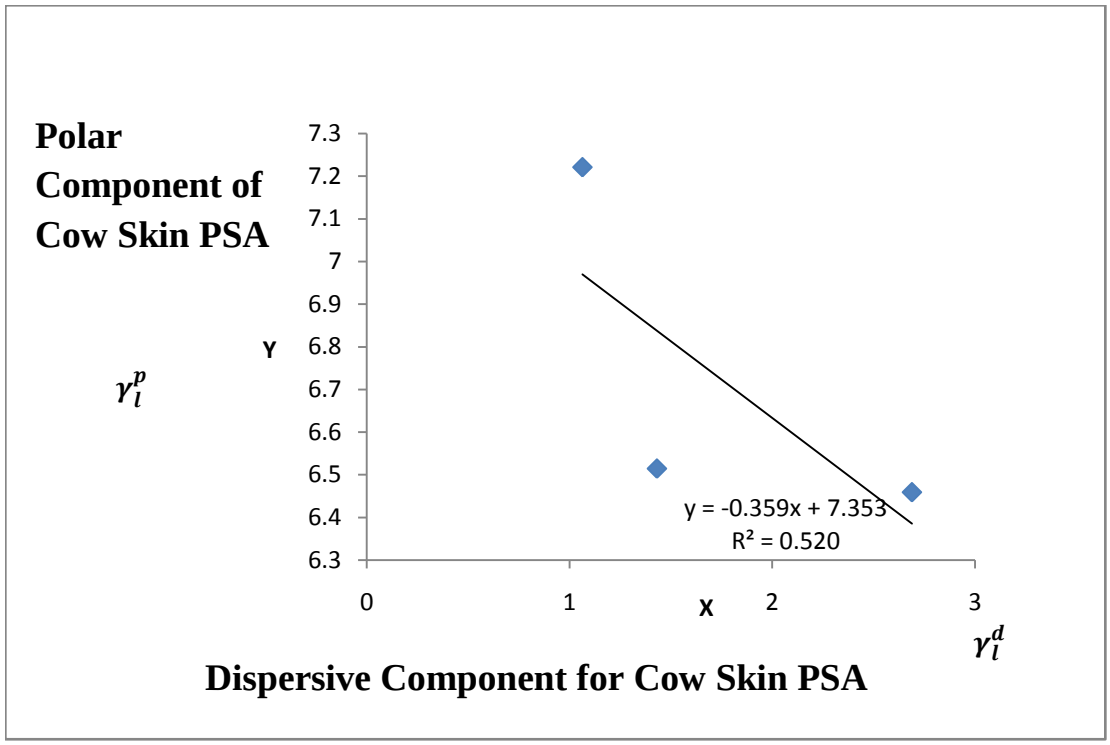

Figure: 4.12Scatter Plot for Cow Skin Pressure Sensitive Adhesive to Derive Surface Free Energy for the Adhesive

Figure 4.12 shows a scatter plot graph. This scatter plot graph was obtained by plotting the polar and dispersive component of the 3 test liquids using the Fowkes equation. The graphical analysis resulted in a regression equation $Y = -0.3599x + 7.3533$. the sum of the squares of the intercept and slope was used to determine the surface free energy of Cow skin pressure sensitive adhesive. The coefficient of determination R^2= 0.5206 or 52.1%. This regression analysis shows that the dependent variable Y representing the surface free energy of cow skin adhesive can be predicted by the result of the values of the polar and dispersive component (independent variables). It shows a strong

relationship between the values of the surface free energy for the cow skin pressure sensitive adhesive and its component (adhesive and polar) surface free energy good regression.

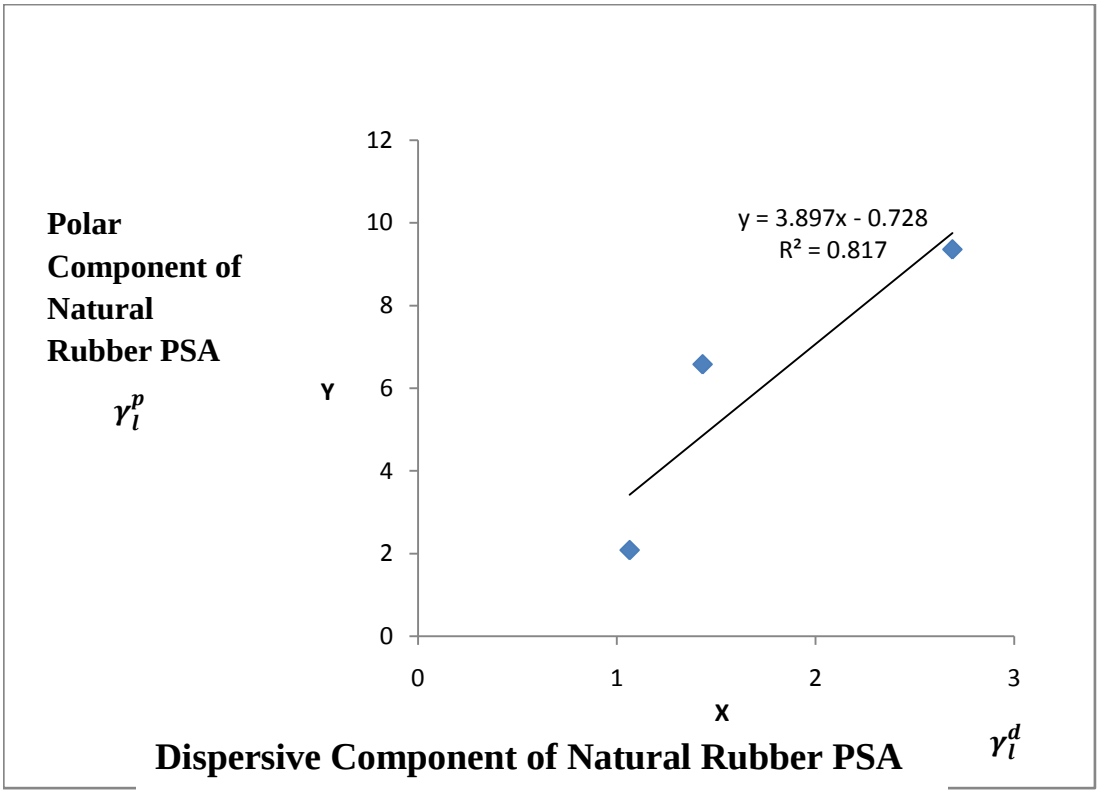

Figure: 4.13Scattered Plot for Natural Rubber Pressure Sensitive Adhesive

Figure 4.13 is the Fowkes Equation Scattered Plot for Natural Rubber Pressure Sensitive Adhesive. It has a linear regression equation $y = 3.8976x - 0.7286$ and coefficient of determination of 0.8173 or 81.73%. The surface free energy was derived from the sum of the squares of the intercept and slope. The coefficient of determination suggests a strong relationship between the value of the surface free energy for the Natural rubber pressure sensitive adhesive and its surface free energy components. (Dispersive and polar). Good regression.

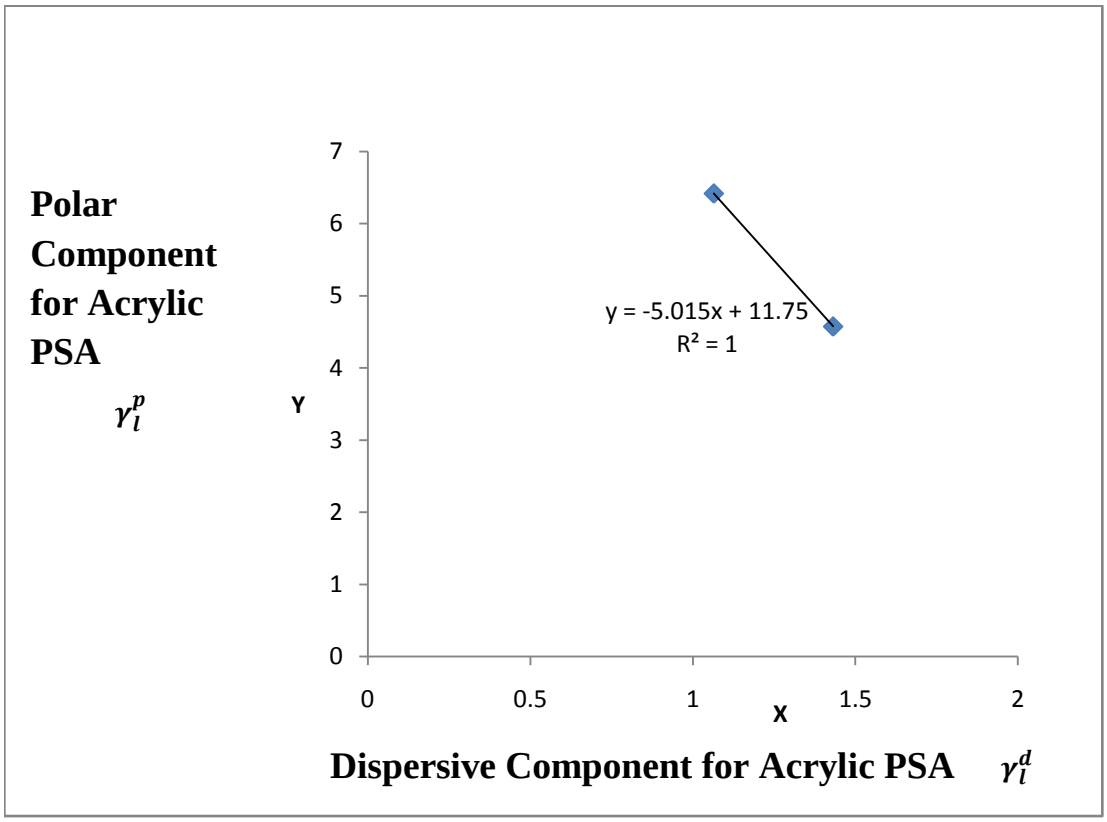

Figure: 4.14 Scattered Plot for Acrylic Pressure Sensitive Adhesive

Figure 4.14 is a scattered plot representing the relationship between polar and dispersive components of acrylic pressure sensitive adhesive. The regression equation is as follows: $y = -5.012x + 11.757$. The sum of the squares of both the intercept and slope give the surface free energy of acrylic adhesive. The regression value is 1. This indicates perfect harmony in the role of dispersive and polar components respectively in determining the value of the surface free energy for the adhesive. However the value of the regression must have been affected by the use of only two test liquids (ethylene glycol and glycerol) for the analysis. The third test liquid ethanol exhibited spontaneous wetting when dropped on the film of the acrylic. This stopped the image of the contact angle

from being derived at snapshot and subsequent calculations were limited. Good regression.

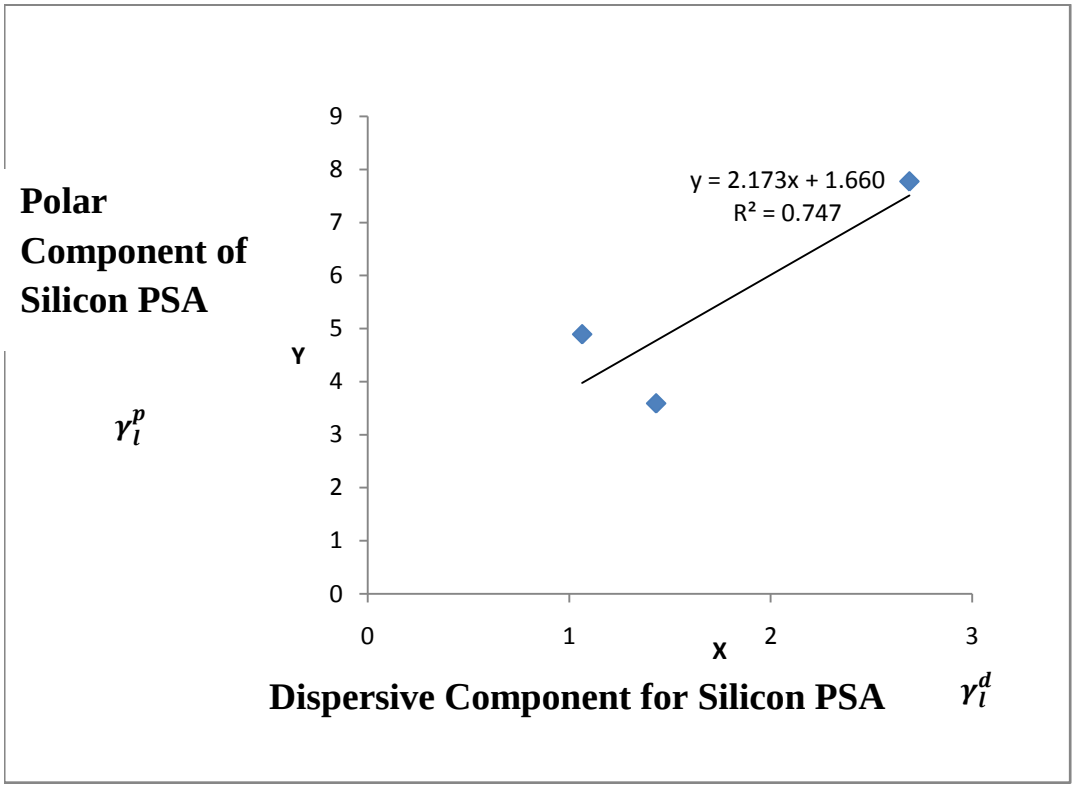

Figure: 4.15Scattered Plot for Silicon Pressure Sensitive Adhesive

Figure 4.15 is a scattered plot representing the relationship between polar and dispersive components of silicone pressure sensitive adhesive, with a regression equation of$y = 2.1735x + 1.6607$. The sum of the squares of both the slope and intercept gives the surface energy of the silicone adhesive. The coefficient determination is 0.7475 or 74.75%. It indicates a strong relationship between the values of the dependent variable the surface free energy and the independent variables the polar and dispersive component. This is a good regression.

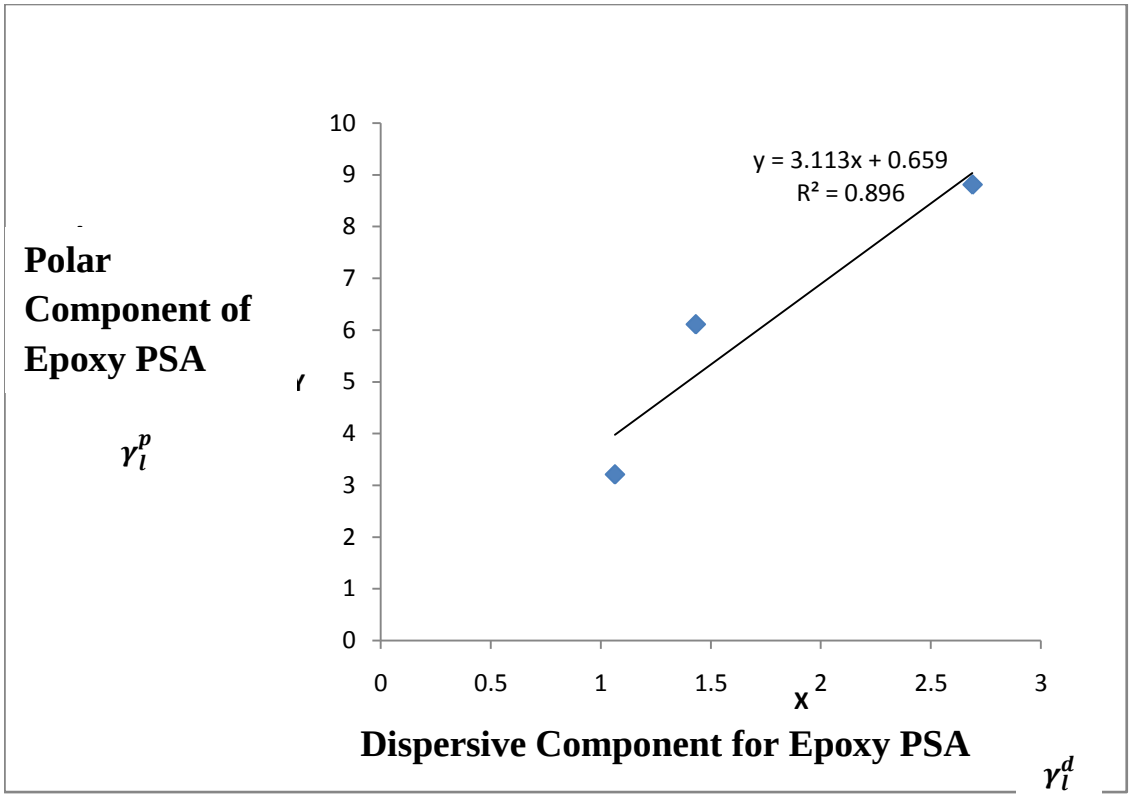

Figure: 4.16 Scattered Plot for Epoxy Pressure Sensitive Adhesive

Figure 4.16 is a scatteredplot representing the relationship between the polar and dispersive component of epoxy pressure sensitive adhesive. The regression equation is as follows: $y = 3.1133x + 0.6593$. The sum of the squares of the slope and intercept give the surface free energy of the epoxy. The value of the coefficient of determination is 0.8968 or 89.68%. The regression shows a strong relationship between the dependent variable (surface free energy) and independent variable (polar and dispersive component). Thus the independent variable can predict the dependent variable by 89.682, good regression.

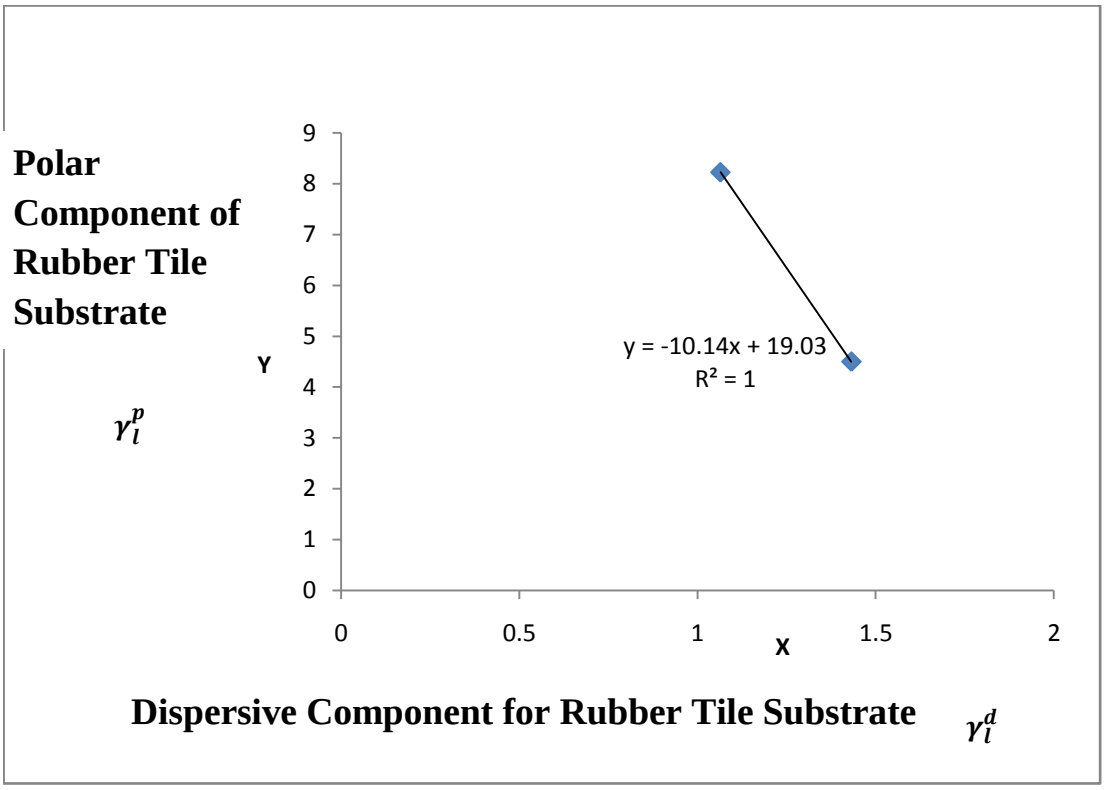

Figure 4.17: Scattered Plot for Rubber Tile Substrate

Figure 4.17 is a scattered plot representing the relationship between polar and dispersive component of rubber tile substrate. The regression equation is$y = -10.48x + 19.01$ and with a regression of 1. The sum of the squares of the slope of the equation and its intercept gives the surface free energy of the rubber tile substrate. The coefficient determination is 1. The regression value at 1 indicates perfect harmony in the prediction of the outcome of the dependent variable (surface free energy) and independent variable (polar and dispersive components). However this regression must have been affected by the use of only 2 test liquid for deriving the contact angle and subsequent calculations.

Ethanol and Glycerol were used while the third test liquid Ethylene glycol caused spontaneous wetting of the rubber tile. Good regression.

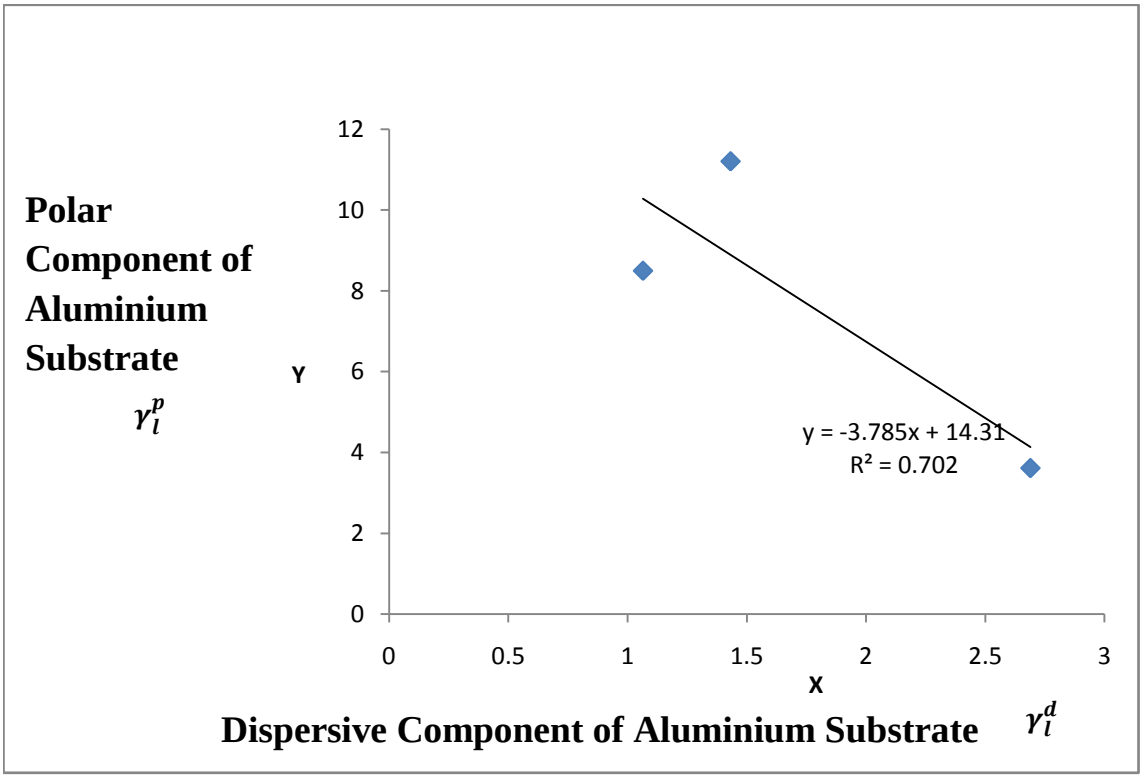

Figure 4.18: Scattered Plot for AluminuimSubstrate

Figure 4.18 is a scattered plot representing the relationship between polar and dispersive component of aluminum substrate. The regression equation is $y = -3.7858x + 14.313$, with a regression of 0.7024. The sum of the squares of both the slope and intercept gives the value of the surface free energy for the aluminum. The coefficient of determination is 0.7024 or 70.24%. This is a strong relationship as this regression of 0.7024 shows that the dependent variable surface free energy dependents on the independent variable components (dispersive and polar) by a factor of 70%.

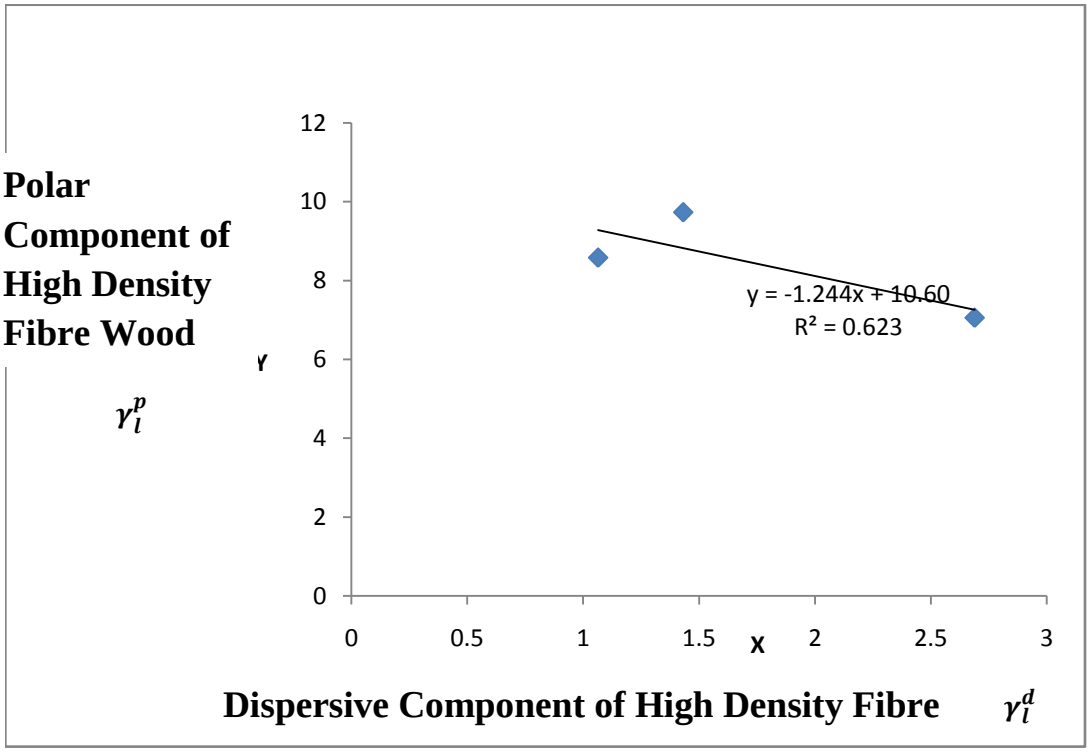

Figure 4.19: Scattered Plot for High Density Fibre WoodSubstrate

Figure 4.19 is a scattered plot representing the relationship between polar and dispersive component of high density fibre wood. The regression equation is as follows: $y = -1.2449x + 10.609$. The sum of the squares of both the slope and intercept of the regression equation gives the surface free energy of the high density fibre wood. The coefficient of determination is 0.6236 or 62.36%. It is a strong relationship between the values of the dependent variable the surface free energy and the independent variable polar and dispersive component. This is a good regression.

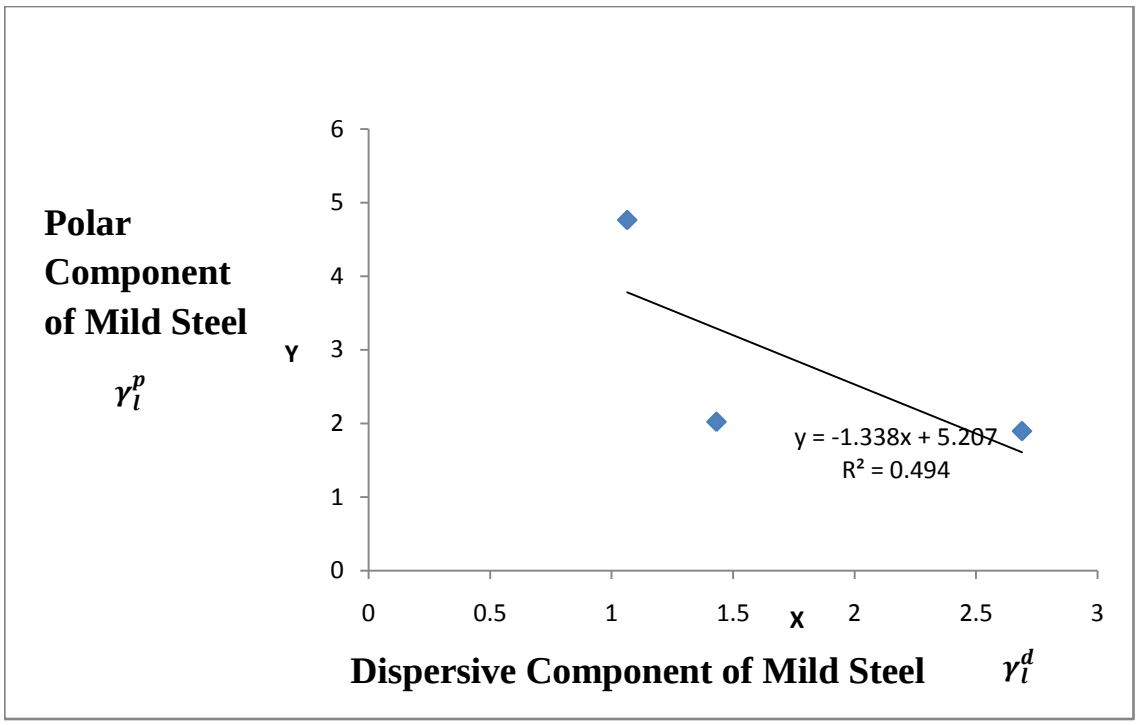

Figure 4.20: Scattered Plot for Mild SteelSubstrate

Figure 4.20 is a scattered plot representing the relationship between the polar and dispersive component of Mild steel. The linear regression is as follows: $y = -1.3385x + 5.2076$ and R^2=0.4945 (coefficient of determination). The sum of the square of both slope and intercept of the regression gives the surface free energy of the Mild steel. The value of the coefficient of determination of 0.4945 is a result of 49.45%. The result gives a moderate regression. Thus the value of the polar and dispersive component predicts the value of the surface free energy by 49.45%.

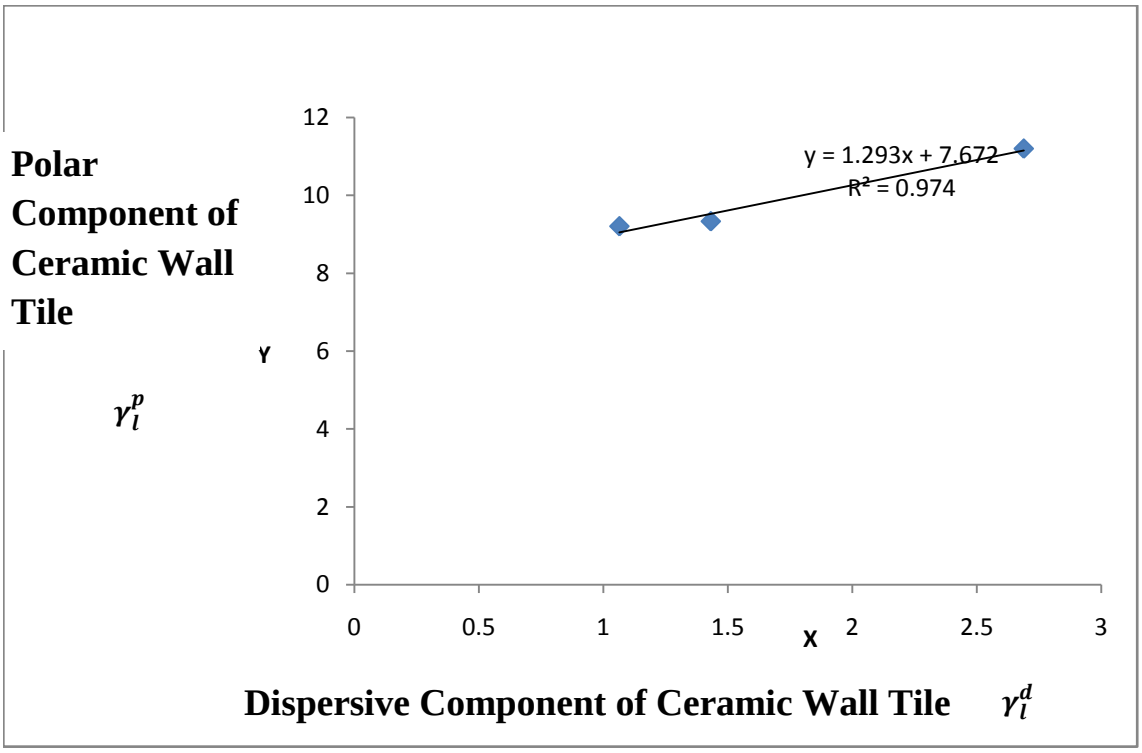

Figure4.21: Scattered Plot for Ceramic Wall TileSubstrate

Figure 4.21 is a scattered plot representing the relationship between the polar and dispersive component of Ceramic wall tile. The linear regression is $y = -1.2939x + 7.6726$ and regression of 0.9746. The coefficient of determination is 0.9746 or 97.46%. The sum of the polar and dispersive component (each square) gives the surface free energy of the Ceramic wall tile. This is a good regression. The surface free energy of Ceramic wall tile value is 97.46% determined by the polar and dispersive component. The Statistical Package for Social Science (SPSS) was used to analyze the relationship between

polar and dispersive components, of both the substrates and the pressure sensitive adhesive. The outcome is expressed in Table 4.9.

Table 4.9: Result of SPSS Correlation and Regression Analysis between Dispersive components and Polar components of Surface Free Energy for both substrates and Pressure Sensitive Adhesives.

	R	R^2	B	T	P value
*Rubber Tile	-	-	-	-	-
Aluminium	0.838	0.702	-3.786	1.536	0.367
High Density Fibre wood	0.790	0.624	-1.245	1.287	0.421
Mild steel	0.703	0.494	-1.338	-0.989	0.504
Ceramic wall Tile	0.987	0.975	1.294	6.194	0.102
Cow skin	0.722	0.521	-0.360	-1.042	0.487
Natural rubber	0.904	0.817	3.898	2.115	0.281
*Acrylic	-	-	-	-	-
Silicon	0.865	0.748	2.173	1.721	0.335
Epoxy	0.947	0.897	3.113	2.948	0.208

**Insufficient samples for analysis*

4.5.3 Relationship between dispersive components and polar components of substrates and pressure sensitive adhesives.

No significant relationship was found ($P > 0.05$). However, the correlation coefficient (R)above 0.7 indicates that there is a very strong linear positive relationship between disperse and polar components. The coefficients of determination (R^2) were above 0.5 indicating that over 50% of the variation in

polar component can be attributed to disperse component. In Table 4.9, the significance relationship was described as P> 0.05. The verbal interpretation is that the relationship between the variables was not feasible. However, this judgment was considered null in the context of this research. This is because validity of significance of relationship which is expected to be P< 0.05 is applicable when the number of variable is at least 200 in number. The number 200 is just sample expected to be picked from major population of variables. This research work has a total of 30 samples formed by the drops of each of the three test liquid on each of the five substrates and five pressure sensitive adhesive respectively. Despite the significance relationship the statistical package for social science analyzing tool stated other valid comments. Amongst them, is that rubber tile substrate and acrylic pressure sensitive posted invalid sample analysis. The acrylic adhesive generated results from two test liquids, ethylene glycol and glycerol while ethanol produced a spontaneous wetting on acrylic sample. The rubber tile substrate generated results from two test liquids ethanol and glycerol while ethylene glycol produced a spontaneous wetting on rubber tile sample. This development limited the analysis of the sample. Table 4.10 shows that data for both dispersive and polar components for both substrates and pressure sensitive adhesive generated a correlation coefficient above 0.7. This means that there is a highly valid relationship between components of surface free energy for both pressure sensitive adhesive and substrates. The correlation helps to compare the ratio between the dispersive and polar components of the surface free energy for either substrates or adhesives. This comparison helps to predict adhesion between substrate and pressure sensitive adhesive. This is because when the ratio between the dispersive and polar component of the surface free energy the adhesives and

substrates are known. It can help to predict adhesion between the two materials. The coefficient of determination across the polar and dispersive components for both substrates and pressure sensitive adhesives yield a value of above 0.5. It indicated that 50% of the variation in the polar component of either the substrate or pressure sensitive adhesive can be attributed to the dispersive component in the both materials. This means that for a substrate or pressure sensitive adhesive to be designated as a polar material, that the outcome of such verdict is influenced by the dispersive component of the surface free energy of such material. For this research work, it can be adduced that the amount of influence dispensed by the dispersive component on the polar component of the free energy is at 50% magnitude. Invariably, it can be stated that the dispersive forces in this research work also influenced the outcome of interfacial energy, wetting, adhesion amongst Substrate and Pressure Sensitive Adhesives. This is because it affects the role the polar component will play in the interfacial interactions.

4.5.43D-Surface Plots (Minitab 3D Surface Plot graphs)

The 3D-Surface Plots shows the relationship between surface free energy and the polar components as well as the dispersive components of the surface free energy for both substrates and adhesives. The surface energy is represented as the Z axis, whereas, polar component of the surface free energy is represented as Y axis. The Dispersive component of the surface free energy is represented as the X axis.

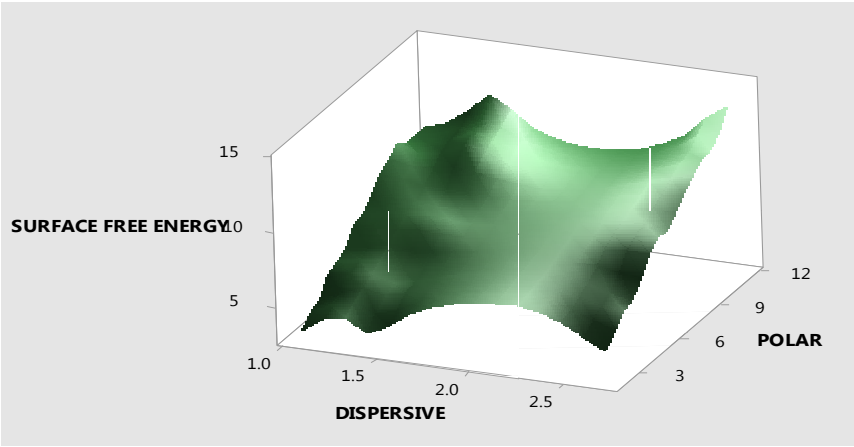

Figure 4.29: 3D Surface Plot of Surface Free energy vsPolar and Dispersive Surface Free Energy for Cow Skin

Figure 4.29 shows a parabola for the relationship of the dispersive free energy component values with regards to corresponding values with the surface free energy. The polar free energy components maintain a linear relationship with a corresponding with a corresponding rise in the values of the surface free energy. The surface free energy of cow skin pressure sensitive adhesive can be expressed as a quadratic function, while the polar is a linear relationship.

This to obtain the value of the surface free energy for the cow skin pressure sensitive adhesive, the contribution of the polar component is a square of the contribution of the dispersive components.

Mathematically the relationship can be expressed as follows.

$$S.F.E \quad \propto p^2\,\gamma \qquad (4.4)$$

Where;

S.F.E is the surface free energy of cow skin pressure sensitive adhesive

P is the polar component of the surface free energy of cow skin pressure sensitive adhesive.

γisthe dispersive component of the surface free energy of cow skin pressure sensitive adhesive.

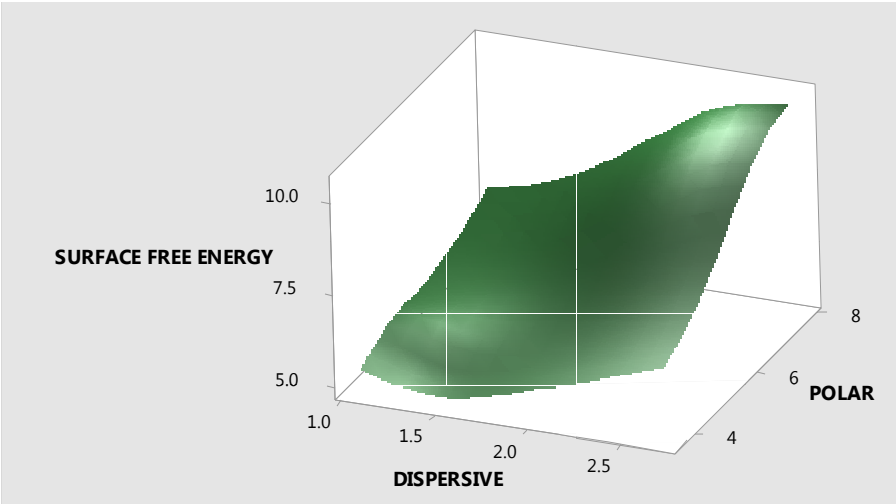

Figure 4.30: 3D Surface Plot of Surface Free energy vs Polar and Dispersive Surface Free Energy for Silicon

Figure 4.30 Show that there exists a linear relationship between the surface free energy of silicon pressure sensitive adhesive and its dispersive and polar components. The graph shows that a rise in values of the polar component is accompanied by a rise in the corresponding values of the surface free energy, likewise the rise in the value of the dispersive component corresponds to rise in the value of the surface free energy. Thus the value of surface free energy for silicon pressure sensitive adhesive is directly influenced by interactions between the polar and dispersive components of the surface free energy. Mathematically the relationship can be expressed as;

$$S.F.E \quad \propto (p, \gamma) \tag{4.5}$$

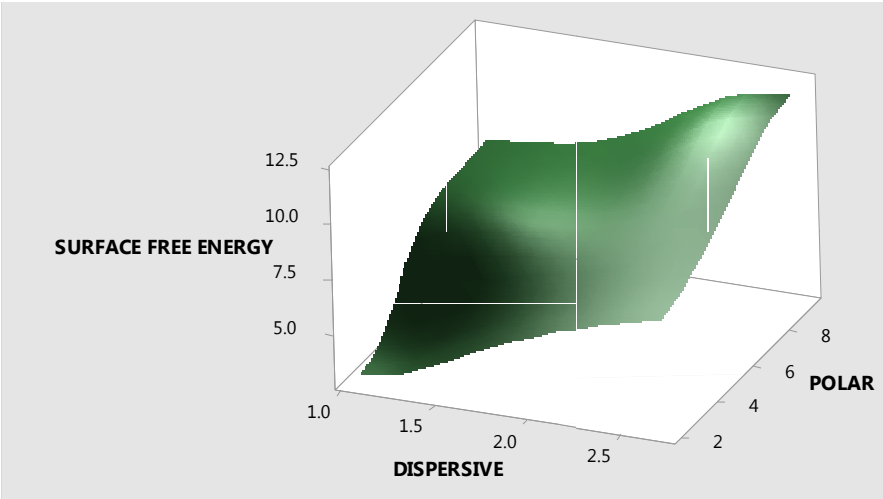

Figure 4.31: 3D Surface Plot of Surface Free energy vs Polar and Dispersive Surface Free Energy for Natural Rubber

Figure 4.31 shows that the surface free energy has a linear relationship with the polar and dispersive components of surface free energy. The graph shows that for each rise in the values of the dispersive component of the surface free energy, there is a corresponding rise in the polar component, and also accompanied by a corresponding rise in the surface free energy.

Mathematically the relationship can be expressed as;

$$S.F.E \quad \propto (p, \gamma) \qquad (4.6)$$

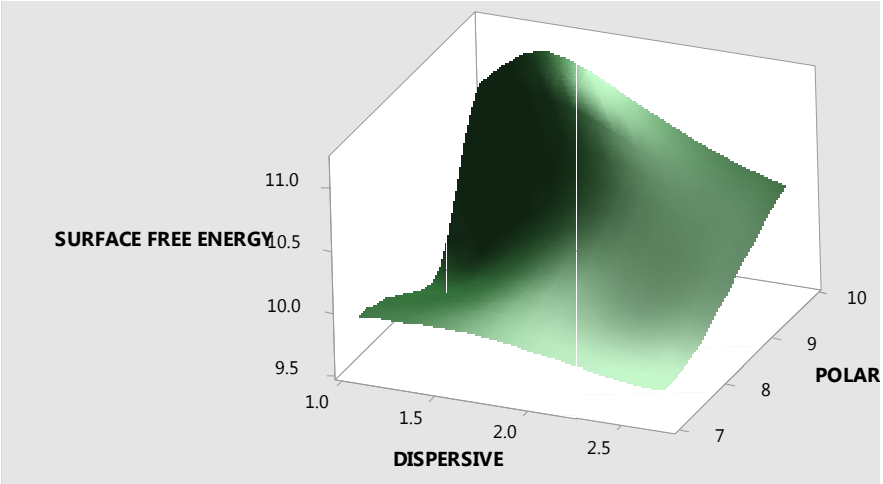

Figure 4.32: 3D Surface Plot of Surface Free energy vs Polar and Dispersive Surface Free Energy for High Density Fibre Wood

Figure 4.32 show a rise in the polar component of surface free energy with a corresponding rise in the value of surface free energy of high density fibre wood. The dispersive component values of the surface free energy remain uniform (constant) accompanying a rise in the surface free energy. Thus the surface free energy of high density fibre wood is mainly influenced by the polar component.

Mathematically the relationship can be expressed as;

$$S.F.E \quad \propto p\,\gamma_l \tag{4.7}$$

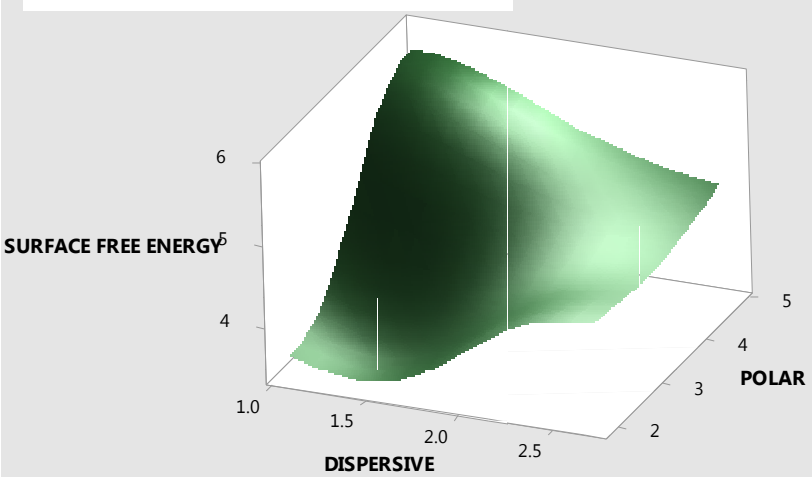

Figure 4.33: 3D Surface Plot of Surface Free energy vs Polar and Dispersive Surface Free Energy for Mild Steel

Figure 4.33 Show a rise in the surface value of the dispersive component of surface free energy and a corresponding rise in the surface free energy value of the mild steel. The polar component values maintain a uniform (constant) relationship with the corresponding surface free energy value. Thus the surface

free energy of mild steel is mainly influenced by the relationship can be expressed as follows:

$$S.F.E \quad \propto \gamma\, p_c \qquad (4.8)$$

Where p_c represents the polar component of the surface free energy of Mild steel pressure sensitive adhesive.

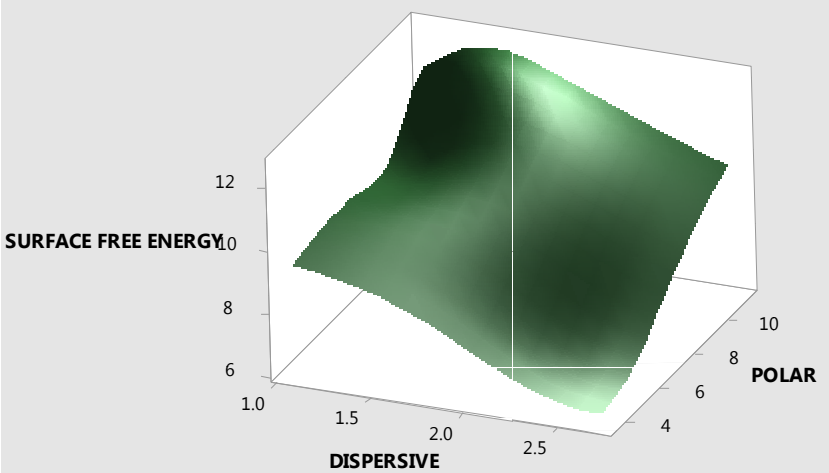

Figure 4.34: 3D Surface Plot of Surface Free energy vs Polar and Dispersive Surface Free Energy for Aluminum Substrate

Figure 4.34 Show an inverse relationship between the surface free energy and the polar and dispersive components of the surface free energy. Here the graph shows a decline in the value of the surface free energy decrease with a rise in the value of the dispersive surface free energy component. The polar component rises in values likewise each corresponding surface free energy.

Mathematically the relationship is expressed as;

$$S.F.E \quad \propto (\rho, {}^{1}/_{\gamma}) \;\therefore\; S.F.E \quad \propto ({}^{p}/_{\gamma}) \qquad (4.9)$$

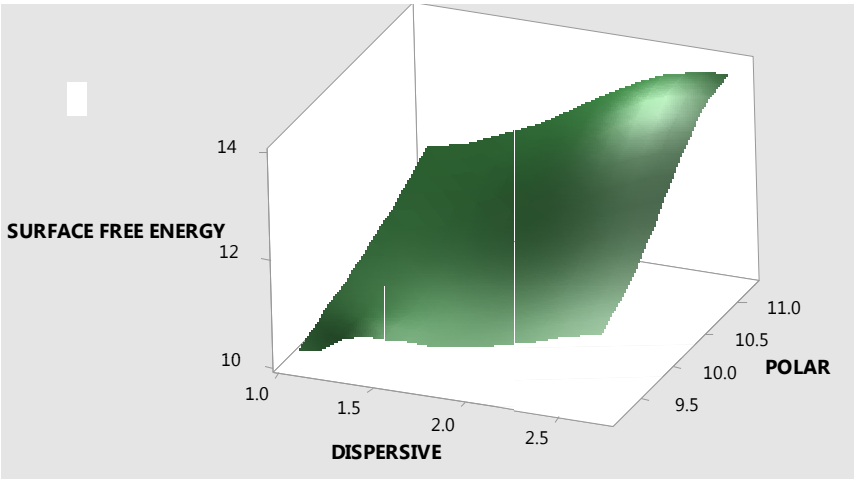

Figure 4.35: 3D Surface Plot of Surface Free energy vs Polar and Dispersive Surface Free Energy for Ceramic Wall Tile

Figure 4.35, shows that the surface free energy has a linear relationship with the polar and dispersive component of the surface free energy. The graph implies that each rise in the value of dispersive component of the surface free energy is followed by a rise in the values of polar component of the surface free energy, there a rise in the corresponding values of the surface free energy. Mathematically the relationship is expressed as follow.

$$S.F.E \quad \propto (\rho, \gamma) \qquad (4.10)$$

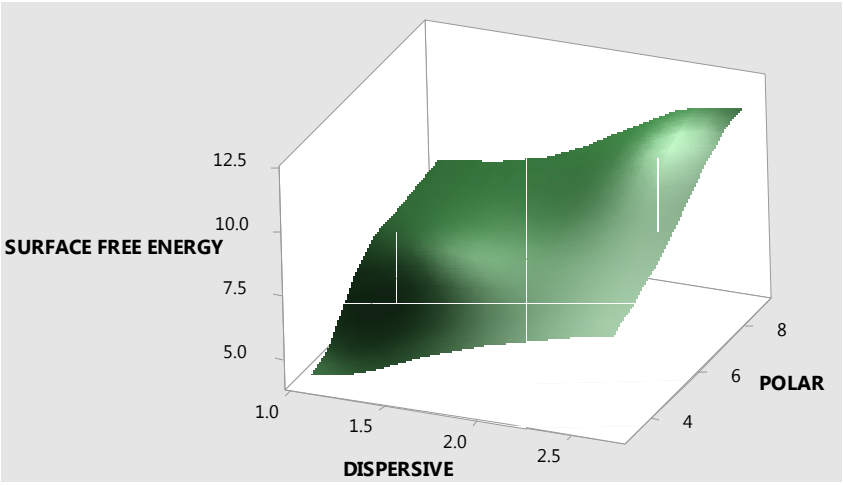

Figure 4.36: 3D Surface Plot of Surface Free energy vs Polar and Dispersive Surface Free Energy for Epoxy

Figure 4.36 show that the surface free energy has a linear relationship with the polar and dispersive components of surface free energy. The graph suggests that for noticed rise in value of dispersive component, there is a corresponding rise in the value of surface free energy (Z axis). Likewise for a rise in the values of polar component of the surface free energy, corresponds with the rise in surface free energy. The value of the surface free energy for epoxy pressure sensitive adhesive is directly influenced by the interactions between the polar and dispersive components of surface free energy.

Mathematically the relationship can be expressed as follows

$$S.F.E \quad \propto (\rho, \gamma) \qquad (4.11)$$

4.6 Analysis of Substrate Surface Characterization and its effect on interfacial adhesion with pressure sensitive adhesives.

The effectiveness of the contributions of the substrate surface chemistry to adhesion performance (with pressure sensitive adhesives) needs be discussed. This is because the chemistry of the substrate top surface defines the

relationship each substrate will exhibit with each pressure sensitive adhesive. This also will influence the quality of the bond available at each substrate/ adhesive interface. Pacholsli, et al, (2015) held that adhesive with corresponding chemistry to substrates showed better adhesion, than adhesive/substrate pair with allied surface energy. Thus the X-ray fluorescent (XRF) was used to produce the result of positive material identification report for every substrate used in the research. The report expressed in Table 4.10 and Appendix B shows the constituent chemistry composition of each substrate surface and their amount in the alloy. The substrates were graded as follows:

- Heavy Density Fibre Wood: Grades Ti-6-22-22(2.22), IMI829(2.35), for Test 1

  (sample A) Ti-6-22-22(2.46), IMI829 (3.12), for Test 2

  Class: Alloy-FP
- Alumunium :Grade, AA-3003(1.06), AA-3005(1.14) for Test 1

  (sample B) Grade, AA-3003(0.04), AA-3005(0.54) for Test 2

  Class: Alloy-LE-FP
- Carbon Steel (Mild steel): Grade C-steel (0.00), C-1020 (0.02) for Test 1

  (sample C) Grade C-steel (0.00), Iron (0.00)

  Class: Alloy-LE-FP
- Rubber Tile: Grades, No Match
- Ceramic Wall Tile: Grades, No Match.

Table 4.10 Result of positive material identification Test for Substrates used for the research

Heavy Density Fibre Wood		Aluminium		Carbon Steel Mild Steel		Rubber Tile		Ceramic Wall Tile	
Test 1 Element Composition %	Test 2 Element Composition %	Test 1 Element Composition %	Test 2 Element Composition %	Test 1 Element Composition %	Test 2 Element Composition %	Test 1 Element Composition %	Test 2 Element Composition %	Test 1 Element Composition %	Test 2 Element Composition %
Titanium 83.93 ±0.746	Titanium 84.74 ±0.755	Aluminum 94.90 ±0.159	Aluminum 96.53 ±0.901	Silicon 0.76 ±0.097	Silicon 0.36 ±0.088	Aluminium 7.32 ±0.371	Aluminium 8.15 ±0.370	Aluminium 11.89 ±0.435	Aluminium 11.47 ±0.378
Manganese 0.37 ±0.37	Manganese 0.31 ±0.082	Manganese 3.33 ±0.133	Manganese 2.28 ±0.067	Titanium 0.13 ±0.020	Titanium 0.09 ±0.019	Silicon 67.19 ±0.537	Silicon 67.36 ±0.530	Silicon 83.53 ±0.658	Silicon 84.00 ±0.597
Iron 8.35 ±0.199	Iron 8.51 ±0.209	Iron 1.45 ±0.066	Iron 0.95 ±0.042	Chromium 0.06 ±0.010	Chromium 0.06 ±0.009	Titanium 7.18 ±0.226	Titanium 6.99 ±0.221	Titanium 0.85 ±0.151	Titanium 0.93 ±0.139
Cobalt 0.21 ±0.040	Cobalt 0.19 ±0.040	Copper 0.12 ±0.012	Copper 0.08 ±0.07	Manganese 0.29 ±0.07	Manganese 0.26 ±0.030	Iron 10.62 ±0.121	Iron 10.28 ±0.117	Iron 1.51 ±0.055	Iron 1.51 ±0.050
Nikel 0.11 ±0.017	Nikel 0.10 ±0.017	Niobium 0.03 ±0.006	Paladium 0.08 ±0.011	Iron 98.77 ±0.253	Iron 99.22 ±0.0253	Zinc 7.35 ±0.061	Zinc 6.91 ±0.058	Zinc 1.95 ±0.030	Zinc 1.83 ±0.027
Copper 0.08 ±0.016	Copper 0.11 ±0.018	Paladium 0.17 ±0.018	Hafnium 0.03 ±0.010			Zirconium 0.03 ±0.007	Zirconium 0.03 ±0.006	Zirconium 0.16 ±0.006	Zirconium 0.14 ±0.005
Zinc 0.34 ±0.025	Zinc 0.39 ±0.026		Tantalum 0.05 ±0.012			Niobium 0.04 ±0.007	Niobium 0.04 ±0.007	Niobium 0.02 ±0.005	Niobium 0.02 ±0.004
Zirconium 0.27 ±0.050	Zirconium 0.39 ±0.052					Paladium 0.13 ±0.024	Paladium 0.18 ±0.023	Paladium 0.09 ±0.017	Paladium 0.10 ±0.015

Niobium 0.29 ±0.054	Niobium 0.29 ±0.017					Tungesten 0.08 ±0.018	Gold 0.07 ±0.012		
Paladium 3.38 ±0.190	Paladium 3.35 ±0.200					Gold 0.06 ±0.010			
Tin 1.25 ±0.422	Chromium 0.37 ±0.087								
Hafnium 0.11 ±0.026	Hafnium 0.11 ±0.029								
Tantalum 0.09 ±0.028									
Tungesten 0.27 ±0.038	Tungesten 0.26 ±0.037								
Gold 0.96 ±0.065	Gold 0.12 ±0.071								

Interfacial adhesion is influenced by interfacial energy between substrate and adhesive. Factors such as corresponding surface chemistry and Vander Waal forcespresent at interface affect the role of interfacial energy in adhesion. The research consider the constituents of each substrate above 3% as an active player in the phenomenon of corresponding chemistry across the substrate/ adhesive interface. Table 4.11 shows the constituent chemical element across each substrates. Table 4.5 show the interfacial energy across each substrate and the various pressure sensitive adhesives. The synthesis of the two premises (Table 4.10 and table 4.5) led to the following inferences. Table 4.5 showed that Aluminum followed by high density fibre wood, then ceramic wall tile turned out the highest values for interfacial energy.The rubber tile and mild steel exhibited the lowest value for interfacial energy between substrate and adhesives.This observation can be traced to the ability of the aluminum to combine very well with constituents of most pressure sensitive adhesives. The constituents include silicon, silica, silanes, glycol, pentanyls, chloro, ethyl and sulphides. The high density fibre wood contain predominantly Titanium, iron, paladium. These share chemical affinity with titanium dioxide, silicon dioxide, phenol, and alkyl, based functional groups for organic compound. Manganese from Aluminum has chemical affinity silica, sulphide, dioxide of silicon and nitriles.The ceramic wall tile which has a high degree of silicon and Aluminum is bound to have chemical affinity with phenols, carbonates, dioxides, silanes, acrylates, nitrile, ethyl/methyl compounds. These components are actively higher in ceramic wall tile than rubber tiles. Meanwhile in rubber tile titanium, iron, zinc, might be competing for chemical affinity with aluminum, thus the low performance at interface.Meanwhile, the chemical affinity between these

substrate/adhesive componentsare built on intermolecular interaction. These interactions include Van-der Waals, electrostatic attraction, metallic charge attraction and other force.

4.7 Analysis of substrate surface modifications useful in enhancing interfacial adhesion (between substrate and the adhesive)

The characterization of the various substrate surfaces revealed the chemical composition of each substrate surface. This led to a proper identification of each surface as the substrate chemical properties played major role in the interfacial adhesion with pressure sensitive adhesives. It is worth mentioning that the various substrate (walls) studied in this research had earlier been engineered to serve particular primary purpose. The hoisting of the emergency sign (Aluminum substrate) bearing materials using designated procedures and abiding by strict regulationcomes later. Thus the surface of the substrate need be modified to create a basis for better adhesion and minimizing failure at the interface.The following procedure which involves identification of sources of contamination for the interface substrates and proffering solutions are suggested ways of remediating failure. The entire suggestion is geared toward promoting better adhesion as contained in table 4.11

Table 4.11:Substrate Surface and Method of Surface Preparation for Adhesive bonding

SUBSTRATES	LIKELY. Sources of contamination	Effects on substrate surface	Suggested solution.
High Density Fabre wood	-Atmospheric Moisture - smut smut - Dust -Mineral oil - Wax - Finger print - Paints	- Atmospheric moisture forms boundary layer which stops surface wetting decrease surface energy, contact angle rises. - Dust, mineral oil wax, finger print paints promote high contact angle formulation, high interfacial tension at interfaceenhances surface voiding	- use sand blast to remove smut - considered heating with flame to remove water -Degrease with trichloroethylene to remove cutting fluid grease, mineral oil, wax, finger prints, paint - use plasma treatment to corona Discharge or flame treatment
Aluminum	-Rust protection oil -Grease -Cutting -Finger print -fluid -Mold -scale	Rust, promotion the formation of oxides which inhibit wettability by adhesive and test liquid -grease, cutting fluid, finger print stop intermolecular and chemical bonding -mole encourage befouling which reduce substrate surface energy.	- plasma treatment - spray cleaning - avcaline cleaning - etching with acid - Corona discharge.
Carbon steel (mild steel)	-Oxides -Scales - Paints - Rust - Atmospheric moisture - Organic soil - Cutting fluids	-Rust, oxides, paint, scale inhibit wettability of the surface cause high contact angle formation -Atmospheric moisture encourage formation boundary layer which interne with adhesive wetting of surface -Organic soil encourage befouling	-Degrease - Sand blast - Plasma treatment - Spray cleaning - Abrading - Chemical treatment
Rubber Tile	- Paint - Dust - Finger print - Dust - Atmospheric moisture - Animal Lubricant - Solid contaminate	-Paint, dust, finger print animal lubricant inhibit wettability, reduce substrate surface tension -Solid contaminate cause void formation interface.	- Decrease - Sand blast, wire brush - Spray cleaning - Clean with water and air dry. - Plasma treatment
Ceramic wall Tile	- Dust - Finger print - Animal Lubricant - Paint - Solid contaminate - Wax - Organic soil	-Solid contaminate encourage low contact point during interfacial adhesion void for matins -Dust, paint, wax, finger print inhibit wetting this reduce adhesion -Organic soil encourage bio fouling	- Degrease - Sand blast - Plasma Treatment - Use wire brushing - Corona discharge

4.8 Analysis Result of Adhesion Prediction

Tack measures adhesive strength and quality. Tack for each pressure sensitive adhesive used for each bond was derived from the mechanical tensile test. The value of the peak force for each bond is regarded as the adhesive tack across each bond. The nondestructive derivation of tacks depends on the analysis of parameters responsible for tack across bonded interface. For this research work, the parameters for such analysis are as follows:

(a) W_A, work of adhesion: which measure the ability of the pressure sensitive to stick to the surface across each bond type.

(b) W_C: work of cohesion: which measure the ability of the pressure sensitive adhesive to remain in contact with its parts across interface

(c) W_S: work of spread, which measure the ability of the adhesive to flow across the interface and locates its use.

(d) W_{AC}: Total work of adhesion which measures the work done while an adhesive sticks to at an interface, while remaining in contact with its parts. This is the work that enable that bond exist.

(e) Adhesive Ratio: measures the bond performance and quality. It is a measure of the relationship between an adhesive wettability potential and work done to maintain an adhesion.

Table 4.12a shows parameters with their corresponding values derived across bond types with regards to respective pressure sensitive adhesives. Across all adhesives (except cow skin) used for the work, there is relatively noticeable spread ability of each adhesive across interface. This shows good wettability. The work of cohesion exhibited by the cow skin adhesive is greater than its work of adhesion. Thus low wettability potential and inadequate for interfacial bonding as spreading parameters indicate negative. Table 4.12b shows a

logarithm value of the peak force and adhesion ratio across different bonds type. The adhesion ratio across each bond type shows the potential for tack for respective bond types with regard to each pressure sensitive adhesive.

Table 4.12a: Result of Force at Peak, Work of Adhesion, Work of Cohesion, Total work of adhesion and Work of Spreading across bond type

Natural rubber BOND TYPE	Force At Peak (N)	W_A (J/m^2)	W_C (J/m^2)	$W_{AC}=W_A+W_C$ (J/m^2)	$W_S=W_A-W_C$ (J/m^2)
HDF/NR/ALU	1525.1	282.91	31.44	314.35	251.47
CWT/NR/ALU	1239.5	199.44	31.44	230.88	168.00
MS/NR/ALU	8418.4	130.60	31.44	162.04	99.16
RT/NR/ALU	1650.9	158.19	31.44	189.63	126.75
EPOXY BOND TYPE					
HDF/Epoxy/ALU	2221.0	275.62	20.26	295.88	255.36
CWT/Epoxy/ALU	419.7	195.10	20.26	215.36	174.84
MS/Epoxy/ALU	7840.9	126.19	20.26	146.45	105.93
RT/Epoxy/ALU	1834.9	92.58	20.26	112.84	72.32
Acrylic BOND TYPE					
HDF/Acrylic/ALU	1655.0	195.17	22.78	217.95	172.39

CWT/Acrylic/ALU	1892.3	126.59	22.78	149.37	103.81
MS/Acrylic/ALU	6041.4	58.15	22.78	80.93	35.37
RT/Acrylic/ALU	1581.9	56.60	22.78	79.38	33.82
Cow Skin					
BOND TYPE					
HDF/CS/ALU	167.1	46.86	108.4	155.26	-61.54
CWT/CS/ALU	1697.6	6.64	108.4	115.04	-101.76
MS/CS/ALU	7120.0	-28.33	108.4	79.77	-136.73
RT/CS/ALU	1826.0	-35.60	108.4	72.50	-144.00
Silicon					
BOND TYPE					
HDF/SI/ALU	1746.8	163.64	14.96	178.60	148.68
CWT/SI/ALU	1810.2	159.19	14.96	174.15	144.23
MS/SI/ALU	5783.4	96.11	14.96	111.07	81.15
RT/SI/ALU	1747.1	70.02	14.96	84.98	55.06

Table 4.12b Result of Log of Force at Peak and Adhesion Ratio

Natural Rubber Bond Type	Logarithm (In) of |Force at Peak(N)	Adhesion ratio (A.R)
HDF/NR/ALU	7.3298	0.8000
CWT/NR/ALU	7.1225	0.7277
MS/NR/ALU	9.0382	0.6119
RT/NR/ALU	7.4091	0.6684
Epoxy Bond Type		
HDF/EPOXY/ALU	7.7057	0.8631
CWT/EPOXY/ALU	6.0395	0.8118
MS/EPOXY/ALU	8.9671	0.7233
RT/EPOXY/ALU	7.5147	0.6409
Acrylic Bond Type		
HDF/ACRYLIC/ALU	7.4116	0.7910
CWT/ ACRYLIC /ALU	7.5455	0.6950
MS/ ACRYLIC /ALU	8.7064	0.4370
RT/ ACRYLIC /ALU	7.3664	0.4261
Cow Skin Bond Type		
HDF/CS/ALU	5.1186	-0.3964
CWT/CS/ALU	7.4370	-0.8846
MS/CS/ALU	8.8707	-1.7141
RT/CS/ALU	7.5099	-1.9862
Silicon Bond Type		
HDF/SI/ALU	7.4655	0.8325
CWT/SI/ALU	7.5012	0.8282
MS/SI/ALU	8.8707	-1.7141
RT/SI/ALU	7.4657	0.6479

Predictive models were developed for the relationship between In of force at Peak and adhesion ratio. It was observed that a lower force at peak

wasaccompanied by lower adhesion ratio. These relations are presented in figures 4.37-4.41.

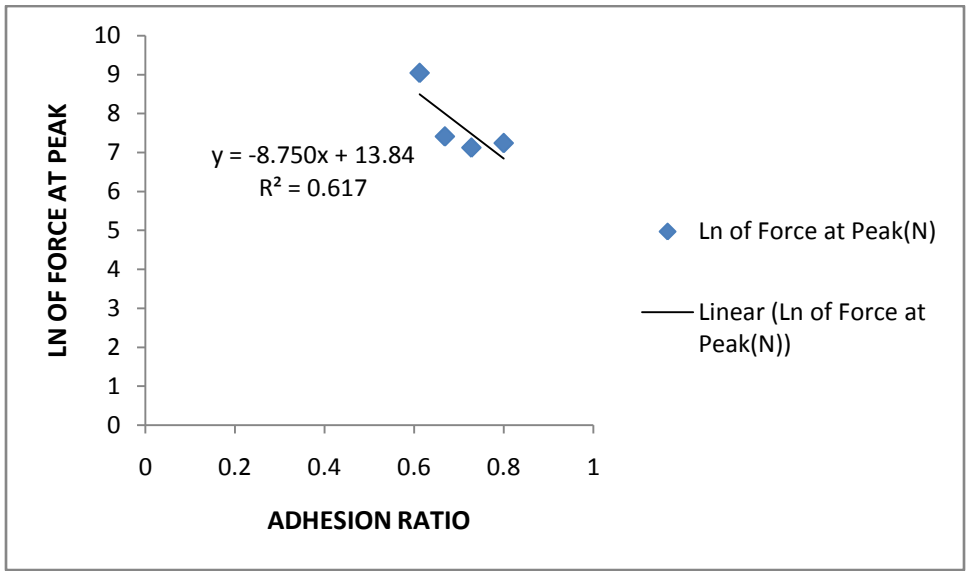

Figure 4.37: Scattered plot of force at peak against adhesion ratio for natural rubber pressure sensitive adhesive

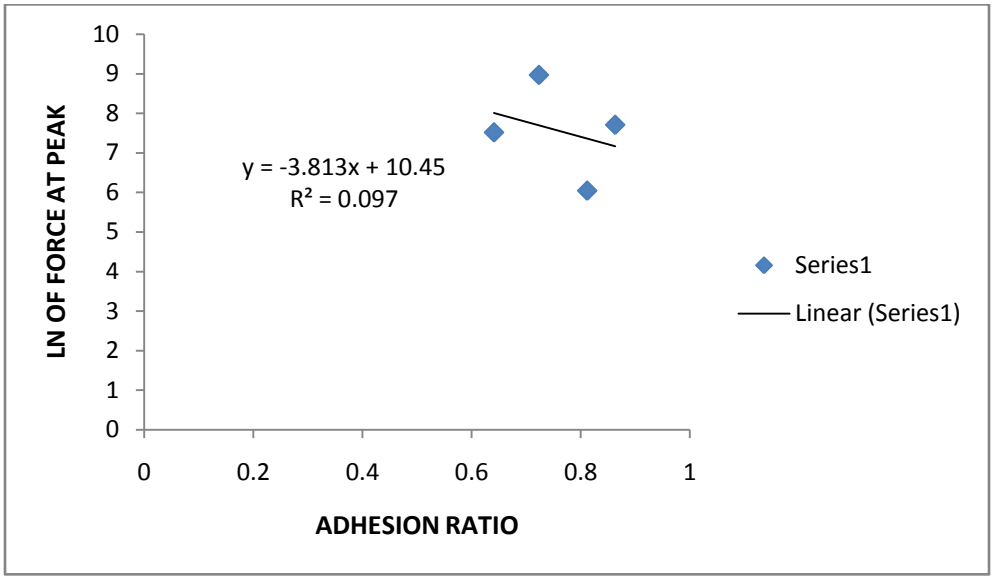

Figure 4.38: Scattered plot of force at peak against adhesion ratio for epoxy pressure sensitive adhesive

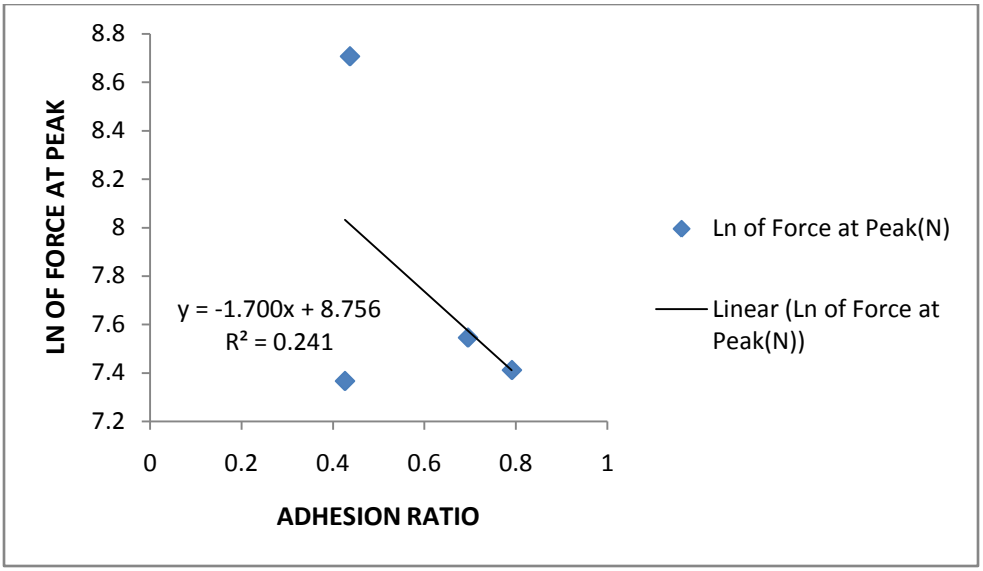

Figure 4.39: Scattered plot of force at peak against adhesion ratio for acrylic pressure sensitive adhesive

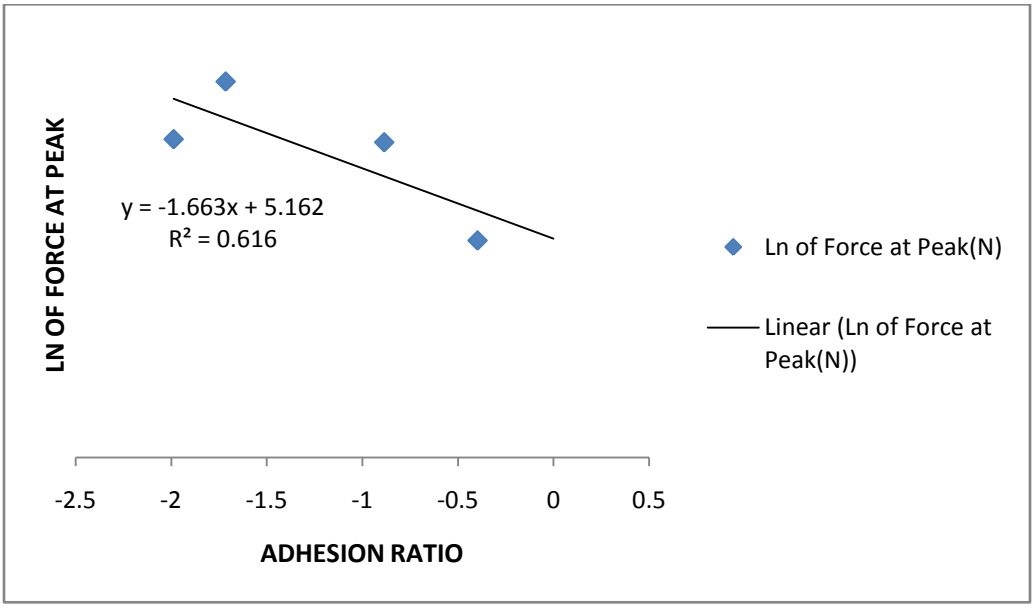

Figure 4.40: Scattered plot of force at peak against adhesion ratio for cow skin pressure sensitive adhesive

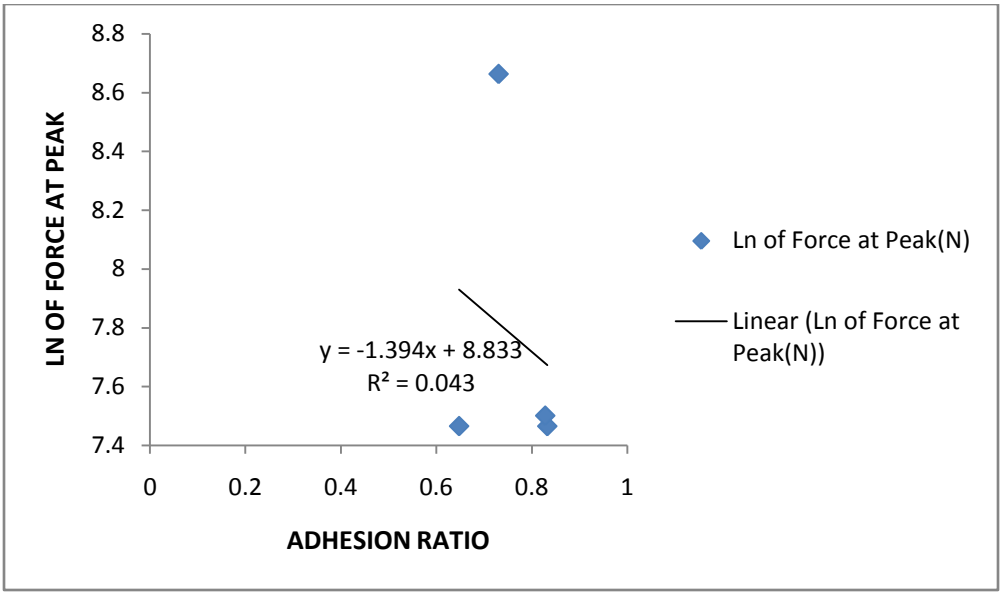

Figure 4.41: Scattered plot of force at peak against adhesion ratio for silicon pressure sensitive adhesive

CHAPTER FIVE

CONCLUSION AND RECOMMENDATIONS

5.1 Conclusion

The role of interfacial parameters on the adhesion of pressure sensitive adhesives was studied. Three test liquids were respectively used to derive the contact angle for each substrate, as well as pressure sensitive adhesive. The contact angles for the substrates range from 55.74^0 to 163.59^0while the adhesives range from 78.69^o to 181.85^o.The contact angle enabled the surface free energy for each substrate and each adhesive to be calculated, through Fowkes law. The Kaelble plot was used to derive the values of polar and dispersive component of the surface free energy. OwendtsWendt law was used to derive interfacial surface energy between substrate and adhesive.

From the result obtained, the following conclusions are drawn;

1. The interfacial energy at bond interface was observed to influence the outcome of thermodynamic work of adhesion across the bond.
2. Surface polarity (dispersive or polar) plays an important role in the determination of adhesive strength.
3. There exists a direct relationship between the thermodynamic work of adhesion and fracture energy.
4. Interfacial parameters indeed influence the adhesion of the emergency sign on the substrate (vertical walls) in the presence of pressure sensitive adhesives.

5.2 Recommendations for future research

Suggestion for future research with respect to the topic should be carried out as follows.

- To understand the impact of surface modification on the relationship between fracture energy and thermodynamic work of adhesion. This will help assess the role of adhesion ratio in predicting bond strength alongside thermodynamic work of adhesion without delamination.
- To ascertain the impact of environmental conditions on adhesion between substrate and pressure sensitive adhesive.
- To establish any role (if any) that similarity in chemical composition between substrate and adhesive would play in delamination at interface. These suggested recommendations if studied will enhance the understanding the conditions for effectual adhesion at interface.

5.3 Contribution to knowledge

1. The influence of interfacial parameters in the adhesion of pressure sensitive adhesive, using multiple pressure sensitive adhesive and multiple substrates, was determined.
2. This work established that when substrate and pressure sensitive adhesives of opposite polarities are bonded at interface, stronger work of adhesion is achieved (This extends the hypothesis that close ratio matching of polarity components between adhesive and substrates predicts stronger adhesion).
3. A parameter to predict adhesion was established, called adhesion ratio. This parameter was derived from a synergy of work of cohesion, work of spreading and thermodynamic work of adhesion across interface between adhesives and substrates.

REFERENCES

Achebe C. H.,Omenyi S. N., Manafa O. P., Okoli D., (2012) "Human Immunodeficiency Virus (HIV)-Blood Interactions: Surface Thermodynamics Approach", *Proceedings of the International Multi-Conference of Engineers and Computer Scientists* 2012, Hong Kong, pp.136-141.

Adelhaye-MohammadY.D, Chaouche M, Chapuis J, Charlaix E, Hinch J, Roux S,VanDamne H., (2012), Tackiness and Cohesive and Cohesive failure of granularpastes,mechanistic aspect. European Physical Journal E, (2012) 35.45.doi 10.1140/epje/.2012-12045-6.

Al-Qadi I.L,Figureueroa H.D, Mason J.F., Mc Ghee K.K., (2008), Adhesion testing procedure for hot poured crack sealant. Research Report ICT-08-026, Illinois centre for Transportation. Series No. 08-026, UILU-ENG 2008-2014, ISSN: 0197-9191.

Alyssa Y.S., Nicholas A.W., Eva L.P, Peter H.N., Ali D. (2014), "Self drying: A gecko innate ability to remove water from wet pads"*PLOS ONE* 9 (7); 1-8.

ASTM, 2019 - American Society for Testing and Materials, Standard Test Method for Pressure Sensitive Tack of Adhesive using an Inverted Probe Machine. D2979-16.

Ana C. Marques, Alexandra Mocanu, Natasa Z. Tomic, et al (2020), Review on Adhesives and Surface Treatments for Structural Applications: Recent Developments on Sustainability and Implementation for Metal and Composite Substrates. *Materials MDPI,* 13; 1-43.

Banerjee S., (2008), Simple derivation of Young,Wenzel and Cassier–Bexter equation and its interpretation. Surface Physics Division,Saha Institute of Nuclear Physic 1/AF Bidhannagar, Kolkata 700064 India.

Baruch R., Sebastin D., Valeri F., et al (2020); "Intermediate State of Wetting on Hierarchical Super Hydrophobic Surfaces", *Langmuir,* 36(20): 5517-5523.

Belnoue J.P.H and Hallets S.R., (2016), Cohesive/ Adhesive failure interaction in ductile adhesive joints. Part 1: A smeared-crack model for cohesive failure. International Journal of Adhesion and Adhesive.Doi: 10.1016/j.ijadhadh.2016.03.03009.

Benedek I., (2004), Pressure sensitive adhesive and application. Second Edition, revised and expanded. Marcel Dekker,lnc. 270 Madison Avenue New York 10016.

Benedek I. and Feldstein M. (2019); "Applications of Pressure-Sensitive Products" *CRC Press,* 1st Edition, 378.

BernardesP.C., Emiliare A. A., Ana Clarissa D.P., Jose F.Q., CarineA.L., Nelio J. D. (2012);"Work of adhesion of dairy products on stainless steel surface",*Brazilian Journal of Microbiology* (2012):1261-1268.

BhutaniGaurau, Khandekar Sameer, Muralidhar K., (2012), Contact angle of pendant drop on rough surface. Proceedings of the thirty-ninth national conference on fluid mechanics and fluid power. December 13-15,2012,SVNITSurat, Gujarat, lndia.

BoxionZ., (2004), The interaction of pressure sensitive adhesive with paper surface.Ph.D dissertation, Chemical Engineering, Mc Master University Hamilton, Ontario Canada.

Bolger J.C., and Michael A.S., (1969), Molecular structure and electrostatic Interaction: Interface conversion P. Weiss and O. Cheevers (Eds),Interface

conversion, Elservier New York, Chapter 1,15-30.

Boyd, A., Gabriela, L., Romain,P., Ray K., Patrice, L., John, M. C., Raghu,R., Alan, S. (2007);"Fundamentals of Wettability". *Schlumberger wettability workshop, Bahrain*, May 2007.

ChaudhuryM., (1996);"Interfacial interaction between low energy surface". *Journal of Material Science and Engineering,* 16: 97-159.

Chengchun Z., Yihua Z., Zhengyong W., et al. (2019); "Non-wet King Fisher Flying in the rain; The Water-repellent Mechanism of Elastic Feather", *Journal of Colloid and Interface Science,* 541: 56-64.

Chukwuneke, J. L., Achebe, C. H., Omenyi, S. N. (2015);"Surface thermodynamic approach to mycobacterium tuberculosis (M-TB) Human Sputum Interaction"*Bioengineering and Biomedical Science,* 5(3); 1-8.

Connor, A. E.,WillenbacherN., (2004); "The effect of molecular weight and temperature on tack properties of model Polyisbutylenes".*International Journal of Adhesion and Adhesive* 24:335-346

Creton, C. and Ciccotti M., (2016),"Fracture and adhesion of soft materials". Reports on Progressin Physics, IOP Publishing, 79(4): 1-9.

Creton, C. (2003), Pressure sensitive adhesive:An introductory course MRS Bulletin, 28,434-439

DeplaceF., Carelli C., Mariot S., RetsosH., Chateauminois A. Ouzinab K., Creton C., (2009), Fine tuning the adhesive properties of soft nanostructure adhesive with rheological measurements.*The Journal of Adhesion*, 85: 18-54.

Du J.,Lindeman D.D., Yarusso D.J., (2004), "Modelling the peel performance of pressure sensitive adhesives". *Journal of Adhesion*, 80 (7): 601-912

Duncan, B. R., Leatherdale, D., Taylor, M. and Musgrove, R., (2005), “Techniques for characterizing the wetting, coating and spreading of adhesive on surface”. NPL REPORT DEPC MPR 020, National physical Laboratory.

Feldstein M., Dormidontova E., Kholhlo A., (2014), Pressure sensitive adhesive based on interpolymer complex.*Progress in Polymer Science* 4: 79-153.

Flinn B.D and Ashley C.T, (2010), Improving adhesive bonding of composite through surface characterization: Variables that affect contact angle measurements on peel ply surfaces. Department of Material Science and Engineering 302 Roberts Hall, MS 352120, University of Washington, Seattle, WA98195.

Fowkes F.M, (1983), Physiochemical aspect of polymeric surface. Mittal Ed), Plenum, New York, 2:583

Fowkes, F. M., (1967), Attractive force at interfaces. Ind. Eng. Chem., 56.40

Fuentes C.A., Brughmans G, Tan L.Q.N, Dupont-Gillian C.,Verposet I., Van-vuure A.W, (2015), “Mechanical Behaviour and Practical Adhesion at bamboo Composite Interface Physical Adhesion and Mechanical Interlocking”.*Journal of Composite science and Technology* 109:40-47.

Fujita, M, Takemura A., Ono, H., Kajiyama, M., Hayashi S., Mizumachi, (2000), Effect of miscibility and viscoelasticity on shear creep resistance of natural Rubberbase pressure sensitive adhesives. *J. Appl. Polymsci*, 75(15): 35-45.

Geiss,L. P., Vogt, D., (2007),“Durability of pressure sensitive adhesive joint,Kaiserlautern University of Technology”,*Faculty of Mechanical and Process Engineering work group material and surface technologies (AWOK)*, 67663,Kaiserslautern, Germany.

Geoghgan M, and Krause G., (2002) Wetting at Polymer Surface and Interface. Progress in Polymer Science 28 (2003) 261-302.

Ghatak, A and Chaudhury,M.K., (2007), "Critical confinement and inelastic instability in thin solid films".*The Journal of Adhesion* 83: 679-704.

Gommes C.J (2014), "Physical chemistry of interfaces". University of Liege, Belgium

Good R.J. and Girifalco L. A., (1957), "A Theory for the Estimation of Surface and Interfacial Energies", *Journal of Physical Chemistry*,61: 904-909

Greensmith, H.W., Mullins, L. and Thomas, A.G., (1960), "Rupture of rubber". *Transaction of Royal Society of Rheology,* 4:177-189.

Gutowski, V. S. and Sheng L. (2014), "Theoretical and technology aspect of surface engineering for adhesion enhancement of polymers and composites". *Advance in manufacturing science and technology*, 38(4):5-21.

Hauschwitz P., Jochova D., Jagdheesh R., et al (2021); "Towards Rapid Large-scale LIPSS Fabrication by 4-Beam ps DLIP", *Optics and Laser Technology,* 133: 1-5.

Howson J.E. (2011), Relationship between Surface Energy and TotalWork of Fracture of asphalt binder and asphalt binder-aggregateInterface.Ph.D dissertation in Civil Engineering, Texas A &MUniversity, United State of America.

Israelachivili J. N. (1992), Adhesion forces between surfaces in liquids and condensable vapors. Surface Science Report, 14 (3) : 109-159.

Jennisen H. P. (2012); "Hyper Hydrophobic Rough Surfaces and Imaginary Contact Angles", *Materialwissenschaft und Werkstofftechnik,* 43(8): 743-750.

Julia,N., Constantino,C., Osvary, R., Lars, S., Tetsuo, Y. and Anke, L. (2010), "Measurement of the receding contact angle at the interface between a viscoelastic material and a rigid surface".*Soft Matter,* 6: 2685-2691.

Kock-Yee L. (2014), “Definitions for Hydrophobicity and Super Hydrophobicity, Getting the Basics Right”, *Journal of Physical Chemistry Letters,* 5(4); 686-688.

Kovacevic, V. (2008), Surface and interface phenomenon in polymer short course. International workshop on advance polymer science and turbulent drag reduction 10-20th march, 2008, Zagreb Croatia.

Kwanwoo S., Jinwook L., Seong O. and Jooyun K. (2019); “Interaction of Surface Energy Components between Solids and Liquid on Wettability and its Application to Textile Anti-Wetting Finish”*Polymer (Base L),* 11(13): 498.

Lake G. J., and Lindley P.B., (1965), “The mechanical fatigue limit of rubber”.*Journal of Applied polymer science*, 9: 1233-1251

Le Quan, N.T., Dupont, C., Verposet, I., Van Vuure, A.W, (2015),“Mechanical Behavior and practical adhesion at bambo composite interface. Physical adhesion and Mechanical Interlocking”.*Composite Science and Technology,* 109: 40-47.

Lifshitz E.M., (1961), the theory of molecular attractive force between solids. Advance Physics 10.165-209

Li-Hua Li, macosko C, Korba G.L., Pocius A.V., TirrellM., (2001)Interfacial energy and adhesion between acrylic pressure adhesive and Release coating Journal of adhesion 77:95-123,2001

Marin G., Derail C., (2006), Rheology and Adherence of pressure sensitive adhesives.*The journal of Adhesion,* 82:469-485.

Mitutoyo America corporation (2009,December), Surface roughness measurement No.1984. Retrieved August 16, 2016 from www.mitutoyo.com

Mohammed l. k., Charalambides M.N., Kinloch A.J., (2016), “Modeling the effect of rate and geometry on peeling and tack of pressure sensitive adhesive”.*Journal of Non-Newtonian Fluid Mechanics,* 233: 85-94

Mohammad l.k, Kinloch A.J, CharalambideM., (2016), Modeling the peeling behaviour of soft adhesive. *Procedia Structural Integrity* 2: 326-333.

Mokhtari,M., Modarikoider, B.H. and Malarino, S. (2017),“Effect of the composite stacking sequence on the failure load of the single lap bonded joint”. *Journal of Theoretical and Applied mechanics*, 55 (4): 1257-1268.

MoslemiM, KhosrawanM., (2015), “Cohesion mode parameter selection for mode 1prediction of interfacial delamination”. *Journal of Mechanical Engineering,* 61(9): 507-516.

Myshkin N.K.,PetrokovetsM. I., KovalevA. V., (2005), Tribology of Polymer Adhesion friction wear and mass transfer tribology international 38(2005) 910-921.

Neuman A. W., Van Oss C. J., Omenyi S. N., Absolom D.R., Viser J., (1983), Measurement of surface tension of blood cells and protein. *Annals New York Academy of Science* 276-298.

Njobuenwu D.O, Oboho E.O., Gunus R.H., (2005), Determinationof contact angle from contact area of liquid droplet spreading on solid substrate. Department of Chemical/ Petroleum Engineering, Rivers State University of Science and Technology, Port Harcourt, Nigeria and Institute of Particle Science and Engineering, School of Process, Environmental and Material Engineering of Leeds United Kingdom.

NooriH. (2015), Assessment of interfacial adhesion in polymer laminated sheet metals Ph.D Thesis, Department of Mechanical Engineering Mc Master University Hamilton Ontario, Canada.

Omenyi S.N, Spelt K, Neuman A.W, Policova Z, Van Oss C. J, Thomson C. (1983), Measurement of surface tensions of blood cell and proteins. New York Academy of Sciences.

Ozawa, T., lshiwataShinichiK.Y. (2001), Adhesive properties of ultraviolet curable pressure sensitiveadhesive tape for semiconductor processing: Interpretation via rheological view point.Furukawa Review, No.20,2001.

Pacholski M., Griiffith B., Keely D. and Powell T. (2015),Correlating substrate surface analysis to adhesive performance. TheDow chemical company.

ParreidtS.TSchmid m, housser C (2017), validation of a novel technique and evaluation of the surface free energy of food. 6(31).

Patil S, Malasi A., Majumder A, Ghatak A., and Sharma A., (2012), Reusable Antifouling viscoetastic adhesive with an elastic skin Langumir,28:42-46.

Person B. N. and Tosatti E. (2001), The effect of surface roughness on the adhesion of elastic solids.*Journal of Chemical Physics,* 115(12).

Phttanarudee, S. (1998), The use of thermodynamic work of adhesion to predict adhesive strength, M.Sc Thesis, Polymer Science and Engineering Le High University

PiltonenPetteri (2013),Prevention of fouling on paper machine surfaces University of Onlu Graduate School University of Onlu, Faculty of Technology, Department of Process and Environmental Engineering,ActaUniversitatisOluensis C Technical.

Qi, (2000), Measurement of surface and interfacial energies between solid material using elastic loop. Master of Science in Engineering Mechanics Thesis,VirginaPolytechnic Institute and State University.

Royalance. D. (2001), Stress-Strain curve, Department of Material Science and Engineering, Massachusetts Institute of Technology, Cambridge. MA 02139

RudenauerY., (2013), Influence of interfacial parameters on the adhesion of soft polymer.Ph.D dissertation, Institute for Mechanical Process Engineering and Mechanics at Karlsruhe Institute of Technology, Germany.

Sara M., Roderick M., Yuting C., et al. (2020); "Hierarchical Structures, with Submillimeter Patterns, Micrometer Wrinkles, and Nanoscale Decorations, Suppress Biofouling and Enable Rapid Droplet Digitization", *Nano-micro Small,* 2004886: 1-9.

Sauliner F., Ondarchu T., Aradian A. and Raphel E., (2004), Micromolecules 37: 1067-1075

ShaominSun,MenglingLi, Ally Liu, (2012),A review of mechanical properties of pressure sensitive adhesive. International Journal of Adhesion and Adhesive 41: 98-106.

Shaw D. and William M., (2013), Simpleradhesive bonding for low surface energy polyolefin plastic, PP.62.Reprinted from design world for Henkel.

Simoncic (2004) Influence of different parameters on the surface energy of finished cotton fabric. Tekstilec 2004, Let 47 Stl-2, St6-12.

Sun J., Zhao X., Illeperuma W., et al. (2012); "Highly Stretchable and Tough Hydrogels", *Nature,* 489: 133-136.

Tangury F., Nicoli M., Linder A. and Creton C., (2014), Quantitative analysisof debonding structure of soft adhesive. The European Physical Journal, E 37, 1-12

Teissire, J., Nallet, F., Fare,P., Gay, C., (2006), Understanding crack versus cavitation in a pressure sensitive adhesive: The role of kinetics retrieved from http://www.cipp-bordeaux.cnis.fr/ext/rubrique.php3?ld-rubrique=8.April 5, 2017.

Theory of surface tension, contact angle, wetting, work of adhesion (4), 2014. Retrieved April 5, 2017 from http://www.surface.tension.org/article/62.htmc.

Toyama M., lko T., Moriguchi H., (2003), Studies on tack of pressure sensitive adhesive tapes. Journal of Applied polymer 14 (8):2039-2048.

ToygarEvienM., ToparliM., SenF., Ali GungorM, (2009), Fracture energy determination and critical crack propagation.Material and Design June 2009. Vol.30(6) 2278-2282.

Tsai M., Morton J. and Mathew F., (1995), Experimental and numerical studies of a laminated composite single-lap adhesive joint. Journal of Composite Materials, 29, 1254-1275.

Vann Oss C. J., Chaudhry M. K. and Good R. J., (1988), Monopolar surface, advance colloidal interface science. Chem Rev. 88:927-941.

Wha-Tong and Wen-Hua Cheng (1995), A study on interfacial adhesion of poly (vinyl fluoride) with substrates in a multilayer structure. Polymer Engineering and Science, 35(8): 1-9.

Wolf and Sparavigna C.S., (2010), Role of plasma surface treatment on wetting and adhesion. Scientific Research Engineering 2010(2): 397-402.

Xiaocong He (2010), Effect of mechanical properties of adhesive on stress distribution in structural bonded joint. Proceeding of World Congress on Engineering, 2010 Vol. II WCE 2010, June 4, 2010, London U.K.

Xpolymer-H-Adhesive-I (2008,December). Retrieved on January 10,2017from,http://nzic.org.nz/…/polymer/WH.pdf.

Yamaguchi F., Koike K., and Doi M., (2007), In situ observation of stereoscopic shape of cavities in soft adhesives, Europhysics letters, 77, 64002

Yana Peykoua, Olga Lebedeva, Alexander Diethert, Peter Miller-Bushbaun and Norbert Willenbacher (2012), Adhesive properties of acrylate copolymers effect of the nature of the substrate and copolymer functionality International Journal of adhesion and adhesive 34(2012) 107-116.

Yang, H. (2006a) Adhesion studies (i) Autohesion of Ethylene/1-octene copolymers.Ph.D Dissertation in Chemistry Virgina Polytechnic Institute and State University, U.S.A.

Yang, H. (2006b) Method development and adhesive characterization of pressure sensitive adhesive in paper laminates for postage stamps.Ph.D Dissertation in Chemistry Virgina Polytechnic Institute and State University, U.S.A.

Zbigniew C., Lukaz B., Arkadiusz K., (2013), How does the surface freeEnergy influences the tack of acrylic pressure sensitive adhesive (PSAS)? Journal of coating Technology. Res.10 (6) 879-885.

Zbigniew C., Magdalena W.,AgnieszkaK., JagodaK. (2012), The influence of residue monomers on selected properties of acrylic pressure sensitive adhesive.Drewno Pr. NaukDoniesKomunik, 2012, 55(188).

Zhang Newby B. M., Chaudhury M. K., and Brown H.R, (1995), Macroscopic evidence of the effect of interfacial slippage on adhesion science, 269,1407-1409

Zhang Y. (2007),The effect of surface roughness parameters on contact and wettability of solid surface.Ph.D dissertation co-major:Mechanical Engineering: Electrical Engineering. Lowa state university Ames,lowa USA

APPENDIX A

The line of best fit across the plots aided in the development of a Kaelble plot. The Kaelbleplot shows the relation between the polar and dispersive components of each measuring liquid, derived through the contact angles. The contact angles were the result of the drops of each measuring liquid on each substrate and each pressure sensitive adhesive.

4.1. Computation of the Surface Free Energy of the Substrates and Pressure Sensitive Adhesive from Kaelble Plot.

The sensitive and polar components are derived by the linear regression equation (equation of straight line) of each Kaelble plot, done on each substrate by the measuring liquid. They are as follows:

Substrates

(A) Surface Free Energy for Aluminum

Equation of linear regression (straight line equation)

$Y = mx+c$

$Y = -3.7857x+14.313$

The polar component of the surface energy is the square of the y intercept plot square ie

The dispersive component of the surface energy is the square of the slope ie

Y = -3.7857x+14.33

Which is (-3857)2=14.3315 approximately

= (14.33)2=205.3489

= 14.3315+205.3489

= 219.6084mJ/m^2

= 220mJ/m^2(approximately)

Surface Free Energy for High density Fibre Wood

(b) Equation of linear regression for high density fibre wood is as follows:

Y = -1.2449x+10.609

$$\gamma^d = m^2, \gamma^p = c^2$$

γ = $(-1.2449)^2$

γ = 1.56225 approximately

γ = $(10.609)^2$

γ = 112.55088mJ/m^2 approximately

$$\gamma^d = m^2, \gamma^p = c^2$$

γ = 1.56225+112.55088

γ = 114.113131mJ/m^2, 114mJ/m^2 approximately

(c) **Surface Free Energy forMild Steel**

Equation of linear regression for mild steel is as follows:

Y = -1.3385x+5.2076

$$\gamma^d = m^2, \gamma^p = c^2$$

γ = (-1.3385)^2

γ = 1.79158mJ/m^2 approximately

γ = (5.2076)^2

γ = 27.11909mJ/m^2

γ = 1.79158+27.11909

v= 28.910678mJ/m2, 28.91mJ/m^2 approximately

Surface Free Energy forCeramic Wall Tile

Equation of linear regression for ceramic wall tile is as follows:

Y = 1.2939x+7.6726

$$\gamma^d = m^2, \gamma^p = c^2$$

γ=(1.2939)^2

γ = 1.674177 approximately

γ = (7.6726)^2

γ = 58.86879 approximately

γ = 1.674177+58.86879

γ = 60.542968mJ/m^2 approximately

γ = 60.54mJ/m^2 approximately

Surface Free Energy forRubber Tile

Equation of linear regression for ceramic wall tile is as follows:

Y' = 7.1634x-6.0988 Y''=3.079x-1.6472

Y'-Y''=(7.1634-3.079)x -(6.0988-1.6472)

= 4.0844x -4.4516

=(4.0844)^2=16.6823mJ/m^2

=(4.4516)^2=19.81674mJ/m^2

$$\gamma^d = m^2, \gamma^p = c^2$$

γ =16.6823mJ/m^2+19.81674mJ/m^2

γ =36.4990mJ/m^2

γ =36.5mJ/m^2 approximately

Surface Free Energy forPressure Sensitive Adhesives

(a) Cow skin animal pressure sensitive adhesive

Equation of linear regression for cow base adhesive is as follows:

γ = -0.3599x +7.3533

γ=(-0.3599)^2

γ = 0.129528mJ/m^2

γ=(7.3533)^2

γ = 54.0710mJ/m^2

$$\gamma^d = m^2, \gamma^p = c^2$$

γ = 0.129528+54.0710

γ = 54.20054

γ = 54.2005 approximately

γ = 54.2mJ/m^2 approximately

(B) Natural Rubber Sensitive Adhesive

Equation of linear regression for natural rubber base adhesive

Y = 3.8979x -0.7286

=(3.8976)^2

= 15.191286mJ/m^2

=(-0.7286)^2

= 0.5308857

$$\gamma^d = m^2, \gamma^p = c^2$$

γ = 15.191286+0.5308857

γ = 15.72214396

γ = 15.72mJ/m^2 approximately

For Epoxy Pressure Sensitive Adhesive

Equation of linear regression for epoxy adhesive

Y = 3.1133x +0.6593

=$(3.1133)^2$

= 9.69263mJ/m^2

=$(0.6593)^2$

= 0.4346764

= 0.4348mJ/m^2

= 9.69263+0.4346764

= 10.127mJ/m^2 approximately

Acrylic Pressure Sensitive Adhesive

Equation of linear regression for acrylic adhesive

Y' = 5.3527x -4.2881, Y''= 3.1439x -1,7121

Y'-Y'' =(5.3527-3.1439)x - (4.2881-1.7121)

Y = 2.1781x -2.5759, where $\gamma^d = m^2, \gamma^p = c^2$

= 4.743684+6.6352, γ^d=$(2.1781)^2$

= 11.37894mJ/m^2, γ^d= 4.743684mJ/m^2

= 11.39mJ/m^2, γ^d=$(2.5759)^2$

γ^p= 6.6352mJ/m^2

Silicone Pressure Sensitive Adhesive

Equation of linear regression for silicone adhesive

Y =2.1735x+1.6607

$$\gamma^d = m^2, \gamma^p = c^2$$

y = $(2.1735)^2$

γ^d = 4.72410mJ/m^2

γ^p = $(1.6607)^2$

γ^p = 2.7579mJ/m^2

$$\gamma^{lv} = \gamma^d \gamma^p$$

γ^{lv} = 4.72410+2.7579

γ^{lv} = 7.48202 γ^{lv} = 7.48mJ/m^2

Component of the interfacial energy between substrate and pressure sensitive adhesive.

a) **For Aluminum**

I. **Aluminum and cow skin sensitive adhesive, (with cow skin represent as 3a)**

$$\gamma_{\acute{\imath}3a} = \gamma_{\acute{\imath}} + \gamma_{3a} - 2\left(\gamma^d_{s\acute{\imath}}\gamma^d_{l3a} + \gamma^p_{s\acute{\imath}}\gamma^p_{l3a}\right)^{1/2}$$

γ_1 represent aluminum substrate surface free energy substituting the values of the variablesstated in equation

$\gamma_{\acute{\imath}}$ For aluminum =220mJ/m^2

γ_{3a} for cow skin pressure sensitive adhesive =54.2mJ/m^2 approximately

$\gamma^d_{s\acute{\imath}}$ for dispersive component of the aluminum =14.3315mJ/m^2

$\gamma^p_{s\acute{\imath}}$ for polar component of the aluminum =205.3489mJ/m^2

γ^d_{l3a} for dispersive component of the cow skin adhesive =0.129528mJ/m^2

γ^p_{l3a} for polar component of the cow skin adhesive =54.0710mJ/m^2

$\gamma_{\acute{\imath}3a}$=220mJ/$m^2$+54.2mJ/$m^2$-2(14.315*0.129528+205.3489*54.0710)$^{1/2}$mJ/m^2

$\gamma_{\text{í}3a}$=274.2mJ/m^2-2(1.856330532+11103.420372)$^{1/}$2mJ/m^2

$\gamma_{\text{í}3a}$ =274.2mJ/m^2-2(11105.276703)$^{1/2}$mJ/m^2

$\gamma_{\text{í}3a}$=274.2mJ/m^2-2(105.38157668)mJ/m^2

$\gamma_{\text{í}3a}$=274.2mJ/m^2-210.76315335mJ/m^2

$\gamma_{\text{í}3a}$ =63.43684mJ/m^2

$\gamma_{\text{í}3a}$=63.45mJ/m^2 approximately

II. Aluminum and natural rubber based pressure sensitive adhesive

$$\gamma_{\text{í}3b} = \gamma_{\text{í}} + \gamma_{3b} - 2\left(\gamma_{s\text{í}}^{d}\gamma_{l3b}^{d} + \gamma_{s\text{í}}^{p}\gamma_{l3b}^{p}\right)^{1/2}$$

$\gamma_{\text{í}}$ representsaluminum substrate surface free energy

$\gamma^{\text{í}}$ substitutingthe values of the variables stated in equation

γ_{3b} foraluminum =220mJ/m^2

$\gamma_{s\text{í}}^{d}$ fornatural rubber based pressure sensitive adhesive =15.72mJ/m^{2}approximately

$\gamma_{s\text{í}}^{p}$ fordispersive component of aluminum =14.3315mJ/m^2

γ_{l3b}^{p} forpolar component of aluminum =205.3489mJ/m^2

$\gamma_{\text{í}3b}$ fordispersive component of the natural rubber adhesive =15.191286mJ/m^2

$\gamma_{\text{í}3b}$ forpolar component of the natural rubber adhesive =0.530857mJ/m^2

$\gamma_{\text{í}3b}$=220mJ/m^2+14.3315mJ/m^2-

2(14.3315*15.19128+205.3489*0.530857)$^{1/2}$mJ/m^2

$\gamma_{\text{í}3b}$=234.3315mJ/m^2-2(217.71382932+109.01090101)$^{1/2}$mJ/m^2

$\gamma_{\text{í}3b}$=234.3315mJ/m^2-2(326.72473033)$^{1/2}$mJ/m^2

$\gamma_{\text{í}3b}$=234.3315mJ/m^2-36.151056986mJ/m^2

$\gamma_{\text{í}3b}$=198.18mJ/m^2 approximately

III. Interfacial Energy between Aluminum and Acrylic based pressure sensitive Adhesive

$\gamma_{\text{í}3c} = \gamma_1 + \gamma_{3c} - 2\left(\gamma_{s1}^{d}\gamma_{l3c}^{d} + \gamma_{s1}^{p}\gamma_{l3c}^{p}\right)^{1/2}$

γ_1 representsaluminum substrate substituting the values of the variable stated in equation.

$\gamma^{\text{í}}$ foraluminum =220mJ/m^2

γ_{3c} foracrylic based pressure sensitive adhesive=

$\gamma_{s\text{í}}^{d}$ fordispersive component of the aluminum =14.3315mJ/m^2

$\gamma_{s\text{í}}^{p}$ forpolar component of the aluminum =205.3489mJ/m^2

γ_{l3c}^{d} fordispersive component of the acrylic adhesive =4.743684mJ/m^2

γ_{l3c}^{p} forpolar component of the acrylic based adhesive=6.6352mJ/m^2

$\gamma_{\text{í}3c}$ =220mJ/m^2+10.127mJ/m^2 -2(14.3315x4.743684+205.3489x6.6352)$^{1/2}$mJ/m^2

$\gamma_{\text{í}3c}$ =230.127mJ/m^2 -2(67.984107246+1362.5310213)$^{1/2}$mJ/m^2

$\gamma_{\text{í}3c}$ =230.127mJ/m^2 -2(1430.5151285) $^{1/2}$mJ/m^2

$\gamma_{\text{í}3c}$ =230.127mJ/m^2 -2(37.822151294)mJ/m^2

$\gamma_{\text{í}3c}$ =230.127mJ/m^2 -75.64430259mJ/m^2

$\gamma_{\text{í}3c}$ =154.4826974mJ/m^2

$\gamma_{\text{í}3c}$ =154.48mJ/m^2

iv. Aluminum and Silicon based sensitive adhesive

$\gamma_{\text{í}3d} = \gamma_{\text{í}} + \gamma_{3d} - 2\left(\gamma_{s\text{í}}^{d}\gamma_{l3d}^{d} + \gamma_{s\text{í}}^{p}\gamma_{l3d}^{p}\right)^{1/2}$

$\gamma_{\text{í}}$ representaluminum substrate free energy

Substitutingthe values of the variables stated in equation

$\gamma_{\text{í}}$ foraluminum =220mJ/m^2

γ_{3d} forsilicon base pressure sensitive adhesive 7.48mJ/m^2

$\gamma_{s\text{í}}^{d}$ fordispersive component of the aluminum =14.3315mJ/m^2

$\gamma_{sí}^{p}$ forpolar component of the aluminum =205.3489mJ/m^2

γ_{l3d}^{d} fordispersive component of the silicon = 4.72410mJ/m^2

γ_{l3d}^{p} forpolar component of the silicon = 2.7579mJ/m^2

γ_{l3d}^{d}= 220mJ/m^2+7.48mJ/m^2-2(14.3315*4.7240+205.3489*2.7579)$^{1/2}$mJ/m^2

γ_{l3d}^{d} = 227.48mJ/m^2-2(47.702006+566.331731)$^{1/2}$mJ/m^2

γ_{l3d}^{d}= 227.48mJ/m^2-2(634.03373731)$^{1/2}$mJ/m^2

γ_{l3d}^{d}= 227.48mJ/m^2-2(25.1800265)$^{1/2}$mJ/m^2

γ_{l3d}^{d}= 227.48mJ/m^2-50.36005311mJ/m^2

γ_{l3d}^{d}= 177.1199468

$\boldsymbol{\gamma_{l3d}^{d}}$= 177.12mJ/m^2

v. Aluminum and epoxy based pressure sensitive adhesive

$$\gamma_{í3e} = \gamma_{í} + \gamma_{3e} - 2\left(\gamma_{sí}^{d}\gamma_{l3e}^{d} + \gamma_{sí}^{p}\gamma_{l3e}^{p}\right)^{1/2}$$

$\gamma_{í}$ representaluminum substrate surface free energy

Substitutingthe values of the variable stated in equation

$\gamma_{í}$ foraluminum = 220mJ/m^2

γ_{3e} forepoxy base pressure sensitive adhesive = 10.127mJ/m^2

$\gamma_{sí}^{d}$ fordispersive component of the aluminum = 14.3315mJ/m^2

$\gamma_{sí}^{p}$ forpolar component of the aluminum = 205.3489mJ/m^2

γ_{l3e}^{d} fordispersive component of the epoxy = 9.69263mJ/m^2

γ_{l3e}^{p} forpolar component of the epoxy = 0.4346764mJ/m^2

$\gamma_{í3e}$= 220mJ/m^2+7.48mJ/m^2-2(14.3315*9.69263+205.3489*0.4346764)$^{1/2}$mJ/m^2

$\gamma_{í3e}$= 227.48mJ/m^2-2(138.90992685+89.2603206)$^{1/2}$mJ/m^2

$\gamma_{í3e}$= 227.48mJ/m^2-2(228.17024745+89.2q603206)$^{1/2}$mJ/m^2

$\gamma_{í3e}$= 227.48mJ/m^2-2(15.105305275)mJ/m^2

$\gamma_{\text{í}3e}$ = 227.48mJ/m^2-30.21061055mJ/m^2

$\gamma_{\text{í}3e}$ = 197.2693894mJ/m^2

$\boldsymbol{\gamma_{\text{í}3e}}$**= 197.27mJ/m^2**

b) For high density fiber wood (HDF-Wood)

c) High density fiber wood and cow base pressure sensitive adhesive

$\gamma_{\text{“I}3a} = \gamma_{\text{“I}} + \gamma_{3a} - 2\left(\gamma_{s\text{“I}}^{d}\gamma_{l3a}^{d} + \gamma_{s\text{“I}}^{p}\gamma_{l3a}^{p}\right)^{1/2}$

$\gamma_{\text{“I}}$ representthe HDF-Wood substrate surface free energy

Substituting the value of the variable stated in equation (4.9)

$\gamma_{\text{“I}}$ forHDF-Wood = 114mJ/m^{2}approximately

γ_{3a} forcow base pressure sensitive adhesive =54.2mJ/m^2

$\gamma_{s\text{“I}}^{d}$ fordispersive component of HDF-Wood = 1.56225mJ/m^2

$\gamma_{s\text{“I}}^{p}$ forpolar component of HDF-Wood = 112.55088mJ/m^2

γ_{l3a}^{d} fordispersive component of the cow base adhesive = 0.129528mJ/m^2

γ_{l3a}^{p} forpolar component of the cow base adhesive = 54.0710mJ/m^2

$\gamma_{\text{“I}3a}$ = 114mJ/m^2+54.2mJ/m^2-

2(1.56225*0.129528+112.55088*54.0710)$^{1/2}$mJ/m^2

$\gamma_{\text{“I}3a}$ = 168.2mJ/m^2-2(0.202355118+6085.7386325)$^{1/2}$mJ/m^2

$\gamma_{\text{“I}3a}$ = 168.2mJ/m^2-2(6085.9409876)$^{1/2}$

$\gamma_{\text{“I}3a}$ = 168.2mJ/m^2-2(78.012441236)mJ/m^2

$\gamma_{\text{“I}3a}$ = 168.2mJ/m^2-156.02488247mJ/m^2

$\gamma_{\text{“I}3a}$ = 12.17511753mJ/m^2

$\boldsymbol{\gamma_{\text{“I}3a}}$**= 12.18mJ/m^2**

ii) High Density Fiber Wood and Natural Rubber

Represent the HDF-Wood substrate surface free energy

Substituting the value of the variable stated in equation

$$\gamma_{\text{I}3b} = \gamma_{\text{I}} + \gamma_{3b} - 2\left(\gamma_{s\text{I}}^{d}\gamma_{l3b}^{d} + \gamma_{s\text{I}}^{p}\gamma_{l3b}^{p}\right)^{1/2}$$

γ_{I} forHDF-Wood = 114mJ/m^2

γ_{3b} fornatural rubber base pressure sensitive adhesive = 15.72mJ/m^2

$\gamma_{s\text{I}}^{d}$ fordispersive component of the HDF-Wood = 1.56225mJ/m^2

$\gamma_{s\text{I}}^{p}$ forpolar component of the HDF-Wood = 112.55088mJ/m^2

γ_{l3b}^{d} fordispersive component of the natural rubber adhesive = 15.1919286mJ/m^2

$\gamma_{\text{I}3b}$ forpolar component of the natural rubber adhesive = 0.530857mJ/m^2

$\gamma_{\text{I}3b}$ = 114mJ/m^2+15.72mJ/m^2-

2(1.56225*15.1919286+112.55088*0.530857)$^{1/2}$mJ/m^2

$\gamma_{\text{I}3b}$=129.72mJ/m^2-2(23.733590+59.748422504)$^{1/2}$mJ/m^2

$\gamma_{\text{I}3b}$=129.72mJ/m^2-2(83.482012504)$^{1/2}$mJ/m^2

$\gamma_{\text{I}3b}$= 129.72mJ/m^2-2(9.1368491562)mJ/m^2

$\gamma_{\text{I}3b}$=129.72mJ/m^2-18.2736988mJ/m^2

$\gamma_{\text{I}3b}$=111.4463mJ/m^2

$\gamma_{\text{I}3b}$=111.45mJ/m^2

Iii) Interfacial Energy between High Density Fiber Wood and Acrylic pressure sensitive adhesive

$$\gamma_{\text{I}3c} = \gamma_{\text{I}} + \gamma_{3c} - 2\left(\gamma_{s\text{I}}^{d}\gamma_{l3c}^{d} + \gamma_{s\text{I}}^{p}\gamma_{l3c}^{p}\right)^{1/2}$$

γ_{I} represents the high density fiber

Substitutingthe values of the variable stated in equation (4.11)

γ_{I} forHDF Wood = 114mJ/m^2 approximately

γ_{3c} foracrylic base pressure sensitive adhesive =

$\gamma_{s\text{"I}}^{d}$ fordispersive component of the HDF-Wood = 1.56225mJ/m^2

$\gamma_{s\text{"I}}^{p}$ forpolar component of the HDF-Wood = 112.55088mJ/m^2

γ_{l3c}^{d} fordispersive component of the acrylic =

γ_{l3c}^{p} forpolar component of the acrylic =

$\gamma_{\text{"I}3c}$ = 114mJ/m^2 +11-39mJ/m^2 -2(1.56225 x 4.743684 + 112.55088x6.6352)$^{1/2}$mJ/m^2

$\gamma_{\text{"I}3c}$ = 125.39mJ/m^2 -2(7.410820329+746.79759898)$^{1/2}$mJ/m^2

$\gamma_{\text{"I}3c}$ = 125.39mJ/m^2 -2(754.20841931)$^{1/2}$mJ/m^2

$\gamma_{\text{"I}3c}$ =125.39mJ/m^2 -2(27.462855265)$^{1/2}$mJ/m^2

$\gamma_{\text{"I}3c}$ = 125.39mJ/m^2 -54.92571053mJ/m^2

$\gamma_{\text{"I}3c}$ = 70.46428947mJ/m^2

$\gamma_{\text{"I}3c}$ = 70.46 mJ/m^2

iv) High Density Wood (HDF-Wood) and silicon based pressure sensitive adhesive

$$\gamma_{\text{"I}3d} = \gamma_{\text{"I}} + \gamma_{3d} - 2\left(\gamma_{s\text{"I}}^{d}\gamma_{l3d}^{d} + \gamma_{s\text{"I}}^{p}\gamma_{l3d}^{p}\right)^{1/2}$$

$\gamma_{\text{"I}}$ represent high density wood substrate surface free

substituting the value of the variable stated in equation (4.12)

$\gamma_{\text{"I}}$ forhigh density wood substrate = 114mJ/m^2

γ_{3d} forsilicon base pressure sensitive adhesive = 7.48mJ/m^2

$\gamma_{s\text{"I}}^{d}$ fordispersive component of HDF-Wood = 1.56225mJ/m^2

$\gamma_{s\text{"I}}^{p}$ forpolar component of HDF-Wood = 112.55mJ/m^2

γ_{l3d}^{d} fordispersive component of silicon = 4.72410mJ/m^2

γ_{l3d}^{p} forpolar component of silicon = 2.7579mJ/m^2

$\gamma_{\text{"I}3d}$ = 114mJ/m^2+7.48mJ/m^2-2(1.56225*4.7240+112.5508*2.7579)$^{1/2}$mJ/m^2

$\gamma_{\text{“I}3d}$ = 121.48mJ/m^2-2(7.380069+310.40407195)$^{1/2}$mJ/m^2

$\gamma_{\text{“I}3d}$ = 121.48mJ/m^2-2(317.68284516)$^{1/2}$mJ/m^2

$\gamma_{\text{“I}3d}$ = 12mJ/m^2-2(17.823659702)mJ/m^2

$\gamma_{\text{“I}3d}$ = 121.48-35.647319404

$\gamma_{\text{“I}3d}$ = 85.83268mJ/m^2

$\boldsymbol{\gamma_{\text{“I}3d}}$ **= 85.83mJ/m^2**

v) High Density Wood (HDF-Wood) and Epoxy pressure sensitive adhesive

$\gamma_{\text{“I}3e} = \gamma_{\text{“I}} + \gamma_{3e} - 2\left(\gamma^d_{s\text{“I}}\gamma^d_{l3e} + \gamma^p_{s\text{“I}}\gamma^p_{l3e}\right)^{1/2}$

$\gamma_{\text{“I}}$represents high density wood substrate surface free energy.

Substituting the value of the variable in equation

$\gamma_{\text{“I}}$forhigh density wood substrate = 114mJ/m^2

γ_{3e} forepoxy base pressure sensitive adhesive = 10.127mJ/m^2

$\gamma^d_{s\text{“I}}$fordispersive component of the HDF-Wood = 1.56225mJ/m^2

$\gamma^p_{s\text{“I}}$forpolar component of the HDF-Wood = 112.55088mJ/m^2

γ^d_{l3e} for dispersive component of epoxy = 9.69263mj/m^2

γ^p_{l3e} for polar component of epoxy = 0.4346764mJ/m^2

$\gamma_{\text{“I}3e}$ = 114mJ/m^2+10.127mJ/m^2-

2(1.56225*9.69263+112.55088*0.43467664)$^{1/2}$mJ/m^2

$\gamma_{\text{“I}3e}$ = 124.127mJ/m^2-2(15.142311217+48.923211335)mJ/m^2

$\gamma_{\text{“I}3e}$ = 124.127mJ/m^2-2(64.065522552)$^{1/2}$

$\gamma_{\text{“I}3e}$ = 124.12mJ/m^{2}7-2(8.004094119)

$\gamma_{\text{“I}3e}$ = 124.127mJ/m^2-16.008188224

$\gamma_{\text{“I}3e}$ = 108.1188117mJ/m^2

$\boldsymbol{\gamma_{\text{“I}3e}}$ **= 108.12mJ/m^2**

CONTACT ANGLE MEASUREMENT FOR RUBBER TILE FROM EACH TEST LIQUID AND ACCOMPANYING GRAPHICAL COMPONENT (X-Y Axis).

RUBBER TILE

S/N	Ethylene Glycol (^{0})	Ethanol (^{0})	Glycerol (^{0})	X	Y	X	Y	X	Y
1	NIL	73.212^0	74.899	NIL	NIL	2.6890	2.8049	1.0646	10.97171
2	-	74.484	76.319	-	-	2.6890	10.6864	1.0646	3.13583
3	-	71.940	73.582	-	-	2.6890	2.28946	1.0646	4.42284
4	-	73.675	74.255	-	-	2.6890	5.62829	1.0646	8.26499
5	-	74.285	73.718	-	-	2.6890	9.56740	1.0646	5.20433
6	-	73.528	75.120	-	-	2.6890	4.6784	1.0646	11.46007
7	-	73.114	74.567	-	-	2.6890	2.2932	1.0646	9.7799
8	-	72.889	74.327	-	-	2.6890	1.28317	1.0646	8.641167
9	-	73.172	75.249	-	-	2.6890	2.59131	1.0646	11.61982
10	-	73.511	74.676	-	-	2.6890	4.5709	1.0646	10.79166

11	-	72.416	74.838	-	-	2.6890	0.08409	1.0646	10.79166
12	-	73.542	73.959	-	-	2.6890	4.7674	1.0646	6.6088
13	-	73.128	74.262	-	-	2.6890	2.3638	1.0646	8.30214
14	-	74.281	73.814	-	-	2.6890	9.543	1.0646	5.76392
Σfx	-	73.542	74.542			2.6889	4.7687	1.0646	9.670885
STD	-	0.70439	0.7289						

ALUMINUM

S/N	Ethylene Glycol (^{0})	Ethanol (^{0})	Glycerol (^{0})	X	Y	X	Y	X	Y
1	163.755	101.147	118.980	1.4318	11.7368	2.6890	12.0518	1.0646	11.2223
2	163.145	102.325	117.250	1.4318	12.0558	2.6890	5.1667	1.0646	2.74034
3	162.859	104.284	119.325	1.4318	11.4420	2.6890	1.2022	1.0646	11.6757
4	164.125	103.374	117.507	1.4318	10.5123	2.6890	0.29356	1.0646	4.10063
5	164.337	101.520	120.435	1.4318	9.527	2.6890	10.2822	1.0646	8.7266
6	163.825	103.546	118.545	1.4318	11.5599	2.6890	0.05307	1.0646	9.76138
7	163.539	102.389	119.845	1.4318	12.1055	2.6890	4.7558	1.0646	11.06577
8	163.673	102.546	118.735	1.4318	11.9721	2.6890	3.7839	1.0646	10.50918
9	162.577	103.579	117.879	1.4318	10.4115	2.6890	0.0290	1.0646	6.24678
10	163.745	102.858	118.250	1.4318	11.7599	2.6890	2.0823	1.0646	8.33232
11	163.409	103.478	117.590	1.4318	12.1934	2.6890	0.12519	1.0646	4.568966
12	164.358	102.565	120.337	1.4318	9.4205	2.6890	3.6706	1.0646	9.2099
13	164.128	101.852	119.517	1.4318	10.499	2.6890	8.2760	1.0646	11.6304
14	162.937	102.547	120.354	1.4318	11.6552	2.6890	3.7780	1.0646	9.12827
$\Sigma\bar{f}x$	163.5983	102.715	118.8965	1.4318	12.0316	2.6890	2.8175	1.0646	15.0810
STD	0.558263	0.8728736	1.10916						

HIGH DENSITY FIBRE WOOD

S/N	Ethylene Glycol (^{0})	Ethanol (^{0})	Glycerol (^{0})	X	Y	X	Y	X	Y
1	112.287	62.782	132.128	1.4318	8.9021	2.6890	13.263	1.0646	11.5891
2	119.643	63.640	130.648	1.4318	11.9910	2.6890	11.220	1.0646	7.4114
3	119.250	62.385	129.168	1.4318	12.100	2.6890	12.6201	1.0646	0.38009
4	118.712	64.920	131.150	1.4318	10.886	2.6890	3.35390	1.0646	9.9258
5	119.541	63.585	130.580	1.4318	12.121	2.6890	11.476	1.0646	7.0254
6	118.457	64.520	129.952	1.4318	9.778	2.6890	5.8589	1.0646	3.4383
7	118.389	63.910	130.853	1.4318	9.439	2.6890	12.8506	1.0646	8.5242
8	117.284	64.581	131.585	1.4318	3.0388	2.6890	5.4586	1.0646	11.30633
9	117.875	64.520	132.885	1.4318	6.4978	2.6890	5.8589	1.0646	9.29705
10	118.540	63.851	132.442	1.4318	10.1691	2.6890	10.1136	1.0646	10.9831
11	118.804	64.625	131.782	1.4318	11.2140	2.6890	5.1725	1.0646	11.60550
12	117.970	65.210	130.485	1.4318	7.0735	2.6890	1.8417	1.0646	6.4773
13	118.887	64.728	131.579	1.4318	11.4720	2.6890	4.5147	1.0646	11.2938
14	119.830	64.125	132.475	1.4318	11.5941	2.6890	8.4547	1.0646	10.889

$\Sigma f x$	118.6764	64.0987	131.2651	1.4318	10.7493	2.6890	8.6243	1.0646	10.3789
STD	0.7224	0.80448	1.0543						

MILD STEEL

S/N	Ethylene Glycol (^{0})	Ethanol (^{0})	Glycerol (^{0})	X	Y	X	Y	X	Y
1	121.545	102.452	72.840	1.4318	2.6875	2.6890	4.3589	1.0646	0.96625
2	122.145	101.952	71.520	1.4318	0.4286	2.6890	2.2449	1.0646	1.51470
3	120.909	103.056	73.060	1.4318	6.3580	2.6890	1.2222	1.0646	1.78607
4	122.350	103.236	74.560	1.4318	0.09012	2.6890	0.6223	1.0646	9.74957
5	121.980	102.576	74.107	1.4318	0.8746	2.6890	1.0614	1.0646	7.4545
6	122.545	102.374	73.560	1.4318	0.01278	2.6890	4.8515	1.0646	4.9285
7	120.389	101.856	72.890	1.4318	9.3522	2.6890	2.42880	1.0646	1.1332

8	121.536	102.327	71.925	1.4318	2.7331	2.6890	1.51723	1.0646	0.31833
9	122.150	103.528	73.285	1.4318	0.41747	2.6890	0.02037	1.0646	2.8264
10	123.427	102.819	74.012	1.4318	2.33158	2.6890	0.66946	1.0646	6.9145
11	121.836	101.568	74.285	1.4318	1.38034	2.6890	2.9474	1.0646	8.4233
12	122.815	102.182	73.870	1.4318	0.25977	2.6890	1.7969	1.0646	6.09096
13	122.457	105.182	75.170	1.4318	0.01293	2.6890	1.8337	1.0646	11.5332
14	121.777	104.71	73.452	1.4318	1.6164	2.6890	0.9603	1.0646	3.7001
$\Sigma f x$	122.815	102.887	73.466	1.4318	0.2597	2.6890	1.9448	1.0646	3.7765
STD	0.76741	1.02682	0.989766						

CERAMIC WALL TILE

S/N	Ethylene Glycol (^{0})	Ethanol (^{0})	Glycerol (^{0})	X	Y	X	Y	X	Y
1	155.334	81.794	55.702	1.4318	5.0389	2.6890	13.225	1.0646	9.71275
2	157.788	79.935	54.468	1.4318	10.7325	2.6890	5.4765	1.0646	2.9908
3	156.590	83.653	56.936	1.4318	11.48328	2.6890	4.04688	1.0646	11.25183
4	155.211	81.500	55.942	1.4318	4.3041	2.6890	13.16284	1.0646	10.6420
5	156.741	82.435	54.892	1.4318	11.8535	2.6890	11.47497	1.0646	5.34125
6	157.180	81.712	55.128	1.4318	12.1693	2.6890	13.2686	1.0646	6.7161
7	155.300	82.159	55.567	1.4318	4.8353	2.6890	12.5290	1.0646	9.0885
8	155.148	80.544	56.238	1.4318	5.9241	2.6890	9.4225	1.0646	11.4049
9	156.890	81.984	55.734	1.4318	12.0906	2.6890	12.97386	1.0646	9.8508
10	156.959	81.234	55.950	1.4318	12.1556	2.6890	12.61856	1.0646	10.66858
11	157.148	80.594	56.284	1.4318	12.1857	2.6890	9.72008	1.0646	11.48121
12	155.210	81.674	55.359	1.4318	4.3041	2.6890	13.2715	1.0646	8.01547

13	156.820	82.156	56.282	1.4318	11.9955	2.6890	12.5383	1.0646	11.4781
14	157.550	81.959	55.815	1.4318	11.5376	2.6890	13.0176	1.0646	10.18155
Σfx	156.82	81.662	55.7355	1.4318	11.9956	2.0890	13.2741	1.0646	9.8573
STD	O.962242	0.91331684	0.6352812						

S/N	Ethylene Glycol (^{0})	Ethanol (^{0})	Glycerol (^{0})	X	Y	X	Y	X	Y
1	129.823	Nil	121.568	1.4318	2.8955	Nil	Nil	1.0646	2.4636
2	130.431	Nil	120.038	1.4318	6.4348	Nil	Nil	1.0646	10.46686
3	128.956	Nil	120.53	1.4318	0.06913	Nil	Nil	1.0646	8.23172
4	129.233	Nil	116.902	1.4318	0.5494	Nil	Nil	1.0646	5.77046
5	128.304	Nil	117.817	1.4318	0.75054	Nil	Nil	1.0646	5.84967
6	128.555	Nil	119.828	1.4318	0.1900	Nil	Nil	1.0646	5.9247
7	131.639	Nil	121.213	1.4318	11.9131	Nil	Nil	1.0646	4.33093
8	130.750	Nil	120.841	1.4318	8.3280	Nil	Nil	1.0646	5.952494
9	130.517	Nil	121.384	1.4318	6.9566	Nil	Nil	1.0646	3.392636
10	129.823	Nil	119.583	1.4318	2.8955	Nil	Nil	1.0646	5.9318
11	130.876	Nil	119.689	1.4318	6.1599	Nil	Nil	1.0646	11.4084
12	131.259	Nil	121.618	1.4318	6.1966	Nil	Nil	1.0646	2.22956
13	130.881	Nil	120.431	1.4318	6.16046	Nil	Nil	1.0646	8.7469
14	130.121	Nil	120.351	1.4318	4.5607	Nil	Nil	1.0646	9.14278

Σfx	130.0834	Nil	120.128	1.4318	4.3399	Nil	Nil	1.0646	10.1272
STD	1.0172274		1.364258						

ACRYLIC

S/N	Ethylene Glycol (^{0})	Ethanol (^{0})	Glycerol (^{0})	X	Y	X	Y	X	Y
1	128.350	92.140	111.259	1.4318	0.62140	2.6890	3.241	1.0646	4.29791
2	127.753	91.370	110.980	1.4318	3.0769	2.6890	2296	1.0646	2.80590
3	126.453	89.877	108.829	1.4318	4.7777	2.6890	4.4128	1.0646	4.43065
4	126.173	88.342	111.019	1.4318	11.4258	2.6890	6.9241	1.0646	3.00283
5	126.895	88.540	112.819	1.4318	8.13140	2.6890	12.1380	1.0646	11.459
6	129.341	87.880	112.115	1.4318	0.85454	2.6890	13.1772	1.0646	9.0854
7	128.283	89.542	110.545	1.4318	0.81328	2.6890	6.5568	1.0646	0.98529
8	128.525	88.670	111.821	1.4318	0.23806	2.6890	11.6256	1.0646	7.5380
9	127.651	89.380	112.728	1.4318	3.6322	2.6890	7..6219	1.0646	5.9275
10	126.578	88.890	110.764	1.4318	9.8231	2.6890	10.5707	1.0646	1.80671
11	129.542	89.318	111.015	1.4318	1.5818	2.6890	8.0498	1.0646	2.9824
12	129.535	88.210	110.824	1.4318	1.5532	2.6890	13.0031	1.0646	2.0673
13	128.611	92.100	111.585	1.4318	0.11478	2.6890	2.9999	1.0646	6.1838
14	127.658	91.580	112.313	1.4318	3.5931	2.6890	0.72713	1.0646	5.9070
$\Sigma f x$	128.025	89.703	111.3154	1.4318	1.4318	2.6890	5.5304	1.0646	4.61797
STD	1.05813	1.4879	1.0649						

SILICONE.

S/N	Ethylene Glycol (^{0})	Ethanol (^{0})	Glycerol (^{0})	X	Y	X	Y	X	Y
1	114.139	139.761	138.537	1.4318	9.179	2.6890	6.9003	1.0646	11.4117
2	113.149	137.851	136.857	1.4318	12.191	2.6890	12.8006	1.0646	6.9900
3	116.089	137.951	135.177	1.4318	0.1733	2.6890	8.5443	1.0646	0.0228
4	115.870	136.742	135.457	1.4318	0.4104	2.6890	7.1841	1.0646	0.39223
5	114.281	134.141	137.328	1.4318	8.4029	2.6890	2.7623	1.0646	9.4644
6	113.754	135.282	136.540	1.4318	6.8920	2.6890	0.12387	1.0646	5.1471
7	114.875	137.105	138.678	1.4318	4.8470	2.6890	9.4966	1.0646	11.1083
8	115.210	135.482	137.908	1.4318	2.9540	2.6890	0.50720	1.0646	11.3843
9	114.890	136.532	135.891	1.4318	6.0725	2.6890	5.7935	1.0646	1.7825
10	113.594	135.748	136.730	1.4318	11.4629	2.6890	1.39161	1.0646	6.2552
11	114.750	136.389	136.485	1.4318	5.6012	2.6890	4.8640	1.0646	4.8293
12	116.389	137.355	137.350	1.4318	5.9764	2.6890	10.8890	1.0646	9.5645
13	115.576	136.833	138.657	1.4318	1.2920	2.6890	7.7850	1.0646	11.1604
14	114.777	137.455	138.421	1.4318	5.4372	2.6890	11.3763	1.0646	11.5786

$\Sigma f x$	114.8102	136.6876	137.138	1.4318	5.2363	2.6890	6.8257	1.0646	8.53362
STD	0.96466	1.33048	1.18358						

NATURAL RUBBER

EPOXY

S/N	Ethylene Glycol (^{0})	Ethanol (^{0})	Glycerol (^{0})	X	Y	X	Y	X	Y
1	129.827	181.850	96.780	1.4318	2.9163	2.6890	12.849	1.0646	1.051583
2	130.520	179.200	97.510	1.4318	6.9747	2.6890	0.0553	1.0646	0.04245
3	131.358	180.889	96.850	1.4318	11.1725	2.6890	8.26103	1.0646	0.82943
	131.510	182.530	96.650	1.4318	11.6270	2.6890	12.9398	1.0646	1.52549
5	130.598	179.858	95.550	1.4318	7.4425	2.6890	10.31909	1.0646	7.39269
6	129.715	179.565	97.130	1.4318	2.3547	2.6890	1.9521	1.0646	0.19542
7	128.570	179.565	96.157	1.4318	0.16809	2.6890	0.794	1.0646	3.9027
8	130.431	182.306	95.890	1.4318	6.4347	2.6890	13.2427	1.0646	5.4254
9	130.413	180.512	96.745	1.4318	5.7153	2.6890	5.7784	1.0646	1.171530
10	130.989	181.589	95.732	1.4318	0.6090	2.6890	12.0236	1.0646	6.34755
11	129.568	182.528	96.28	1.4318	1.6098	2.6890	12.9439	1.0646	3.24121
12	128.670	181.019	96.540	1.4318	0.0557	2.6890	9.0814	1.0646	198,375
13	130.818	182.716	95.749	1.4318	8.7087	2.6890	12.449	1.0646	6.24853
14	131.214	181.285	95.870	1.4318	10.6337	2.6890	10.6169	1.0646	5.5420
$\Sigma f x$	130.2929	181.8515	96.4095	1.4318	5.5931	2.6890	12.8479	1.0646	2.5874
STD	0.922676	1.13372	0.6229						

APPENDIX B

OXFORD INSTRUMENTS

Name	Class	Date	Time	Duration
ENGER SAMPLE B	Alloy_LE_FP	08/12/2018	16:08:09	15.5 s

Element	Al %	Mn %	Fe %	Cu %	Nb %	Pd %
	94.90	3.33	1.45	0.12	0.03	0.17
±	1.159	0.103	0.066	0.012	0.006	0.018

Grades: AA-3003 (1.06), AA-3004 (1.14)
Reference:

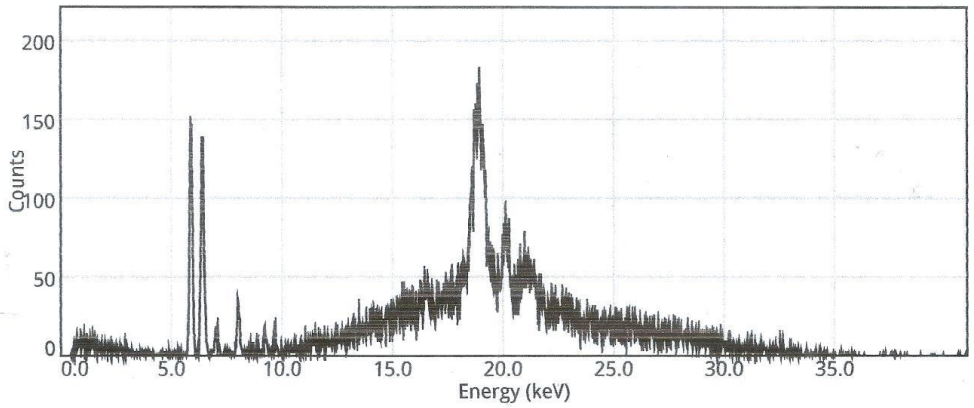

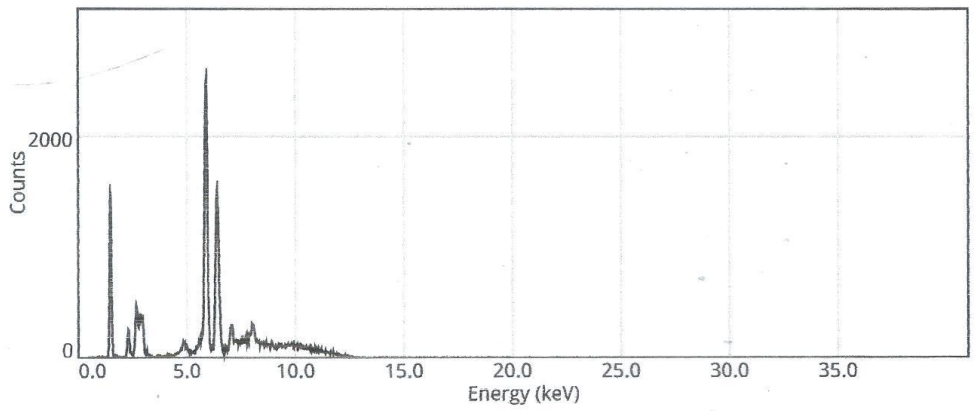

Name	Class	Date	Time	Duration
ENGER SAMPLE B	Alloy_LE_FP	08/12/2018	16:08:57	15.6 s

Element	Al %	Mn %	Fe %	Cu %	Pd %	Hf %	Ta %
	96.53	2.28	0.95	0.08	0.08	0.03	0.05
±	0.901	0.067	0.042	0.007	0.011	0.010	0.012

Grades: AA-3003 (0.44), AA-3005 (0.54)
Reference:

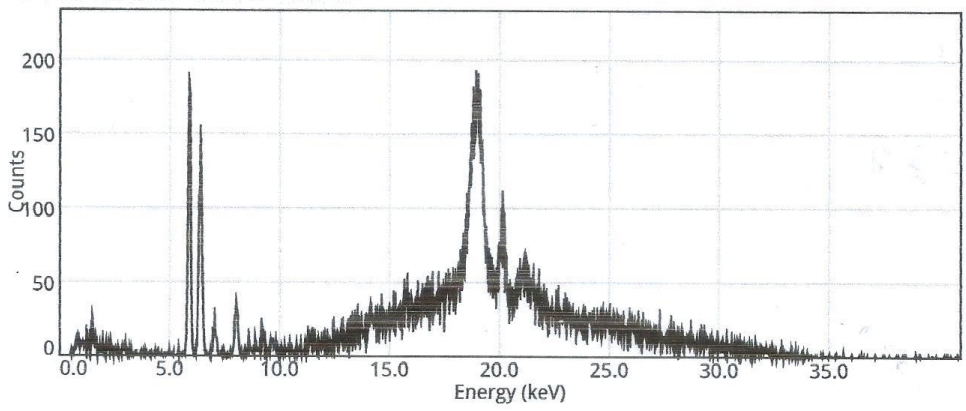

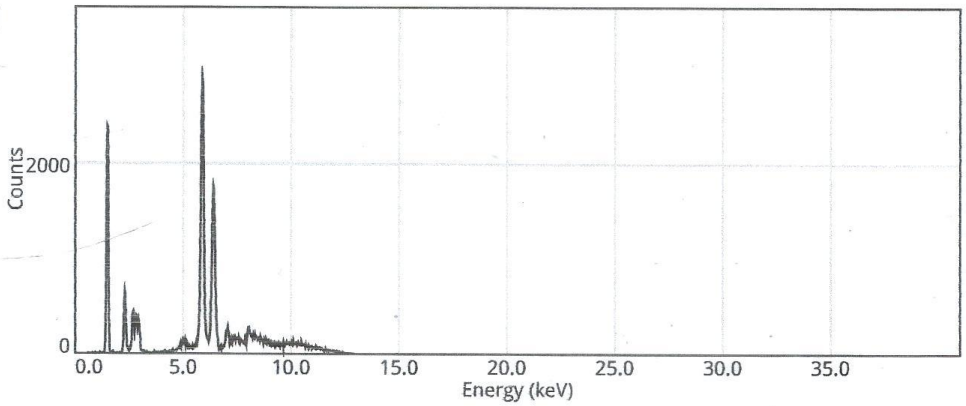

Name	Class	Date	Time	Duration
ENGER SAMPLE C	Alloy_LE_FP	08/12/2018	16:10:57	15.5 s

Element	Si %	Ti %	Cr %	Mn %	Fe %
	0.76	0.13	0.06	0.29	98.77
±	0.097	0.020	0.010	0.030	0.253

Grades: C-Steel (0.00), C-1020 (0.02)
Reference:

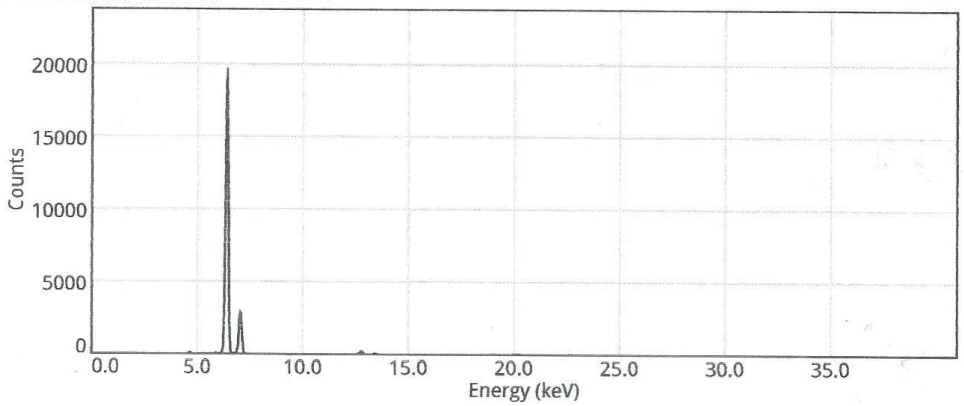

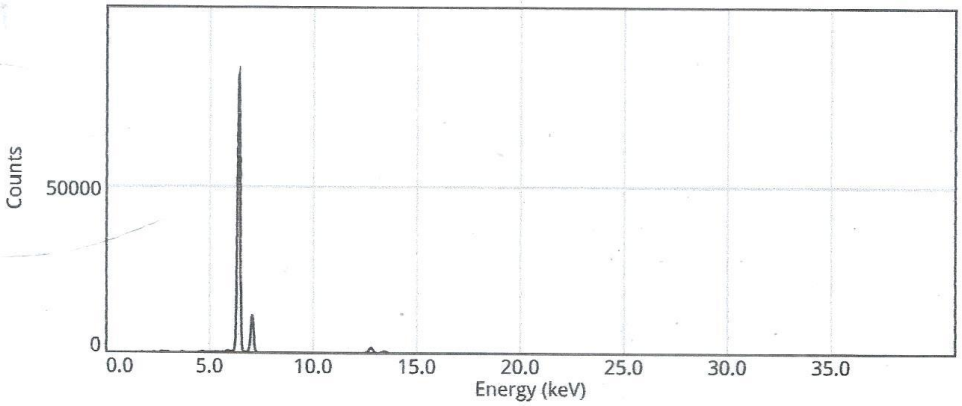

Name	Class	Date	Time	Duration
ENGER SAMPLE C	Alloy_LE_FP	08/12/2018	16:11:29	15.5 s

Element	Si %	Ti %	Cr %	Mn %	Fe %
	0.36	0.09	0.06	0.26	99.22
±	0.088	0.019	0.009	0.028	0.253

Grades: C-Steel (0.00), Iron (0.00)
Reference:

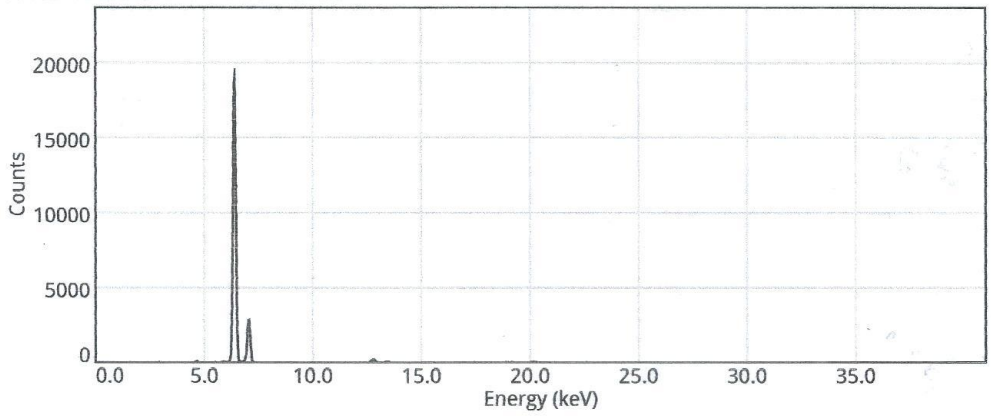

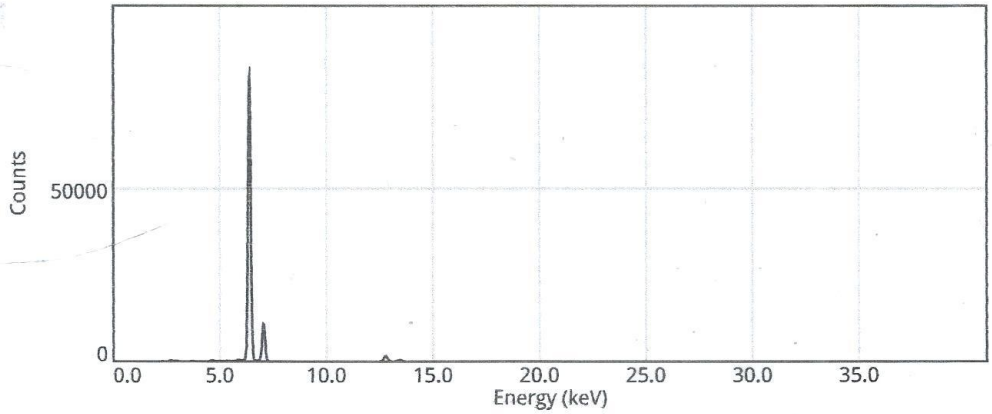

Name	Class	Date	Time	Duration
ENGER SAMPLE D	Alloy_LE_FP	08/12/2018	16:15:55	15.5 s

Element	Al %	Si %	Ti %	Fe %	Zn %	Zr %	Nb %	Pd %	W %	Au %
	7.32	67.19	7.18	10.62	7.35	0.03	0.04	0.13	0.08	0.06
±	0.371	0.537	0.226	0.121	0.061	0.007	0.007	0.024	0.019	0.010

Grades: No Match
Reference:

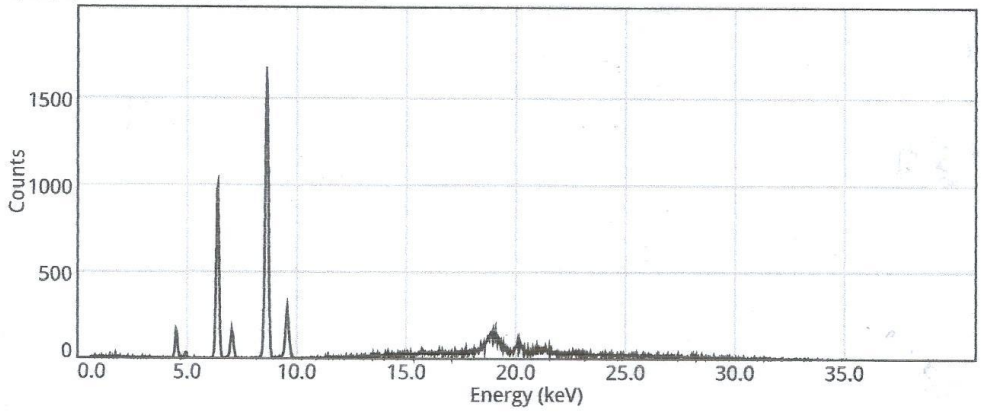

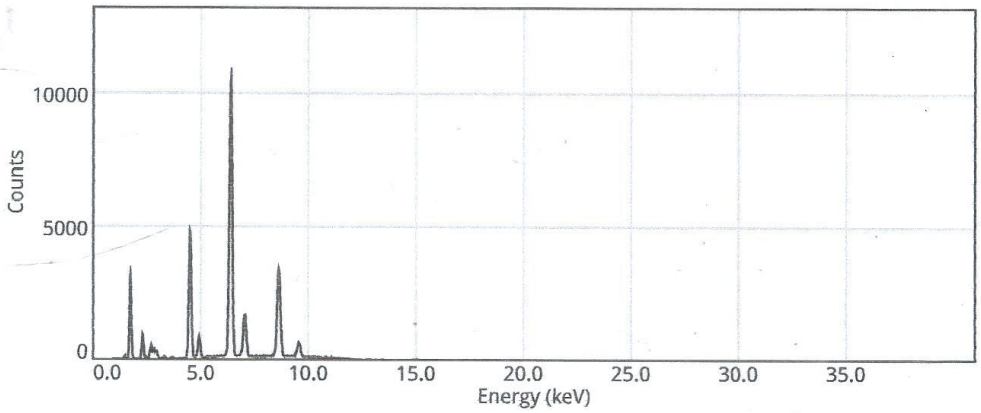

Name	Class	Date	Time	Duration
ENGER SAMPLE D	Alloy_LE_FP	08/12/2018	16:16:19	15.5 s

Element	Al %	Si %	Ti %	Fe %	Zn %	Zr %	Nb %	Pd %	Au %
	8.15	67.36	6.99	10.28	6.91	0.03	0.04	0.18	0.07
±	0.370	0.530	0.221	0.117	0.058	0.006	0.007	0.023	0.012

Grades: No Match
Reference:

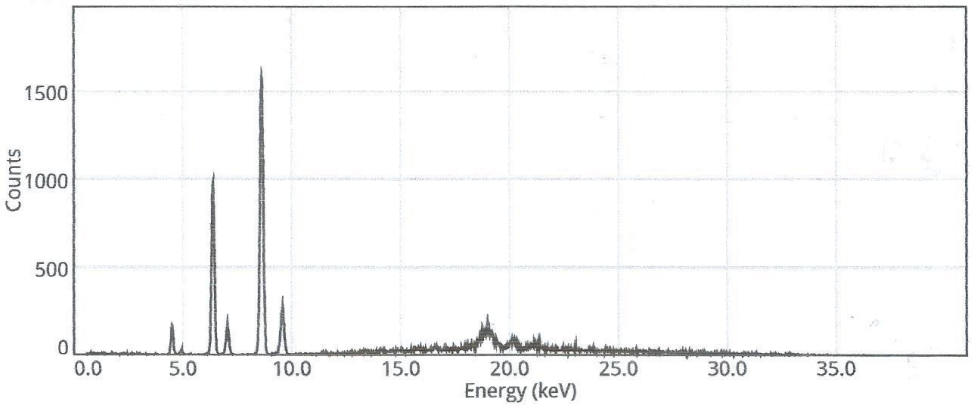

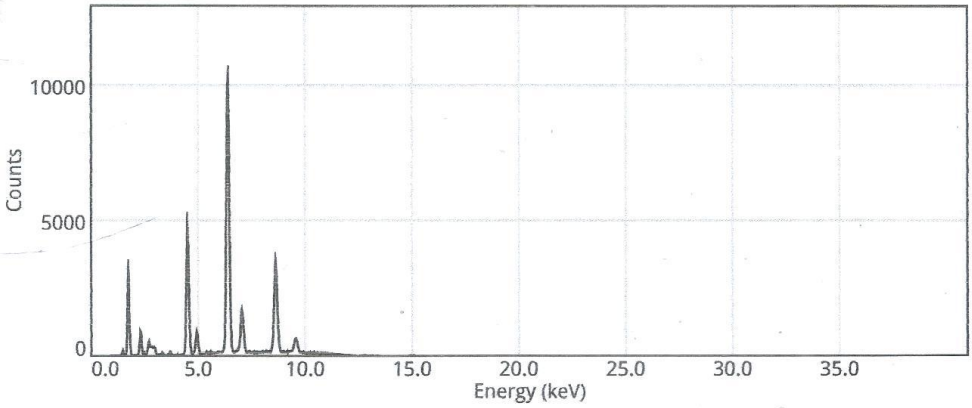

Name	Class	Date	Time	Duration
ENGER SAMPLE E	Alloy_LE_FP	08/12/2018	16:17:39	15.5 s

Element	Al %	Si %	Ti %	Fe %	Zn %	Zr %	Nb %	Pd %
	11.89	83.53	0.85	1.51	1.95	0.16	0.02	0.09
±	0.435	0.658	0.151	0.055	0.030	0.006	0.005	0.017

Grades: No Match
Reference:

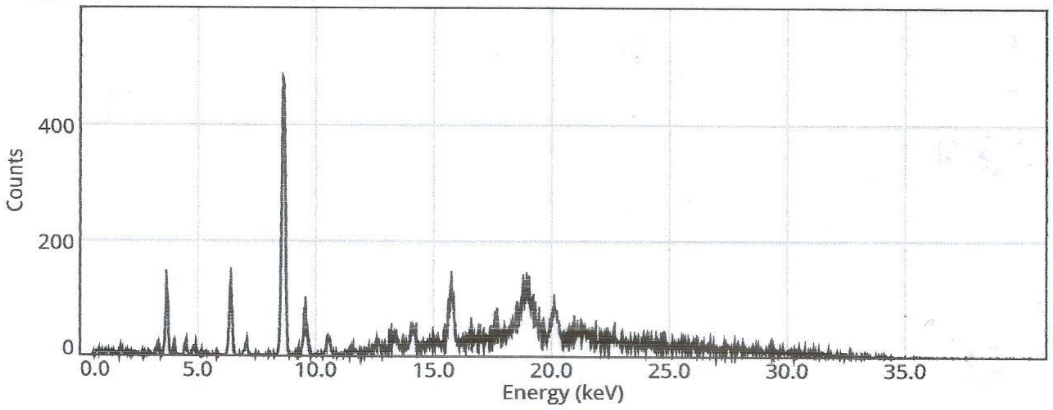

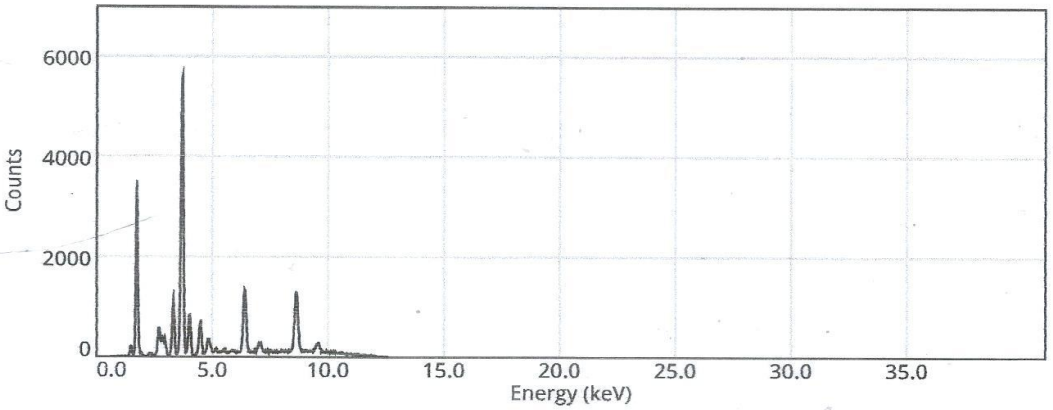

Name	Class	Date	Time	Duration
ENGER SAMPLE E	Alloy_LE_FP	08/12/2018	16:18:04	15.5 s

Element	Al %	Si %	Ti %	Fe %	Zn %	Zr %	Nb %	Pd %
	11.47	84.00	0.93	1.51	1.83	0.14	0.02	0.10
±	0.378	0.597	0.139	0.050	0.027	0.005	0.004	0.015

Grades: No Match
Reference:

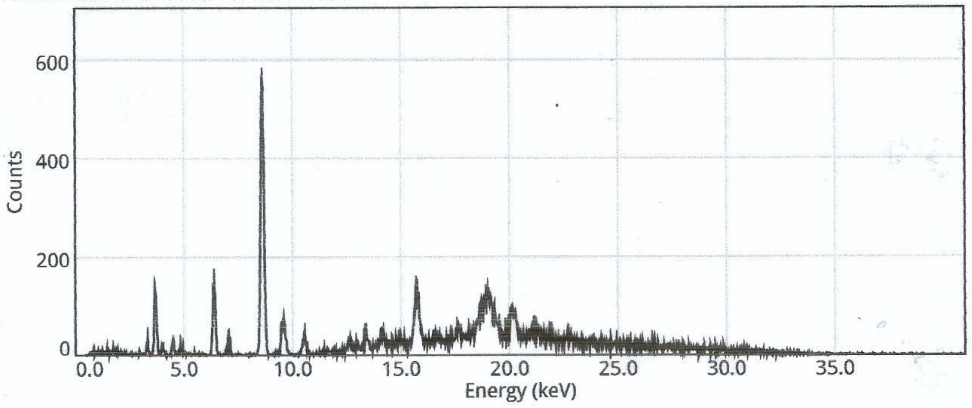
600
400
200
0
Counts
0.0
5.0
10.0
15.0
20.0
25.0
30.0
35.0
Energy (keV)

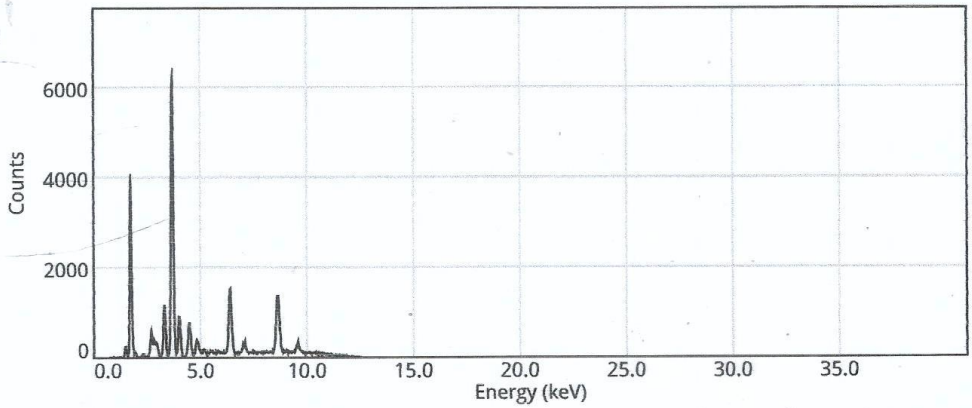
6000
4000
2000
0
Counts
0.0
5.0
10.0
15.0
20.0
25.0
30.0
35.0
Energy (keV)